Evolutionary history, connectivity and habitat-use of annelids from deep-sea chemosynthesis-based ecosystems, with an emphasis on the Arctic mid-Ocean Ridge and the Nordic Seas

Mari Heggernes Eilertsen

Thesis for the Degree of Philosophiae Doctor (PhD)
University of Bergen, Norway
2018

UNIVERSITY OF BERGEN

Evolutionary history, connectivity and habitat-use of annelids from deep-sea chemosynthesis-based ecosystems, with an emphasis on the Arctic mid-Ocean Ridge and the Nordic Seas

Mari Heggernes Eilertsen

Thesis for the Degree of Philosophiae Doctor (PhD)
at the University of Bergen

2018

Date of defence: 16.03.2018

Year: 2018

Title: Evolutionary history, connectivity and habitat-use of annelids from deep-sea chemosynthesis-based ecosystems, with an emphasis on the Arctic mid-Ocean Ridge and the Nordic Seas

Name: Mari Heggernes Eilertsen

Print: Skipnes Kommunikasjon / University of Bergen

Contents

Scientific environment

This PhD project was financed through a four-year PhD position funded by the University of Bergen, was carried out in the Marine Biodiversity research group at the Department of Biological Sciences, and as part of the Centre for Geobiology (NFR project number 179560) and K. G. Jebsen Centre for Deep Sea Research at the University of Bergen.

The project has also been funded in part by the Norwegian Academy of Science and Letters and the Norwegian Deep-Sea Program (the taxonomy fund), the Norwegian Taxonomy Initiative (project number 70184227, “Polychaete diversity in the Norwegian Sea – from coast to the deep sea”), the NFR project Norwegian Barcode of Life (NorBOL), and student grants from the Meltzer Foundation.

UNIVERSITY OF BERGEN
Faculty of Mathematics and Natural Sciences

The Research Council of Norway

L. MELTZERS HØYSKOLEFOND

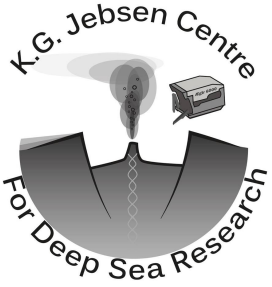

ARTSDATABANKEN

Acknowledgements

Although a doctoral thesis is supposed to be an individual achievement, this thesis would not have been possible without the great team of people I have had around me. Firstly, Hans Tore has been a very supportive and accessible supervisor, and I could always knock on his office door if I needed to discuss something. He allowed me to travel a lot to participate in courses, conferences and field trips, which has been very rewarding both scientifically and personally, and for that I am very grateful. Hans Tore has also given me a lot of freedom to pursue the projects and ideas I wanted, while still helping me to stay on the right track, and providing the knowledge of the study system to help placing my results in a larger perspective.

I also had two very helpful co-supervisors, who were always available to discuss my work. As supervisor of my master thesis, Manuel got me interested in phylogenetics and taught me scientific writing, both through the thesis work and the papers we wrote together afterwards. The training I got then has been of great help to me in my PhD work, and I was very happy to have him as co-supervisor of my PhD as well. My other co-supervisor, Jon, is the main reason my project ended up being all about worms, with his infectious enthusiasm and knowledge about these animals. His taxonomic expertise has been invaluable for my work, and we have had many long discussions about evolution and taxonomy, from which I have learned a lot.

I have had the privilege of collaborating with several researchers from other institutions, and in particular I am very grateful to Greg Rouse and Josefin Stiller from the Scripps Institution of Oceanography, and Magdalena Georgieva, Helena Wiklund and Adrian Glover from the Natural History Museum in London, for sharing material with me and contributing to our collaborative papers. I want to thank Marina Cunha, Ascensão Ravara and Ana Hilário for sharing material, and for hosting us in Aveiro, Portugal. I am also indebted to Kenneth Halanych and Viktoria Bogantes, Cindy L. Van Dover, Igor Jirkov, Lenaick Menot and Andrew Thurber for sending me material. This

thesis has also benefited from material from the MAREANO project, the German Centre for Marine Biodiversity Research (DZMB), the EAF-Nansen Programme, the Gulf of Guinea LME (GCLME) and the Canary Current LME (CCLME).

I want to thank all the members of the Marine Biodiversity research group, who have helped me out with many things, and always showed an interest in my work. Especially, I want to thank the technicians, Solveig, Louise, Kenneth and David, who were a great help with the lab work and always available for discussions on troubleshooting or data analysis. I am also very grateful to Rolf Birger Pedersen and the rest of the staff and students of the Centre for Geobiology and K. G. Jebsen Centre for Deep Sea Research for bringing me along on cruises and helping me out with sampling.

I have had assistance from many staff members at the University Museum of Bergen as well. I would like to thank Endre Willasen for help with phylogenetics, Katrine Kongshavn for producing maps, Nataliya Budaeva for help with acquiring material and with labwork and Tom Alvestad for identifying and subsampling specimens. Through these five years I have been looking forward to coming to work every day (or at least nearly every day), because of the warm and including working environment in our research group. This is to a large degree because of the great team of PhD students and postdocs I have been working with (past and present), which have also become some of my closest friends. In particular I want to thank Carrie and Joana, who have helped make this thesis better through productive scientific discussions and help with text whenever I got stuck.

Lastly, I could not have completed this thesis without the support of my family and friends. I am very grateful to my parents and in-laws for babysitting so I could go to work many a weekend. I am incredibly lucky to have a husband who recently finished his PhD, and understands what it takes to complete such a project. Especially the last year, he has taken more than his share of the work at home, delivered and picked up our girl in kindergarten so I could work longer, and cooked dinner for us almost every

day. I could not have done this without his love and support, and the healthy distractions of our daughter Solveig.

Summary

The enigmatic fauna of chemosynthesis-based ecosystems (CBEs), i.e. hydrothermal vents, cold seeps and organic falls, has been the subject of intensive research over the last decades. However, there are still many aspects of these ecosystems that are poorly understood. There are many shared families and genera of animals between the different types of CBEs, which shows that there is an evolutionary link between them, but the prevalence of shared species and present-day connectivity between different CBEs is debated. The existence of "intermediate" habitats such as sedimented hydrothermal vents and hydrothermal seeps, led to the suggestion that CBEs should be considered a continuum of reducing conditions, rather than completely distinct phenomena. However, it is not clear which environmental factors are most important in structuring the fauna of CBEs, or what determines the habitat specificity of taxa. Evolutionary studies of CBE-adapted taxa often show a gradual adaptation to more extreme environments, with organic falls or cold seeps serving as evolutionary stepping-stones into the hydrothermal vent habitat. Most of these studies, however, have been focused on symbiotrophic taxa, and the evolutionary role of intermediate habitats has not been assessed in a phylogenetic context. Sampling of CBEs is still patchy and biased, both in terms of geographic regions and habitats, which hampers our understanding of biogeographic patterns.

The main objective of this project was to contribute to filling these knowledge gaps by focusing on the annelid fauna of CBEs on the Arctic Mid-Ocean Ridge and in the Nordic Seas. The target taxa were worms in the family Ampharetidae, which are commonly found in all types of CBEs around the world, and *Sclerolinum contortum* and *Nicomache lokii*, which are abundant habitat-builders in Arctic CBEs. The project aimed to: 1 – describe the new species of Ampharetidae from Loki's Castle Vent Field (LCVF), 2 – reconstruct the evolutionary history of Ampharetidae, 3 – assess the relationship between the Arctic populations of *Sclerolinum contortum* and *Nicomache lokii*, and populations in other oceans, 4 – reassess the links between the annelid

fauna of Loki's Castle Vent Field and vent faunas of other oceans, and 5 – evaluate which environmental factors may be driving the habitat-specificity and distributions of the studied species.

The new species of Ampharetidae from Loki's Castle were formally described as *Pavelius smileyi* sp. nov. and *Paramytha schanderi* gen. et sp. nov. Phylogenetic reconstructions and inference of ancestral habitats revealed that adaptation to CBEs has happened multiple times independently within Ampharetidae. Multiple independent colonisations of CBEs within a family is unusual, but may be more common in heterotrophic taxa. The habitat transitions recovered were both from seep to vent and vent to seep, which contradicts the notion of gradual adaptation into more and more extreme habitats, with hydrothermal vents considered the most extreme. Sedimented vents were involved in two of the three transitions inferred, which supports the hypothesis that sedimented vents are important in linking vents and seeps, and a novel link between organic falls and sedimented vents was also shown in a clade comprising the genera *Paramytha* and *Decemunciger*.

Both *Sclerolinum contortum* and *Nicomache lokii* were shown to be distributed all the way from the Arctic to the Antarctic, which is the widest geographic range of animals from CBEs known to date. This corroborates findings by other authors indicating that wide geographic ranges might not be unusual for annelids from CBEs. *S. contortum* shows a stronger geographic structure in the haplotype networks than *N. lokii*, but whether this is due to different dispersal capacities or reflects the geographic isolation of the sampled localities is unclear. Two distinct mitochondrial lineages of *N. lokii* are present in the Antarctic, which may be the result of two independent colonization events. The wide ranges observed in these species may be facilitated by their ability to colonize different types of CBEs, and it is likely that population connectivity is maintained through presently unknown populations.

The presence of taxa at LCVF belonging to genera common at Pacific vents such as *Amphisamytha* and *Nicomache*, led to the hypothesis that the fauna at LCVF was

partly formed by migrations from the Pacific. However, the results presented here show that ampharetid species from LCVF belong to globally distributed clades and have no clear geographic affinities. In addition, the wide distributions of *Sclerolinum contortum* and *Nicomache lokii* indicate a higher degree of connectivity between Arctic and Atlantic CBEs than previously recognized.

Although most ampharetids are specific to one type of CBE, a review of the habitat-use of ampharetid species showed that they are quite flexible in terms of substratum, temperature and fluid flux. Depth and biological interactions may play a role in determining the habitat specificity and distributions of ampharetids, but we will probably find more examples of ampharetids inhabiting multiple CBEs in the future. Observations on the environmental conditions inhabited by *Sclerolinum contortum* and *Nicomache lokii* indicates that *S. contortum* may be able to occupy areas of lower sulphide levels, but is limited by high temperatures. On the other hand, *N. lokii* seems to be more temperature tolerant, but may require higher levels of sulphide. These findings support the notion that environmental factors varying across habitats, such as fluid flux, are important in shaping the faunal composition of CBEs.

The results presented in this thesis shows that there is still a lot of undescribed biodiversity in CBEs, and illustrates the need for integrative taxonomic work. The importance of comparing across habitats and geographic regions is also demonstrated, and future collaborative projects will hopefully enable a better understanding of large scale patterns and the underlying processes in CBEs

List of publications

Paper I

Kongsrud, J.A., Eilertsen, M.H., Alvestad, T., Kongshavn, K. & Rapp, H.T. (2017) New species of Ampharetidae (Annelida: Polychaeta) from the Arctic Loki Castle vent field. *Deep Sea Research Part II Topical Studies in Oceanography*, **137**: 232-245. https://doi.org/10.1016/j.dsr2.2016.08.015

Paper II

Eilertsen, M.H., Kongsrud, J.A., Alvestad, T., Stiller, J., Rouse, G.W., Rapp, H.T. (2017) Do ampharetids take sedimented steps between vents and seeps? Phylogeny and habitat-use of Ampharetidae (Annelida, Terebelliformia) in chemosynthesis-based ecosystems. *BMC Evolutionary Biology,* **17:** 222. https://doi.org/10.1186/s12862-017-1065-1

Paper III

Georgieva, M. N., Wiklund, H., Bell, J. B., Eilertsen, M. H., Mills, R. A., Little, C. T. S., & Glover, A. G. (2015). A chemosynthetic weed: the tubeworm *Sclerolinum contortum* is a bipolar, cosmopolitan species. *BMC Evolutionary Biology*, **15**: 1-17. https://doi.org/10.1186/s12862-015-0559-y

Paper IV

Eilertsen, M.H., Georgieva, M.N., Kongsrud, J.A., Wiklund, H., Glover, A.G. Rapp, H.T. Genetic connectivity from the Arctic to the Antarctic: *Sclerolinum contortum* and *Nicomache lokii* (Annelida) are both widespread in reducing environments. Manuscript submitted to *Scientific Reports**.

*The version included here has been formatted to match the thesis, and figures and tables have been embedded in the text for readability.

1. Introduction

1.1 Chemosynthesis based ecosystems

In the deep sea, below 200 m, there is no sunlight, and no photosynthetic primary production. The deep sea in general is therefore food limited, and most deep-sea organisms are dependent on nutrient input from surface waters. The level of nutrient input decreases with depth, and both the density and average body-size of fauna decreases accordingly (Rex et al., 2006). Considering these characteristics of the deep sea, it came as a big surprise when high densities of large bivalves and tubeworms were discovered at 2600 m depth around hydrothermal vents on the Galapagos Ridge (Lonsdale, 1977).

Hydrothermal vents are areas where heated seawater, enriched in reduced compounds such as hydrogen sulphide (H_2S), streams out of the seafloor (Van Dover, 2000). It was soon discovered that the fauna at the hydrothermal vents get their energy from a different kind of primary production; microbial chemosynthesis (Rau & Hedges, 1979). The primary producers at hydrothermal vents are bacteria and archaea that utilize energy from the reduced compounds in the hydrothermal fluids to produce biomass (Jannasch & Wirsen, 1979). The chemosynthetic microorganisms form the basis of the food-web, and are found both free living, and as symbionts of metazoans (Cavanaugh et al., 1981). Shortly after the first discovery of hydrothermal vent ecosystems, similar high-density assemblages of animals were discovered around methane seeps (Paull et al., 1984), and later also at organic falls such as whale carcasses and sunken wood (Smith et al., 1989; Bienhold et al., 2013). Cold seep and organic fall ecosystems have in common with hydrothermal vents that they are based on chemosynthetic primary production, and these are collectively termed chemosynthesis-based ecosystems (CBEs).

There are some additional habitats that host chemosynthetic primary production, such as oxygen minimum zones (OMZs; Tunnicliffe et al., 2003) and seagrass beds

(Stewart & Cavanaugh, 2006). However, in this thesis the discussion on CBEs will be restricted to deep-sea habitats (below 200 m), and OMZs will not be covered as these habitats do not show the high level of endemicity characteristic of other CBEs (Levin et al., 2010).

1.2 Abiotic characteristics of CBEs

Hydrothermal vents

Hydrothermal vents occur in seafloor spreading centres along plate boundaries (mid-ocean ridges and back-arc spreading centres), but also on mid-plate seamounts, which are located above mantle hot-spots (Van Dover, 2000). Initially, hydrothermal venting was believed to occur only on fast-spreading ridges, but this was proven wrong by the discoveries of vents on the slow spreading Mid-Atlantic Ridge (MAR; Rona et al., 1986) and later on the ultraslow spreading Arctic Mid-Ocean Ridge (AMOR; Pedersen et al., 2010) and Indian Ocean Ridge (IOR; Copley et al., 2016). Individual vent fields are ephemeral in nature, but the longevity can vary by several orders of magnitude, from tens of years at fast-spreading ridges, to tens of thousands of years at slow-spreading ridges (German & Parson, 1998).

Although the vent fluids supply the reduced compounds that sustain life at hydrothermal vents, they also have properties that make the vent habitat challenging to live in. The vent fluids can reach temperatures of up to 400°C (Connelly et al., 2012), have divergent pH values from ambient seawater [from very acidic (pH 1 at Kemp Caldera; Cole et al., 2014) to very alkaline (pH 11 at Lost City; Kelley et al., 2005)], low oxygen content, and they contain toxic elements such as hydrogen sulphide and high levels of heavy metals (Nakamura & Takai, 2014). The temperature of the fluids, however, decreases rapidly away from the vent edifice, and vent fields usually have areas of diffuse flow, where the temperatures are considerably lower. Most vent animals occupy a temperature range between ambient seawater temperatures up to around 20 °C (Sen et al., 2013). The most heat-tolerant vent animal known is the

annelid worm *Alvinella pompejana*, which always lives close to the vent edifice and can tolerate temperatures well above 40 °C (Ravaux et al., 2013). H_2S, in addition to supplying energy for chemosynthesis, is also a toxic chemical. Animals living at hydrothermal vents have different adaptations for dealing with H_2S toxicity, either by avoiding absorbing the chemical through behavioural adaptations or structural modifications of the body surface, or by developing a tolerance of higher internal H_2S concentrations (Tobler et al., 2016). Vent animals are also able to tolerate heavy metals by using metal-binding proteins to detoxify ingested metals (McMullin et al., 2007). All of these adaptations probably come at a high energetic cost, but judging by the incredible densities of animals clustering around vents, the access to nutrients through chemosynthesis outweighs the cost of the adaptations (Tobler et al., 2016).

Hydrothermal vents come in many forms, with different environmental characteristics. The majority of hydrothermal vents on mid-ocean ridges are dominated by bare-rock substrata, but in some areas, vents also occur in sedimented settings (Pedersen et al., 2010; Bernardino et al., 2012; Portail et al., 2015). When vent fluids interact with the sediment, it leads to increased levels of methane (CH_4), ammonium (NH_4^+), hydrocarbons and increased pH (Baumberger et al., 2016). One locality on the Costa Rica margin has been reported to have a mix of low temperature venting of hydrothermal origin and methane seepage, and was thus designated a "hydrothermal seep" (Levin et al., 2012). Another very unique type of vent system are serpentinite-hosted vents, with relatively low temperature venting (<90 °C) of highly alkaline fluids driven by subsurface exothermic reactions between seawater and mantle peridotite (Kelley et al., 2005).

Cold seeps

In contrast to hydrothermal vents, cold seeps are usually found along continental margins, and in sedimented settings. Cold seeps are areas where hydrocarbon-rich fluids or gases seep out of the seafloor at temperatures near the ambient seawater (Van Dover, 2000). Seeps sometimes have increased temperatures compared to the

surrounding seawater, but usually not more than around 5 °C above background temperatures (LaBonte et al., 2007; Levin et al., 2012). Bacterial breakdown of CH_4 in the sediments generates H_2S, and fauna at seeps can host either methanotrophic (methane-oxidizing) or thiotrophic (sulphide-oxidizing) symbionts (Tunnicliffe et al., 2003). Seeps can have special features such as hypersaline brine pools, pockmarks from rapid gas expulsions, mud volcanoes, carbonate rocks or gas hydrates (Cordes et al., 2010). Carbonate rocks are produced by anaerobic methane oxidizing microbes, and provides a hard substratum that can increase biodiversity at a seep site (Levin et al., 2015).

Levels of H_2S are usually lower at seeps than at hydrothermal vents, and seep fluids do not have the high levels of heavy metals that vents have. However, there are other physiological challenges at seeps, such as hypersaline brines, crude oil and anoxic sediments (McMullin et al., 2007). The fluid flow at cold seeps is considered to be more stable and long-lasting than at hydrothermal vents (Sibuet & Olu, 1998), but on a smaller spatial scale there are shifts in the flow patterns causing one patch of chemosynthesis-based fauna to die out and a new community to establish at new seepage sites (Jollivet et al., 1990).

Organic falls

Large parcels of organic matter such as dead cetaceans, pieces of wood or kelp provide patches of high nutrient input to the deep sea. Organic falls of terrestrial origin or from kelp forests are naturally more common close to the continents, and the same is true for smaller cetaceans, but some of the great whales have a more oceanic distribution and can provide falls to the abyssal plains (Smith et al., 2015). The bacterial breakdown of organic falls generates H_2S and CH_4, which forms the basis for chemosynthetic primary production (Treude et al., 2009; Bienhold et al., 2013). Natural organic falls are rare to come upon in the deep sea, but numerous deployment experiments have been undertaken to explore the breakdown and colonization of organic falls (e.g. Bienhold et al., 2013; Cunha et al., 2013; Hilario et

al., 2015). Evidence from these experiments indicates that the organic input needs to be of a certain size to generate sufficiently sulfidic conditions to support a chemosynthesis-based community (Cunha et al., 2013). The size of the fall also determines the longevity of the habitat, and carcasses of great whales have been shown to support chemosynthesis-based communities for decades (Smith et al., 2002). Wood falls are also believed to last for decades before they are completely consumed (Bienhold et al., 2013), which makes the longevity of large organic falls comparable to hydrothermal vents on fast-spreading ridges.

1.3 Habitat endemism

A large proportion of the fauna of CBEs is habitat endemic, meaning that they are only found in these habitats. In a global dataset of vent fauna, 85% of species were never recorded outside the vent habitat (Wolff, 2005), while in cold seeps the degree of endemism is lower (e.g. 50% in Levin et al., 2010). In a colonization experiment in the Atlantic, using cow carcasses to mimic whale falls, 18 of 33 species were considered organic fall specialists [corrected to also include "*Amphisamytha* cf. *lutzi*" which was later described as a bone specialist belonging to the genus *Paramytha*, Queirós et al. (2017)] and three species were known from vents or seeps (Hilario et al., 2015). This gives an overall endemism of 54%, if one considers all organic falls as one habitat type. Some species in CBEs are very specialized, and may only occur in a specific temperature zone of hydrothermal vents (e.g. alvinellids; Levesque et al., 2003; Fontanillas et al., 2017), while others are able to inhabit a multitude of reducing habitats, including both vents, seeps and falls (Black et al., 1997). Non-specialized fauna (background fauna) is usually found in the fringes of the habitats, where environmental conditions are more hospitable (Levin, 2005).

CBE-endemism is probably a product of physiological tolerance to the conditions in CBEs and trophic dependence on chemosynthesis, either directly through chemosynthetic symbionts or indirectly through, for example, bacterivory. It is easy

to understand the habitat endemism of symbiotrophic organisms, which have reduced or absent digestive tracts, and are completely reliant on nutrients from chemosynthetic symbionts (Childress & Fisher, 1992). It is less obvious why heterotrophic organisms are restricted to CBEs, but one explanation could be that the energetic cost of the physiological adaptations to the conditions of CBEs makes them dependent on the abundant food available in CBEs. One factor that may reinforce habitat specificity is settlement cues that enable larvae to recognize suitable habitats to settle in (Adams et al., 2012). There are examples of species which are found at very high densities in one CBE, but also occur in lower densities at other CBEs or in the background fauna (Smith & Baco, 2003). These species may be specialized to the habitat where they are most abundant, although they are not completely endemic. There is a clear effect of depth on the degree of endemism in all CBEs. Hydrothermal vents, cold seeps and organic falls all have a much lower degree of habitat endemics when found in depths of less than 300 m (Levin, 2005; Tarasov et al., 2005; Smith et al., 2015). This has been suggested to be due to higher food abundance outside the CBEs in this zone, and thus lower evolutionary pressure to develop complex adaptations (Tarasov et al., 2005).

There are many higher taxa (genera, families) shared among different CBEs (vents, seeps, falls), indicating a strong evolutionary link between them, but until now there has been few species recorded from multiple habitat types (Wolff, 2005). In addition to habitat specific factors such as temperature and heavy metal toxicity, it has been suggested that factors varying across habitats, such as fluid flux, substratum availability and depth may be important in affecting the faunal composition of CBEs (Watanabe et al., 2010; Bernardino et al., 2012; Portail et al., 2015). In areas where vents and seeps occur in close proximity at similar depths and in sedimented settings, there can be a high degree of overlap in fauna (Watanabe et al., 2010; Portail et al., 2015). In contrast, high variability has been demonstrated between hydrothermal vent communities in close proximity, but in different geological settings (Goffredi et al., 2017). Given the wide variation in physiochemical characteristics within each

category of CBEs, and the existence of “intermediate” habitats such as sedimented hydrothermal vents and hydrothermal seeps, it has been suggested that CBEs should be considered a continuum of reducing conditions, rather than completely distinct phenomena (Levin et al., 2012). In light of these findings it is almost surprising that there are not more species found in multiple types of CBEs, but sampling of CBEs is still patchy, and these numbers may increase as more habitats are thoroughly sampled.

1.4 Diversity and ecology

CBEs have low levels of biodiversity compared to the surrounding deep sea. Low diversity, mainly caused by very low evenness with a few very dominant species, is typical of habitats with high levels of productivity (Van Dover, 2000). Within CBEs, diversity decreases towards the areas with highest concentration of reduced chemicals (e.g. Portail et al., 2015; Bell et al., 2016), most likely due to the increased physiological stress, which requires special adaptations. Cold seeps have higher diversity than hydrothermal vents, and it has been suggested that this is due to the higher stability of seepage, but a comparison of diversity at vent and seep sites concluded that it is more likely that diversity is higher at seeps due to a lower physiological threshold to colonizing the seep habitat (Turnipseed et al., 2003). Whale falls can harbour very high levels of species richness (Baco & Smith, 2003), although the diversity seems to vary with the age of the carcass (Hilario et al., 2015). The high richness of whale fall communities may be related to the substratum availability (both hard substratum provided by the fall itself, and organically enriched sediments around the whale fall) and high trophic diversity (Hilario et al., 2015). The distance between habitats is probably an important factor influencing the biodiversity, because more isolated habitats will have a lower degree of larval colonization from other localities, and thus higher extinction rate. For example, the shorter-lived, but more closely spaced vent fields of the East Pacific Rise (EPR) have a higher diversity than the more stable, but more isolated vent fields on the MAR (Van Dover, 1995).

Within CBEs there are strong gradients of environmental conditions such as temperature, concentrations of reduced chemicals and oxygen levels. These environmental gradients commonly lead to a zonation pattern with characteristic fauna in each zone. As the conditions change over time, for example due to a decreasing rate of fluid flow, a succession pattern in the fauna can be observed (e.g. Smith et al., 2002; Cordes et al., 2005; Sen et al., 2014). When the flow of vent or seep fluid is initiated at a given site, the first organisms colonizing the site will be those which are able to tolerate the high-flow conditions (very hot, sulphide rich fluids at hydrothermal vents), and are able to get to the new site quickly, either by motile adults or larvae with good dispersal potential (Sen et al., 2014). As flow diminishes these will be gradually replaced by species preferring more diffuse flow conditions, and when the flow dissipates completely, background fauna will take over (Cordes et al., 2005; Sen et al., 2014). The patchy spatial distribution of fluid conduits with various flow intensities at seeps and within vent fields, generates a complex mosaic of microhabitats.

At whale falls, succession goes through at least three stages; 1 – an initial mobile-scavenger stage, where large, motile organisms such as fish and crustaceans remove the soft tissue from the bones, 2 – an enrichment-opportunist stage, where heterotrophic organisms form a dense assemblage on the bones and in the enriched sediments around it, 3 – a sulfophilic stage, where bacterial breakdown of tissue and bone lipids generates sulphide, which forms the basis for chemosynthesis (Smith et al., 2015). The breakdown of the bones is enhanced by “bone-eating” worms in the genus *Osedax*, which secrete acid to burrow into the bones, and have heterotrophic bacterial symbionts that degrade organic compounds inside the bones (Rouse et al., 2004). There may also be a fourth stage after the sulfophilic stage, the reef stage, where suspension feeders take advantage of the hard substratum provided by the bones (Smith & Baco, 2003). Wood falls follow a similar succession pattern, although since wood is not as easily digested as the flesh of whale falls, the initial stage of colonization of wood falls has a number of specialized taxa that are able to feed on

wood, such as wood-boring bivalves and wood-feeding urchins or amphipods (Bienhold et al., 2013; Tandberg et al., 2013).

Since CBEs are extreme and variable habitats, it has often been assumed that physical conditions alone are structuring the fauna (e.g. Luther et al., 2001). The understanding of biotic interactions at deep-sea CBEs has been hampered by the difficulty of performing detailed observations and experiments in these remote habitats. Even so, experimental manipulations have demonstrated that predation, for example by fish or crabs, has an effect on the relative abundance of smaller invertebrates at hydrothermal vents (Micheli et al., 2002). Studies of spatial distributions, body size and stable isotopes have shown that competition can lead to food resource partitioning in heterotrophic vent taxa, for example alvinellid worms (Levesque et al., 2003) and gastropods (Govenar et al., 2015). It has also been shown that structure-forming animals are important in facilitating other species (Cordes et al., 2005). Although this field of study is in the early stages still in CBEs, it is clear that the distribution of fauna within CBEs is not only shaped by physical parameters, but also by biological interactions.

1.5 Evolutionary history of CBE-adapted fauna

Many specialized taxa have diversified within CBEs, and whole genera or even families may be exclusively found in these habitats (Van Dover et al., 2002). Over the last decades, a number of phylogenetic studies have elucidated the evolutionary histories of fauna from CBEs. Many of these studies support a stepping-stone mode of evolution, with a gradual adaptation to more extreme habitats (e.g. Distel et al., 2000; Schulze & Halanych, 2003; Decker et al., 2012). The most famous example of this is found in the bathymodiolin mussels, which evolved from wood-dwelling ancestors and made several transitions to cold seeps and hydrothermal vents (the "wooden steps to deep-sea vents" hypothesis; Distel et al., 2000; Thubaut et al., 2013). A similar pattern has been found in several other taxa, with either organic falls or seeps

functioning as evolutionary stepping-stones into the vent habitat (Schulze & Halanych, 2003; Decker et al., 2012; Roterman et al., 2013).

Recently, a biogeographic network analysis of the global mollusc fauna in CBEs revealed that all links in the network between bare rock vents and cold seeps went through sedimented vents (Kiel, 2016). The analysis was based on genus-level data, and indicates that sedimented vents may play an important role in the evolutionary history of vent and seep fauna, perhaps as an evolutionary stepping stone between bare-rock vents and cold seeps. However, the role of sedimented vents as an evolutionary stepping-stone has not been assessed in a phylogenetic framework. The same study also found that organic falls only showed a very weak link to vents and seeps, which would indicate that they are less important as evolutionary stepping-stones (Kiel, 2016). However, the data included on organic falls was limited, and it has been debated whether it is possible to draw any conclusions with regards to the evolutionary role of organic falls based on this study (Kiel, 2017; Smith et al., 2017).

1.6 Biogeography

There have been numerous attempts at inferring a biogeographical model for the global hydrothermal vent fauna, and the model has been gradually expanded to include new regions as these were discovered (e.g. Van Dover et al., 2001; Rogers et al., 2012). However, the clustering approach employed in most of these studies has some methodological weaknesses, and it has been problematic to reach a consensus regarding the number of biogeographic provinces (see Rogers et al., 2012). The application of a network approach resolved some of these problems, and supported a biogeographic model for hydrothermal vent fauna with five biogeographical provinces: East Pacific Rise (EPR), Northeast Pacific (NP), Western Pacific (WP), Indian Ocean (IO) and Mid-Atlantic Ridge (MAR) (Moalic et al., 2012). However, this analysis did not include the high latitude vent fields in the Arctic and Antarctic, which may comprise additional biogeographic provinces (Pedersen et al., 2010; Rogers et al.,

2012). The network analysis by Moalic et al. (2012) recovered the Western Pacific as most central in the network, which may imply that this region played an important role in the early evolution of hydrothermal vent fauna, followed by a global diversification.

Most of the biogeographic analyses published have focused on hydrothermal vent fauna only, but given the close relationship between hydrothermal vent fauna and the fauna of other CBEs (cold seeps and organic falls) it is probably artificial to treat the biogeography of these habitats separately. The only biogeographical analysis to date including all CBEs was the network analysis by Kiel (2016). This analysis recovered eight provinces: 1 - IO, 2 - WP, 3 - the Juan de Fuca Ridge, 4 - the EPR plus the Galapagos Ridge, 5 - the MAR plus the East Scotia Ridge, 6 - NE Pacific back-arc basin vents plus seeps from the same region, 7 - seeps in the Atlantic Equatorial Belt, 8 - seeps in the Mediterranean Sea (see Figure 1.1). In general, hydrothermal vents showed much stronger connectivity to one another, while seeps and organic falls were much more weakly linked (Kiel, 2016). The Artic CBEs were only represented by the shallow hydrothermal vents on the Mohns Ridge and the Håkon Mosby Mud Volcano (see section on Arctic CBEs below), and these showed only very weak connections both to one another and to other sites (the closest site was the Ghost City serpentinazion vent in the Atlantic). It should be pointed out that the analysis by Kiel (2016) only included data on molluscs (bivalves and gastropods), and analyses including other prominent CBE-taxa, such as annelids, may reveal different patterns.

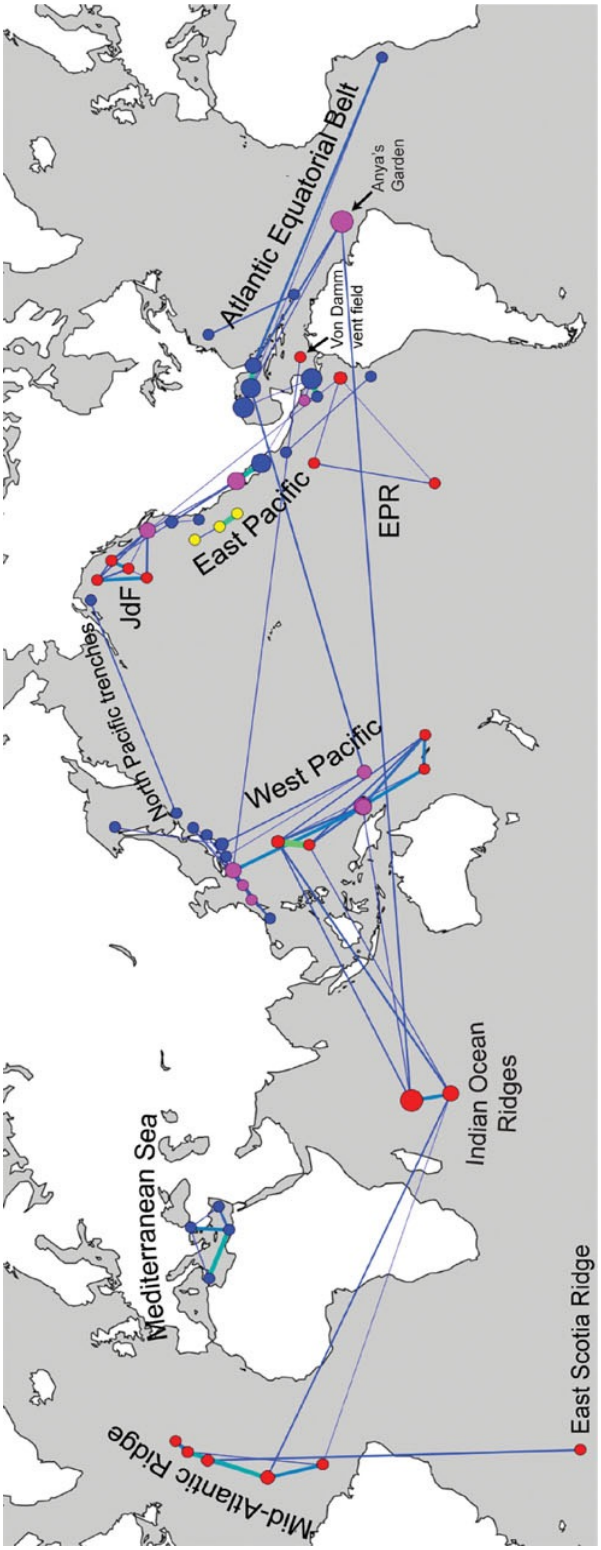

Figure 1.1. Biogeographic network of fauna from deep sea CBEs at a threshold of 0.7 (unconnected nodes at this threshold are not included). Nodes are coloured by habitat: blue – cold seep, purple – sedimented hydrothermal vent/hydrothermal seep, red – bare-rock hydrothermal vent, yellow – whale fall. The thickness of the links represents their weight in the network based on the Bray-Curtis dissimilarity index. Abbreviations: EPR – East Pacific Rise, JdF – Juan de Fuca Ridge. Figure reprinted from Kiel (2016) with permission from the author.

There are several issues preventing a good understanding of the biogeographic patterns of CBEs as of today. Firstly, the sampling of CBEs is still patchy and biased, both in terms of geography and habitat. The East Pacific is probably the best sampled geographic area, in part because hydrothermal vents were first discovered in this region, but also due to the geographic proximity to prominent scientific institutions. On the other hand, CBEs at high latitudes in the Arctic and the Antarctic were only discovered in the last decade (Pedersen et al., 2010; Rogers et al., 2012), and the fauna of CBEs in these regions is still incompletely known. Secondly, there is a bias in the sampling coverage of habitats, for example organic falls are still very under sampled, and the data available is dominated by samples from the East Pacific (Smith et al., 2017). Lastly, there is still a lot of work to be done on the taxonomy of CBE-fauna, and the description of synonymous species in different habitats or geographic regions may confound biogeographic patterns (Vrijenhoek, 2009; Teixeira et al., 2013).

1.7 Dispersal and connectivity

Given the fragmented distribution of CBEs, the animals endemic to these habitats have to disperse across areas of unsuitable habitat to colonize new habitats and maintain connectivity between populations. Adding to that the ephemeral nature of these habitats, especially the short lived hydrothermal vents on fast spreading ridges and organic falls, it was recognized early on that dispersal had to be important for the fauna inhabiting them (Corliss et al., 1979). Many of the invertebrates that are obligate to CBEs are sessile as adults, and they mainly disperse in the larval stage. The dispersal capacity of marine species is often inferred indirectly, for example by larval characteristics such as feeding mode or pelagic larval duration (PLD), but there is an increasing recognition that larval characteristics are not good predictors of realized dispersal (Weersing & Toonen, 2009; Vrijenhoek, 2010). CBE-adapted species with planktotrophic larvae that are able to disperse in surface waters, such as bivalves in the genus *Bathymodiolus* spp. (Won et al., 2003; Faure et al., 2015) or shrimp in the

genera *Alvinocaris*/*Rimicaris* (e.g. Teixeira et al., 2011; Teixeira et al., 2013), can maintain genetic connectivity over large geographic distances. However, the classical view that animals with lecithotrophic larvae have a limited dispersal potential compared to those with planktotrophic larvae is not supported by measures of gene flow based on genetic markers (Vrijenhoek, 2010). Species with lecithotrophic larvae may prolong their pelagic larval duration (PLD), and thus improve their dispersal potential, by arrested development [for example *Alvinella pompejana*, Pradillon et al. (2001)] or by having very large yolk reserves [for example *Branchipolynoe* spp., Jollivet et al. (1998)]. Combining a good knowledge of larval biology and regional current patterns, it is possible to infer how far a species can disperse (e.g. Marsh et al., 2001), but unfortunately the information available on larval biology is very limited for most taxa.

Genetic divergence between populations is often used as a proxy for the degree of dispersal between them. Most of the population genetic studies on CBE-inhabiting species has been performed on hydrothermal vent taxa, and the vents along the EPR and Galapagos Ridge have been particularly well studied. Hydrothermal vents on mid-ocean ridges are distributed in a linear fashion, and vent animals disperse in a stepping-stone pattern along the ridge, with higher levels of dispersal between adjacent vents (Vrijenhoek, 2010). This is expected to generate a pattern of positive correlation between genetic and geographic distance (isolation by distance; IBD, Audzijonyte & Vrijenhoek, 2010b). However, along-ridge dispersal may be disrupted by geographic barriers such as lateral offsets of ridge axes, gaps in the distribution of vents or cross-axis currents (Hurtado et al., 2004; Jang et al., 2016). The degree to which species are affected by such dispersal barriers depends on reproductive characteristics such as egg size, buoyancy and larval mode (Plouviez et al., 2009). It is important to note that gaps in the sampling scheme (unsampled populations) can give a false impression of barriers to gene flow (Audzijonyte & Vrijenhoek, 2010b). Cold seeps, organic falls and hydrothermal vents in back-arc settings have a more complex spatial distribution. Predicting the level of gene flow between these is not as

straightforward as on a linear mid-ocean ridge, and requires detailed knowledge about the regional current systems (e.g. Mitarai et al., 2016).

1.8 CBEs of the Arctic Mid-Ocean Ridge and the Nordic Seas

The Nordic Seas comprise the ocean basins between Iceland to the south and Svalbard to the north (Figure 1.2). The deep basins of the Nordic Seas are isolated from the Atlantic by the Greenland-Iceland-Faroes ridge (GIF-ridge), which has a deepest point at around 600 m in the Denmark Strait between Iceland and Greenland (Hjartarson et al., 2017). The main current patterns across the GIF-ridge consists of a shallow, northward inflow of relatively warm water from the Atlantic, and a southward overflow of cold, deep water that feeds the global thermohaline circulation (Hansen & Østerhus, 2000). The southward flow of deep water forms an additional barrier to immigration from the deep Atlantic, and the fauna of the deep Nordic Seas is characterised by high degrees of endemism (Svavarsson et al., 1993; Stuart & Rex, 2009).

The Arctic Mid-Ocean Ridge (AMOR) is a northward extension of the MAR, but Iceland poses a barrier between the MAR and AMOR at around 65°N. Hydrothermal venting on the AMOR occurs at shallow depths in the Kolbeinsey and Grimsey vent fields near Iceland (~100 m; Fricke et al., 1989), the Seven Sisters vent field on the northern Kolbeinsey Ridge (140 m; Olsen et al., 2016) and the Jan Mayen vent field on the Mohn Ridge (500-750 m; Schander et al., 2010b). However, the faunal composition of these vent fields is dominated by background fauna with only very few vent specialists (Olsen et al., 2016). In 2008 a deeper vent field, named Loki's Castle, was discovered at 2350 m depth in the junction between the Mohn and Knipowich Ridges (Figure 1.2), which showed a rich and endemic vent fauna (Pedersen et al., 2010). The Loki's Castle Vent Field (LCVF) has four black smoker chimneys, and also an area with diffuse, low temperature venting and unique barite chimneys (Steen et al., 2015). The vent field is influenced by sediments from the Bear Island sediment fan, and there is a clear

signature of sedimentary influence on the vent fluids, which have high alkalinity and also high concentrations of ammonium, hydrogen and methane (Baumberger et al., 2016).

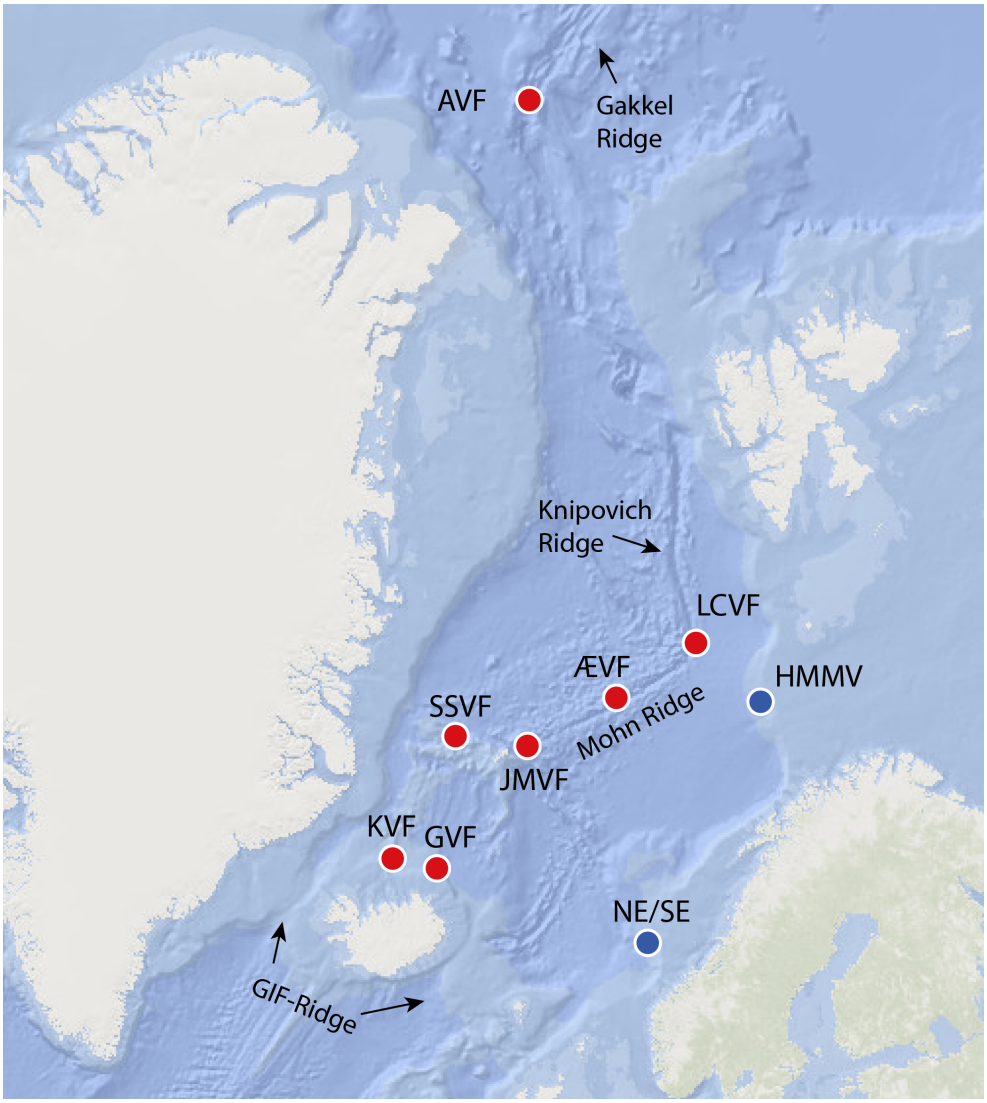

Figure 1.2. Map of the CBEs on the Arctic Mid-Ocean Ridge and in the Nordic Seas. Hydrothermal vents are indicated with a red circle, and cold seeps with a blue circle. Localities are abbreviated as follows: AVF – Aurora Vent Field, GIF-Ridge – Greenland-Iceland-Faroes Ridge, GVF – Grimsey Vent Field, HMMV – Håkon Mosby Mud Volcano, JMVF – Jan Mayen Vent Field, KVF – Kolbeinsey Vent Field, LCVF – Loki's Castle Vent Field, NE – Nyegga seeps, SE – Storegga seeps, SSVF – Seven Sisters Vent Field, ÆVF – Ægir Vent Field. The map was generated using the Ocean Basemap from ESRI.

The most abundant CBE-endemic fauna at LCVF includes the amphipod *Exitomelita sigynae* (Tandberg et al., 2012), the siboglinid worm *Sclerolinum contortum*, the maldanid worm *Nicomache lokii* (Kongsrud & Rapp, 2012), two species of ampharetids, one of which was originally believed to belong to the genus *Amphisamytha*, and two small gastropod species (*Pseudosetia griegi* and *Skenea* sp.; Pedersen et al., 2010, see Figure 1.3). Annelida is the most diverse taxon at LCVF in terms of CBE-adapted species, with 14 species, of which most are new to science (J.A. Kongsrud, pers. comm.). A complete faunal inventory of the LCVF has not yet been published, but initial data indicates that the fauna shows similarities to nearby cold seeps at Håkon Mosby Mud Volcano (HMMV) and Nyegga and to vent sites in the Pacific (Pedersen et al., 2010). In 2015, the Ægir vent field was discovered at 2200 m on the central Mohn Ridge, and based on video footage the fauna seems to have some similarities to LCVF, but without the sedimentary areas with polychaetous mats found at LCVF (Olsen et al., 2016). There is also hydrothermal venting further north on the Gakkel Ridge, and a video survey showed abundant biological activity in a location named the Aurora vent field (Edmonds et al., 2003), but the faunal composition of this field has not been documented yet.

The HMMV is located quite close to the LCVF, at 1270 m depth in the southwestern Barents Sea (Figure 1.2). The mud volcano has methane seepage, and also features abundant methane hydrates and a somewhat elevated temperature in the sediments (Ginsburg et al., 1999; Perez-Garcia et al., 2009). The most abundant species at the HMMV are the siboglinid worms *Sclerolinum contortum* and *Oligobranchia haakonmosbiensis* (Smirnov, 2000; Gebruk et al., 2003), and recently *Nicomache lokii* was also recorded from this locality (this thesis). The remaining animals at the HMMV are also present in the background fauna, but are found at increased densities in the mud volcano (Gebruk et al., 2003). Further south in the Norwegian Sea two additional cold seep sites are found; the Storegga Slide and Nyegga Area. These are located at around 730-740 m depth, and the fauna at these sites are dominated by the same two

species of siboglinids as at HMMV (Van Gaever et al., 2010; Błażewicz-Paszkowycz & Bamber, 2011).

There is not much information about the fauna of organic falls in the Arctic. A colonization experiment using a whale carcass that was sunk to about 125 m in a Swedish fjord, was colonized by a species of the “bone-eating” worm genus *Osedax* (Siboglinidae), but no other fauna associated with the whale fall was reported from the experiment (Glover et al., 2005). A wood fall in a Norwegian fjord (around 660 m depth) was found to harbour the wood-burrowing bivalve *Xylophaga dorsalis* and the siboglinid *Sclerolinum brattstromi*, which was lining the burrows made by the bivalve (Schander et al., 2010a). Although both of these falls were colonized by organisms that rely on chemosynthetic symbionts, the shallow depth and sheltered fjord habitat in which they were located would probably limit any colonization by vent and seep fauna. A wood fall recovered from 2800 m depth near the LCVF was found to harbour a new species of amphipod in the genus *Exitomelita*, of which the only other species was described from the LCVF (Tandberg et al., 2013). The fall was also colonized by *Pseudosetia griegi* and *Skenea* sp., the same two gastropods that have been reported from the LCVF and the Jan Mayen vent field (Tandberg et al., 2013).

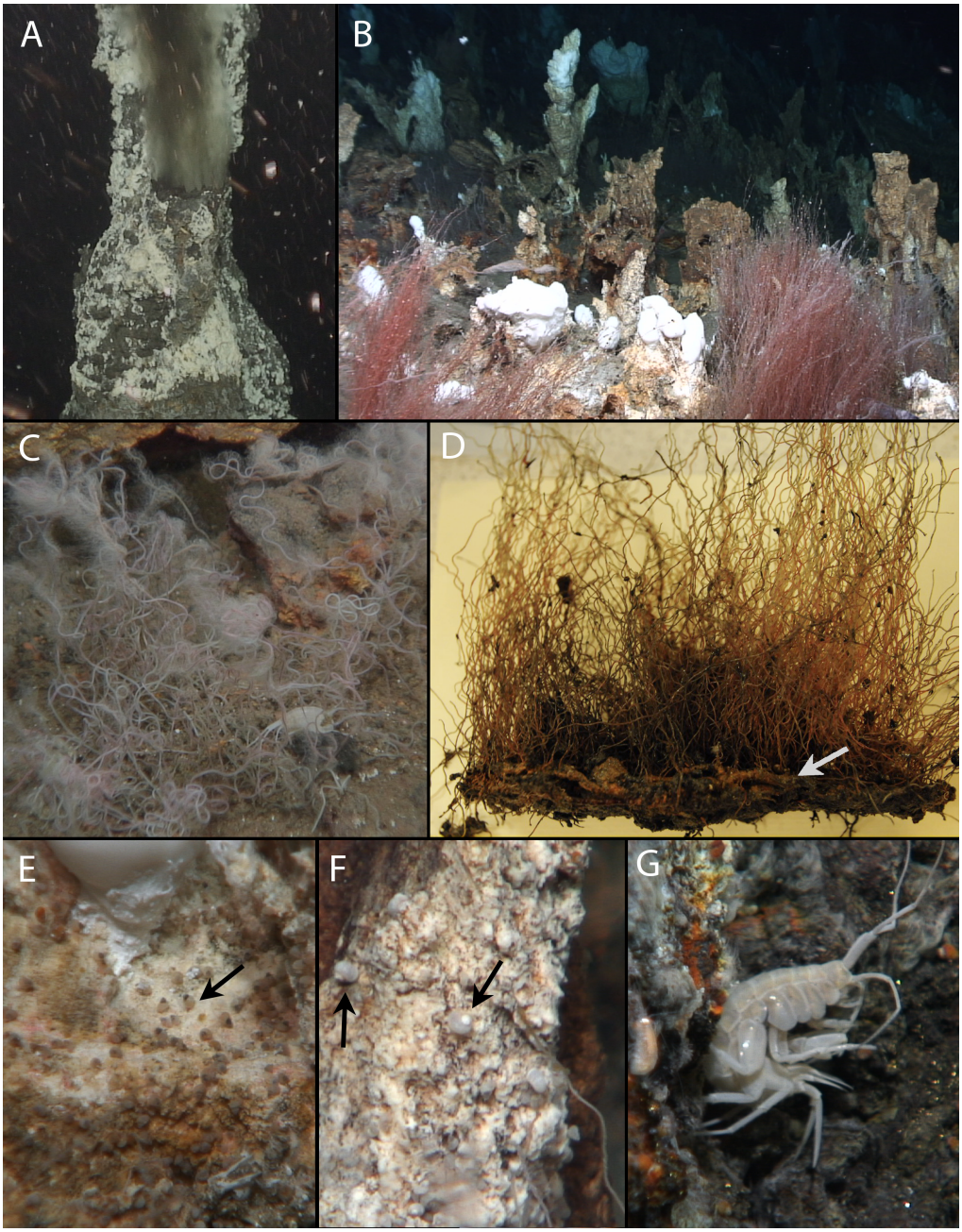

Figure 1.3. Dominant fauna of Loki's Castle Vent Field. A – black smoker chimney, B – diffuse flow barite-field with "bushes" of *Sclerolinum contortum* in the foreground, C – close-up of *S. contortum*, tubes are covered by bacterial filaments, D – polychaetous mat from the barite field, the arrow indicates tubes of *Nicomache lokii* at the base of the mat, E – *Pseudosetia griegi*, arrow indicates one of the snails, F – *Skenea* sp., two snails are indicated with arrows, G – *Exitomelita signyae*. Images: Centre for Geobiology/K. G. Jebsen Centre for Deep Sea Research.

1.9 Study taxa

Annelid worms are one of the most diverse and most iconic animal groups in CBEs, and has been the focus of a large amount of research over the last decades. Yet, most of the studies published to date have been centred around a few annelid taxa, such as the large and enigmatic vestimentiferans (e.g. Marsh et al., 2001; Coykendall et al., 2011), the "bone-eating" *Osedax* (e.g. Vrijenhoek et al., 2009), and the heat-loving alvinellids (e.g. Levesque et al., 2003; Fontanillas et al., 2017). Many annelid taxa are small in size and easily overlooked, and their identification requires taxonomic expertise. This has probably limited research efforts, and there are many annelid groups common in CBEs where basic knowledge about their biodiversity and ecology is still lacking – not to mention large scale processes such as evolutionary history. The taxa which are the focus of this thesis, namely the annelid family Ampharetidae, the siboglinid worm *Sclerolinum contortum* and the maldanid worm *Nicomache lokii* are examples of such poorly understood groups.

Ampharetidae

Worms in the family Ampharetidae are a widespread and common group in deep-sea sediments, with approximately 300 species described belonging to around 100 genera (Jirkov, 2011). This high number of genera illustrates that the taxonomy of Ampharetidae is problematic, with many genera being monospecific and with poor diagnoses (Jirkov, 2011). There is also a lack of consensus on which morphological characters to emphasize in the much-needed revision of the family (Reuscher et al., 2009; Salazar-Vallejo & Hutchings, 2012). Ampharetids are one of the most commonly encountered taxa in CBEs, and prior to this thesis 17 species of ampharetids, representing 8 genera, were described from CBEs (Zottoli, 1982; Reuscher et al., 2012; Stiller et al., 2013; Reuscher & Fiege, 2016; Queirós et al., 2017). Ampharetids are tube-dwellers and they deposit feed by extending their tentacles outside the tube to the surrounding substratum, and then particles get stuck in the mucus on the tentacles (Zottoli, 1983). Evidence from gut content, stable isotopes and fatty acid

analyses indicate that Ampharetids in CBEs do not harbour chemosynthetic symbionts, but feed on chemosynthetic bacteria (Thurber et al., 2013; Portail et al., 2016). Most ampharetid species in CBEs are habitat-specific, and the same species are usually not found at vents and seeps, even when these habitats occur in close geographic proximity (Stiller et al., 2013).

Prior to this thesis there had only been one phylogenetic analysis of Ampharetidae, which focused on the genus *Amphisamytha* (Stiller et al., 2013). *Amphisamytha* has 9 described species, and 7 of these are exclusively known from CBEs, while the remaining two (including the type species *A. japonica*) are shallow water species (Stiller et al., 2013). The species *Amphisamytha galapagensis* was until recently considered the widest distributed vent species known, with records both from the east and west Pacific and also the Atlantic, but the work of Stiller et al. (2013) showed that this species was a species complex, and that *A. galapagensis* is restricted to the EPR and Galapagos Ridge.

Sclerolinum contortum

Sclerolinum contortum was originally described from HMMV (Smirnov, 2000), but was later also reported from LCVF and from cold seeps in the Gulf of Mexico (Pedersen et al., 2010; Eichinger et al., 2013). At LCVF *S. contortum* is found in high densities in the diffuse flow area, where it forms a three-dimensional structure together with the maldanid worm *Nicomache lokii*, which generates a habitat for other small invertebrates (Kongsrud & Rapp, 2012). Worms in the genus *Sclerolinum* live in thin, hair like tubes, and inhabit a multitude of reducing habitats such as decaying wood, cold seeps and hydrothermal vents (e.g. Ivanov & Selivanova, 1992; Sahling et al., 2005; Schander et al., 2010a). They belong to the family Siboglinidae, which lack a functional digestive system and rely on chemosynthetic bacterial symbionts (Schulze & Halanych, 2003; Li et al., 2016). There are seven described species of *Sclerolinum*, but also several populations of putatively undescribed species belonging to this genus, for example at Loihi Seamount near Hawaii, off Kushiro, Japan and at

sedimented hydrothermal vents in the Bransfield Strait, Antarctica (Kojima et al., 1997; Sahling et al., 2005).

Nicomache lokii

Nicomache lokii was originally described from the LCVF, where, as mentioned above, it is found in high densities in the diffuse venting area (Kongsrud & Rapp, 2012). *N. lokii* is, however, also present on the chimney walls, but there the individuals are smaller and their tubes form a thin crust covered in ferrous material (Kongsrud & Rapp, 2012). *N. lokii* is a grazer that feeds by scraping particles from the substratum, and isotope analyses suggests it acquires a significant part of its nutrients from chemosynthetic bacteria (Kongsrud & Rapp, 2012). Three other species of *Nicomache* are also known from CBEs, namely *N. arwidsoni* from vents on the EPR (Blake, 1985), *N. ohtai* from cold seeps in Sagami Bay off Japan (Miura, 1991) and *N. venticola* from Juan de Fuca ridge, NE Pacific (Blake & Hilbig, 1990).

1.10 Objectives

Although the enigmatic fauna of CBEs has been the subject of intensive research over the last decades, there are still many aspects of these ecosystems that are poorly understood. As outlined above, one of the main knowledge gaps concerns the relationship between hydrothermal vent fauna and the fauna of cold seeps and organic falls, both in an evolutionary and ecological context. In addition, the understanding of the biogeography of CBEs and the geographic ranges of species has been hampered by sampling gaps and taxonomic impediments.

The main objective of this thesis was to contribute to filling these knowledge gaps by focusing on the CBEs of the Arctic Mid-Ocean Ridge and the Nordic Seas, and exploring the relationships between the fauna found there and close relatives in other world oceans. More specifically, this project aimed to:

Describe the species of Ampharetidae from Loki's Castle Vent Field

The first aim of this thesis was to describe two new species of Ampharetidae from LCVF, with support of a molecular phylogeny to establish the generic affiliation of the species (**Paper I**).

Reconstruct the evolutionary history of Ampharetidae

The second aim was to reconstruct a phylogeny of Ampharetidae with a comprehensive taxon sampling of both CBE-adapted species and non-CBE taxa (**Paper II**). Using this phylogeny, I tested the hypothesis of multiple evolutionary origins of CBE-adapted ampharetids and assessed the frequency and directionality of habitat shifts between different CBEs in the Ampharetidae. Special attention was paid to whether intermediate habitats such as sedimented vents or hydrothermal seeps may have served as evolutionary stepping stones between vents and seeps.

Assess the relationship between the Arctic populations of *Sclerolinum contortum* and *Nicomache lokii*, and populations in other oceans

Initially, the aim was to explore the relationship between the Antarctic population of *Sclerolinum* sp. and other populations of *Sclerolinum* worldwide, including *Sclerolinum contortum* from the Arctic and Gulf of Mexico (**Paper III**). Subsequently, we acquired material of worms morphologically similar to *Nicomache lokii* from previously undescribed populations at mud volcanoes in the Barbados Trench and hydrothermal vents in Antarctica. Based on the results from **Paper III**, which expanded the range of *S. contortum* to the Antarctic, I aimed to further test the conspecificity of the populations of *S. contortum* in **Paper IV** with additional mitochondrial and nuclear markers, and also to test whether *N. lokii* might have the same wide range.

Reassess the links between the annelid fauna of Loki's Castle Vent Field and vent faunas of other oceans

The hypothesis that the fauna of the LCVF is more similar to Pacific than Atlantic vent fauna was largely based on the presence of *Nicomache lokii* and *Amphisamytha* sp. at LCVF, which both belong to genera that are common at Pacific vents. Based on the results of **Papers I-IV**, I aimed to re-evaluate this hypothesis.

Evaluate which environmental factors may be affecting the habitat-specificity and distributions of the studied species

The fifth aim was to review the habitat-use of ampharetids from CBEs, with an emphasis on temperature, substratum and depth, to assess if these factors may be affecting the habitat-specificity of the species (**Paper II**). I also made some observations on the environmental conditions inhabited by *S. contortum* and *N. lokii* in **Paper IV**, and hypothesized about the factors limiting which habitats they colonize.

2. Methods

2.1 Molecular markers

The choice of molecular markers in this thesis was largely a matter of practicality. For phylogenetic analyses, I used the mitochondrial markers COI and 16S and the nuclear markers 18S and 28S (the three first markers in **Paper I** and all four in **Paper II** and in the phylogenetic analysis of *Nicomache* in **Paper III**). These markers are all relatively easy to amplify using universal or clade-specific primers, and sequencing success is quite good even on material that has been stored for some time after fixation (for example specimens from museum collections).

Ideally, species tree estimation under the multispecies coalescent model (MSC; discussed below) should be based on multiple, freely recombining markers (Heled & Drummond, 2010). Since the mitochondrial genome is inherited as a unit with low levels of recombination, if any, multiple mitochondrial markers cannot be considered independent markers. MtDNA has the advantages of high mutation rates and low effective population size due to maternal inheritance, which means that it is less prone to incomplete lineage sorting and more likely to reflect the species tree than nuclear markers (Corl & Ellegren, 2013). However, mitochondrial DNA appears to introgress more often than nuclear DNA, which may confound the species tree inference (Ballard & Whitlock, 2004), which further emphasizes the importance of including nuclear markers.

To increase the number of independent markers, I attempted to sequence several other nuclear genes in addition to the ones that were used in the end, but these either failed to amplify (e.g. Elongation factor 1α), produced multiple PCR products (Internal Transcribed Spacers) or showed low levels of variation and lack of phylogenetic signal (Histone 3). One marker that showed some promise was Alg11, which has previously been used with success in phylogenetic reconstruction of sponges (Belinky et al., 2012; Hestetun et al., 2016), but sequencing success was too low for the data to be

useful in this thesis. The best option to obtain more nuclear markers is probably genomic approaches such as transcriptomics (Weigert et al., 2014), genome-skimming (Richter et al., 2015) or sequence capture (Blaimer et al., 2016), but these approaches were not possible within the timeframe of this thesis.

For the population genetic study of *Sclerolinum contortum* and *Nicomache lokii*, we applied three mitochondrial (COI, 16S and COB) and one nuclear marker (28S). Although the mitochondrial markers are closely linked, as discussed above, they have different mutation rates, and the sequencing of several mitochondrial markers may thus give a more complete picture of the gene flow of mtDNA. Most nuclear genes are too conserved to provide much information on the intraspecific level, but in this case, 28S showed variation both within and between populations, and I decided to use this marker in addition to the mitochondrial markers.

Nuclear introns, so called EPIC markers (exon-primed, intron-crossing), have been used in population genetic studies of marine invertebrates (Jennings & Etter, 2011; Cowart et al., 2013). These markers are more variable than traditional nuclear markers, and universal primers have been developed that may allow amplification across many invertebrate phyla (Gérard et al., 2013). For *S. contortum* and *N. lokii* I attempted to amplify five putatively intron-containing genes (Actin, ATP-B, Cyclophilin A, Calmodulin and Haemoglobin subunit B2) using primers from Jarman et al. (2002), Audzijonyte and Vrijenhoek (2010a), Jennings and Etter (2011) and Cowart et al. (2013). However, these primers either amplified multiple products of different length (indicated by multiple bands on electrophoresis gels) or amplified products of a length that indicated the absence of introns. Haemoglobin subunit B2, which has previously been used as a population genetic marker in siboglinids (Cowart et al., 2013), showed electrophoresis gel bands of a length that would indicate the presence of an intron, but cloning of the PCR product and subsequent sequencing of clones revealed that two strongly divergent sequences had been amplified from the same specimen. These problems could have been overcome by designing taxon-specific

primers, but this was not possible since genome data was not available for *S. contortum*, *N. lokii* or any closely related species.

2.2 Phylogenetic analyses and species delimitation

Gene trees do not necessarily reflect the species tree, so to accurately estimate a species tree it is important to sample several markers. The inference of multigene phylogenies has until recently mainly relied on the concatenation or supermatrix approach, which assumes that all genes share the same evolutionary history. However, it is now widely recognized that this is often not the case, and applying a concatenation-based analysis on a dataset displaying gene tree discordance, due to for example incomplete lineage sorting, can lead to the inference of erroneous trees with high support (Kubatko et al., 2007). A great advance in phylogenetic estimation was made with the multispecies coalescent model (MSC), which specifically models the relationship between gene and species trees (Degnan & Rosenberg, 2009). The Bayesian applications of the MSC, for example *BEAST, co-estimates gene trees and the species tree within one MCMC run (Heled & Drummond, 2010). Estimating species trees under the MSC should as far as possible include multiple specimens per species, and even going from one to two specimens per species can increase the accuracy and precision of the analysis significantly (Camargo et al., 2012).

For the phylogenetic analyses in **Papers I and III** we did not have the possibility to include multiple specimens per species, other than for the focal species, and thus a concatenation approach was applied. In **Paper II,** the dataset for the ampharetids was greatly expanded, both in terms of taxon sampling, adding another nuclear marker (28S), and also by including multiple specimens per species for most of the species, allowing the dataset to be analysed under the MSC. Due to computational constraints, I initially performed an analysis in MrBayes of the complete dataset concatenated, and subsequently realigned the two clades containing species from CBEs and analysed these under the MSC implemented in STACEY. This approach also reduced the

proportion of ambiguously aligned regions in the alignments, allowing a higher number of basepairs to be included.

*BEAST requires species to be defined *a priori*, and erroneously delimited species can negatively affect the phylogenetic reconstruction. In STACEY, however, species delimitation is incorporated in the same MCMC run as the MSC species tree reconstruction (Jones, 2017). There are some caveats to species delimitation using the MSC, for example the MSC assumes that there is random mating within a species, and may thus delimit population structure as species (Sukumaran & Knowles, 2017). It does, however, appear that the BPP implementation of species delimitation under the MSC is more sensitive to this model violation than STACEY (Barley et al., 2017). The MSC also assumes no gene flow between species, but recognizing that species barriers can be semi-permeable (Harrison & Larson, 2014), and that lineages may be recognized as different species despite some degree of gene flow (De Queiroz, 2007), this assumption may be violated in real datasets. It seems like STACEY is more sensitive to violations of this assumption than population structure, and may cluster lineages together as the same species if there has been recent gene flow, for example in a secondary contact scenario (Barley et al., 2017). Given these limitations, I have tried to interpret the species delimitation results in **Paper II** and **Paper IV** with care, and to consider other lines of evidence where available.

2.3 Population genetic methods

For the population genetic analyses of *Nicomache lokii* and *Sclerolinum contortum* in **Papers III and IV***,* we applied a standard set of statistics for genetic diversity calculated in DnaSP and MEGA (Librado & Rozas, 2009; Kumar et al., 2016). To visualize the geographic distribution of haplotypes, haplotype networks were generated in TCS (Clement et al., 2000). Analyses of molecular variance (AMOVA) were performed in Arlequin (Excoffier & Lischer, 2010) using the F_{ST} statistic (**Paper III**) or in GenAlEx using

the PhiPT statistic (**Paper IV**), which is an F_{ST} analogue that takes genealogical information into account (Peakall & Smouse, 2012).

Since most of the markers used in **Paper IV** were mitochondrial, there were some limitations as to which analyses could be applied. MtDNA has been shown to be prone to selective sweeps, which makes inference about demographic processes problematic (Bazin et al., 2006). The low number of populations is also a limitation, for example at least four populations are needed to identify an isolation by distance pattern (Audzijonyte & Vrijenhoek, 2010b). Isolation with migration models are a powerful tool to identify asymmetric gene flow and divergence times between populations, but this model assumes that there are no unsampled populations exchanging genes with the sampled populations (Hey, 2010), which is an unrealistic assumption for the dataset in **Paper IV**, and thus I chose not to employ these models.

3. Results and discussion

3.1 Taxonomy and evolutionary history of Ampharetidae

Taxonomy and diversity

In **Paper I**, we described two new species of ampharetids from the LCVF; *Pavelius smileyi* and *Paramytha schanderi* (Figure 3.1). The genus *Pavelius* was monotypic until recently, with the single species in the genus described from cold seeps in the Sea of Okhotsk in the North-West Pacific (Kuznetsov & Levenstein, 1988). While **Paper I** was in press, another species in the genus, *Pavelius makranensis*, was described from cold seeps on the Makran accretionary prism, off Pakistan (Indian Ocean; Reuscher & Fiege, 2016). The phylogenetic analysis in **Paper I** revealed a close relationship between the genera *Pavelius* (represented by *P. smileyi* and *P. uschakovi*) and *Grassleia* (represented by *Grassleia* cf. *hydrothermalis*), which was suspected based on morphology. The most abundant ampharetid species at LCVF, which was initially identified as *Amphisamytha* sp. (Pedersen et al., 2010), was in **Paper I** shown to belong to a new genus, *Paramytha*. Around the same time, another species in this genus was described from a bone colonization experiment in the Atlantic (Setúbal Canyon, off Portugal; Queirós et al., 2017), and the congeneric status of these species was supported by the phylogeny in **Paper I**.

A phylogenetic result with taxonomic implications, was the recovery of Alvinellidae (represented by two species of the genus *Paralvinella*) within Ampharetidae (**Paper I** and **Paper II**, see Figure 3.2). This result was previously indicated by Stiller et al. (2013), and in **Paper II** we confirm their finding with a much more comprehensive taxon sampling and including an additional molecular marker. This result is not surprising from a taxonomic point of view, as alvinellids were originally described as a subfamily of Ampharetidae (Desbruyeres & Laubier, 1980). However, ecologically alvinellids are very unique, with a highly heat-tolerant physiology adapted to occupy the warmest zones at hydrothermal vents (Fontanillas et al., 2017). Unfortunately,

the exact position of Alvinellidae within Ampharetidae could not be recovered in the phylogeny in **Paper II**, and further efforts are needed to resolve the status of the subfamilies of Ampharetidae.

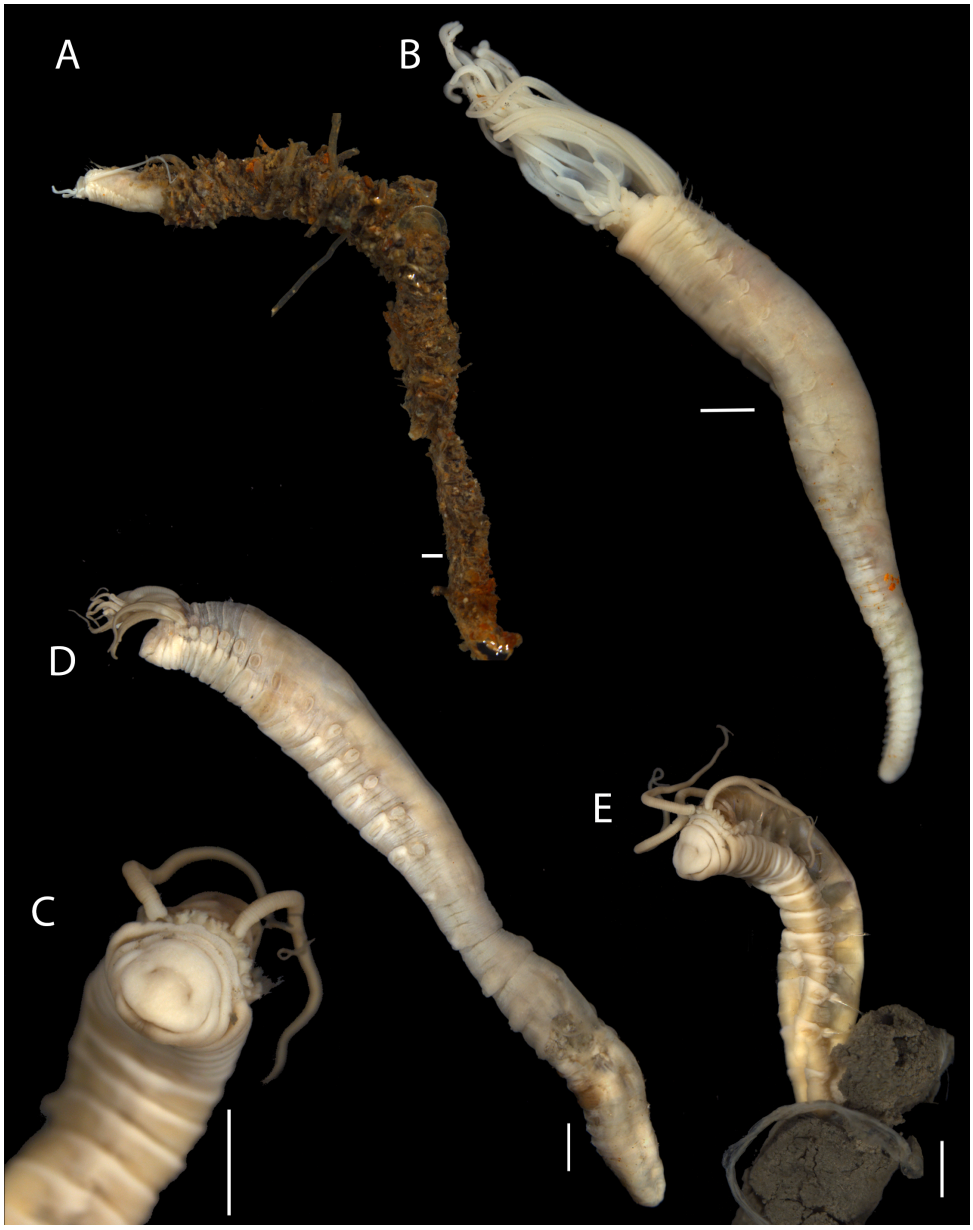

Figure 3.1. External morphology of *Paramytha schanderi* (A and B) and *Pavelius smileyi* (C – E). Scale bars: A and B – 1 mm, C, D and E – 2 mm. Figure adapted from **Paper I.**

The problematic taxonomy of Ampharetidae at the generic level is clearly demonstrated in **Paper I** and **Paper II**. Intrageneric variation in the morphological characters traditionally used to define genera in the family, namely the number of thoracic chaetigers and presence or absence of chaetae on the second segment, have been demonstrated in several genera, including *Pavelius* and *Paramytha* (**Paper I**). In **Paper I,** we commented that there are clear morphological similarities between *Paramytha* and *Decemunciger*, which is a monotypic genus described from wood falls in the North-East Atlantic (Zottoli, 1982). However, the new species could not be assigned to this genus due to morphological differences related to the shape of the prostomium. Recently, a putatively new species of *Decemunciger* was recorded from the East Pacific (Bernardino et al., 2017), and a comparison of COI sequences of this species with our data supports the close relationship between *Paramytha* and *Decemunciger* (commented in **Paper II**). This further demonstrates that some of the morphological characters used to define genera, such as prostomium shape in this case, may be more suitable at the species level.

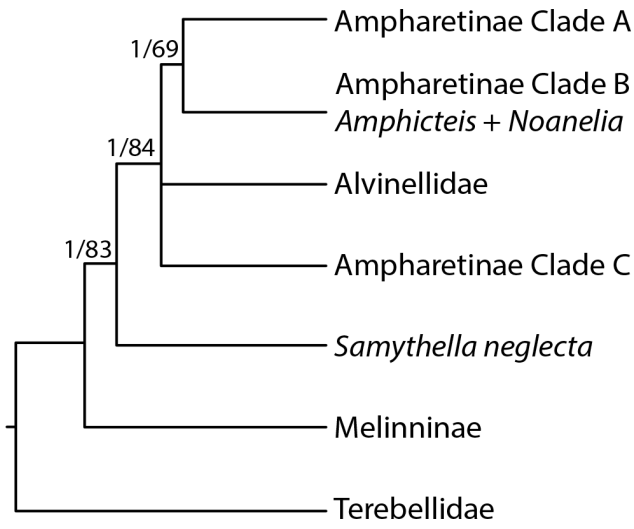

Figure 3.2. Cladogram showing the phylogenetic relationships between the main clades of Ampharetidae. Node support values are given as PP/BS. Figure adapted from **Paper II.**

There have been previous efforts to reduce the number of genera in Ampharetidae, but there is a lack of consensus about which morphological characters should be emphasized (Jirkov, 2011; Salazar-Vallejo & Hutchings, 2012). The phylogenetic results presented in **Paper I** and **Paper II** (see Figure 3.3) do not support the synonymizations of the genera *Mugga* with *Sosane* and *Sabellides* with *Ampharete* (Parapar et al., 2012). The genus *Amphisamytha* was not recovered as monophyletic, with the deep-sea species forming a monophyletic clade together with two species of *Amage*, and the shallow water species *Amphisamytha bioculata* recovered outside that clade (Figure 3.3). These results clearly demonstrate that molecular phylogenetics will be important in the much-needed taxonomic revision of Ampharetidae, and the sequence data generated for **Paper II** will feed into a larger scale phylogeny aiming to revise the taxonomy of the family (Kongsrud et al. *in prep*).

Five years ago, there were only nine species of ampharetids described that were exclusively known from CBEs [seven from vents and seeps; reviewed in Reuscher et al. (2012) and two from organic falls; Zottoli (1982)], while today there are over twice as many (19 described species, see **Paper II**). Still, there is an evident taxonomic lag in the description of fauna in CBEs, as demonstrated by the undescribed species of ampharetids included in the phylogeny in **Paper II**. There are also numerous examples of putatively new and undescribed species from CBEs in the literature [e.g. undescribed species of ampharetids from cold seeps in the Gulf of Mexico (Levin & Mendoza, 2007) and a whale fall off Brazil (Sumida et al., 2016)]. In addition, there are many undiscovered CBEs yet to be found, for example there are very few organic falls documented to date, and even fewer with proper sampling of the sediments around the fall where ampharetids may be found (Smith et al., 2017). Ampharetids are small in size, and easily overlooked, and their absence from species lists of CBEs may in some cases be due to insufficient sampling. Considering all of the above, it is clear that there is still a lot of undescribed ampharetid diversity in CBEs.

Evolutionary history

The phylogeny in **Paper I** indicated that adaptation to CBEs has happened multiple times independently within Ampharetidae, and this was further supported by the phylogenetic analyses and ancestral habitat reconstruction in **Paper II** (see Figure 3.3). Based on the results presented in **Paper II** and the taxonomic affinity of the species that are described from CBEs, but were not included in the analyses, the transition into CBEs has happened at least four times independently in Ampharetidae. This shows that the barrier to colonizing CBEs is probably not so high for ampharetids. Still, there are multiple species in each CBE-adapted clade, which shows that the initial colonization is followed by a subsequent diversification within CBEs. This would indicate that there is some adaptive innovation acquired in the initial colonization of CBEs that opens the door to the colonization of other CBEs. To the best of my knowledge, the annelid family Dorvilleidae is the only other group where multiple independent adaptations into CBEs within a family has been shown (Thornhill et al., 2012). Ampharetidae and Dorvilleidae have in common that they are heterotrophic, which may explain why these taxa seem to colonize CBEs with relative ease compared to symbiotrophic taxa. The acquisition of symbionts is probably a larger evolutionary "step" which happens more rarely, and is followed by a larger adaptive radiation (e.g. Lorion et al., 2013).

There are several habitats represented in each of the CBE-adapted clades in Ampharetidae, which shows that shifts between different types of CBEs are common in this family. Two out of five clades have only two species found in different habitats, and ancestral states could thus not be reconstructed. The ancestral state for subclade A1 (*Pavelius*/*Grassleia*) is cold seeps, with a transition to sedimented vents for *Pavelius smileyi* (Figure 3.3). This is in line with findings in other taxa that seeps or organic falls serve as stepping stones into the vent habitat (e.g. Schulze & Halanych, 2003; Thubaut et al., 2013). However, in subclade C1 and C2 (*Amphisamytha* spp.), the ancestral state is recovered as bare-rock vents, with subsequent colonization of

sedimented vents and cold seeps. This is in contrast with the notion of gradual adaptation into more and more extreme habitats, with hydrothermal vents considered the most extreme. Two of the habitat transitions recovered involve sedimented vents, and thus support the hypothesis that sedimented vents are important in linking vents and seeps. The third transition is in clade C1, where the ancestor of *Amphisamytha jacksoni* and *Amphisamytha vanuatuensis* is recovered as vent-dwelling, while *Amphisamytha vanuatuensis* is known from the Edison Seamount and from hydrothermal vents in North Fiji and Lau basins. It is not completely clear what kind of habitat Edison Seamount should be classified as. Elevated levels of methane and H_2S have been measured, but no temperature anomaly, so in **Paper II** we followed Stecher et al. (2003) in calling the site a cold seep. However, Stecher et al. (2003) suggested that this site may be a "blur" between a cold seep and hydrothermal vent, and Kiel (2016) defines it as a sedimented vent. Thus, it is possible that the transition in clade C1 should be vent to vent/sedimented vent, which would strengthen the support for the central role of sedimented vents even further.

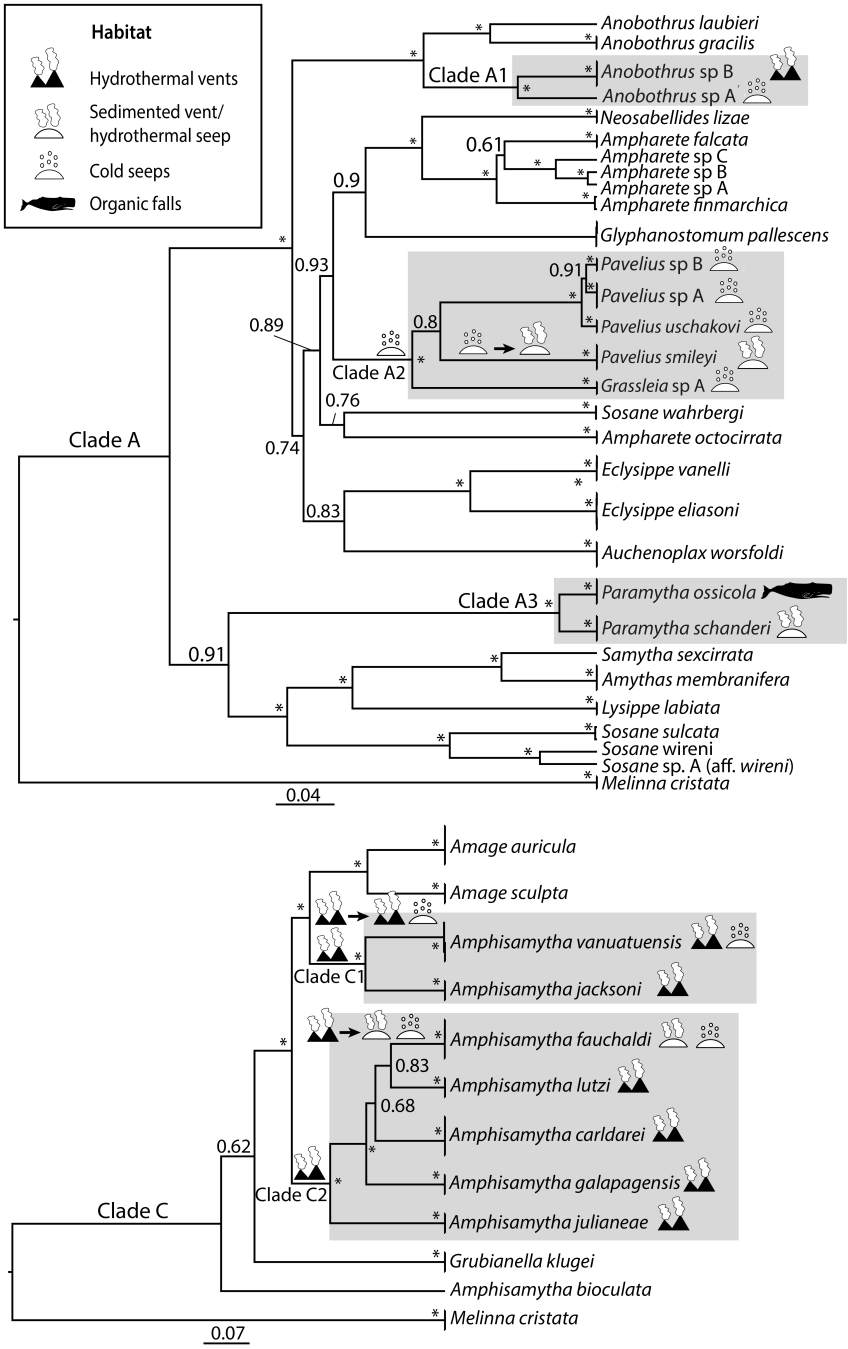

Figure 3.3. Species trees of Clades A and C inferred under the MSC in STACEY with *Melinna cristata* as outgroup. Node values are posterior probabilities, and PP > 0.95 is illustrated with a *. Ancestral states for habitat are illustrated at the base of the subclades where they could be resolved and supported transitions between habitats are also shown. Figure adapted from **Paper II.**

3.2 Biogeographic ranges and population connectivity of *Sclerolinum contortum* and *Nicomache lokii*

In **Paper III**, the geographic range of *Sclerolinum contortum* was extended from the Arctic and the Gulf of Mexico, to the Antarctic giving it a total range of nearly 16 000 km. A phylogenetic analysis based on three molecular markers (COI, 16S and 18S) supported that the Antarctic population belongs to *S. contortum*, and clearly separated this species from other congeneric species. Haplotype analyses of COI showed low levels of COI divergence between the three sampled populations, but clear geographic structure of the haplotypes. In **Paper IV**, similarly low levels of divergence were demonstrated in two additional mitochondrial markers (16S and COB), and the nuclear marker 28S, supporting the conspecificity of these populations. In addition, *Nicomache lokii* was shown to share the same wide distribution, but with less pronounced geographic structure (Figure 3.4). There are two mitochondrial lineages of *N. lokii* in the Antarctic, one which is very similar to the Arctic and central populations, and one which is quite divergent (Lineage A, see Figure 3.4). Species delimitation analyses supported that both of these lineages are conspecific to *Nicomache lokii*, but the conspecificity of Lineage A should be re-evaluated with a higher number of more variable nuclear markers (discussed in **Paper IV**).

Several recent studies have indicated that wide geographic ranges may not be unusual for annelids species from deep-sea CBEs (Borda et al., 2013; Copley et al., 2016). The growing evidence of species distributions spanning several ocean basins contrasts with biogeographic analyses of vent fauna, which have shown high levels of endemicity (95% on the species level) within biogeographic provinces (Moalic et al., 2012). This discordance may be partly due to taxonomic inaccuracies, such as the presence of synonymous species in different regions (Vrijenhoek, 2009; Teixeira et al., 2013). More work on poorly understood and taxonomically challenging taxa will probably improve our understanding of the biogeography of CBEs in the years to come. It also appears that the recent efforts in describing the fauna of CBEs in poorly

explored regions such as the Indian Ocean (e.g. Copley et al., 2016), Southern Ocean and the Arctic (this thesis) are revealing more links between CBEs around the world.

It is interesting to speculate on how these low levels of genetic divergence across massive geographic distances have come to be. Three non-exclusive hypotheses may be put forward: 1 – that these species have a higher than expected dispersal capacity, 2 – the presence of unrecorded habitats functioning as stepping stones for dispersal, and 3 – dispersal through intermittent long-distance dispersal events. Unfortunately, there is very little known about the larvae of either species (discussed in **Paper IV**), but the egg size of both species would indicate lecithotrophic larvae. There are no shared COI haplotypes between the populations of either *S. contortum* or *N. lokii*, which indicates that either dispersal between the known populations happens rarely, or gene flow goes through presently unknown populations. The existence of undocumented populations is highly likely, and there are some records in the literature of putative populations of *Nicomache lokii* (see **Paper IV**). *Sclerolinum contortum* is able to inhabit decaying wood, which may provide stepping stones to dispersal for this species (Gaudron et al., 2010). Modelling of currents has shown that at depths of around 1000 m, long-distance dispersal between the west Pacific basins may occur once every few 10k to 100k years (Mitarai et al., 2016). The distances between the west Pacific basins are much shorter than the distances between the populations of *S. contortum* and *N. lokii*, and it seems unlikely that long-distance dispersal alone can explain the genetic pattern shown in **Paper IV**. In my opinion, the most probable explanation is a combination of unknown populations with one, or both of the other hypotheses, depending on the spatial distribution of available habitats.

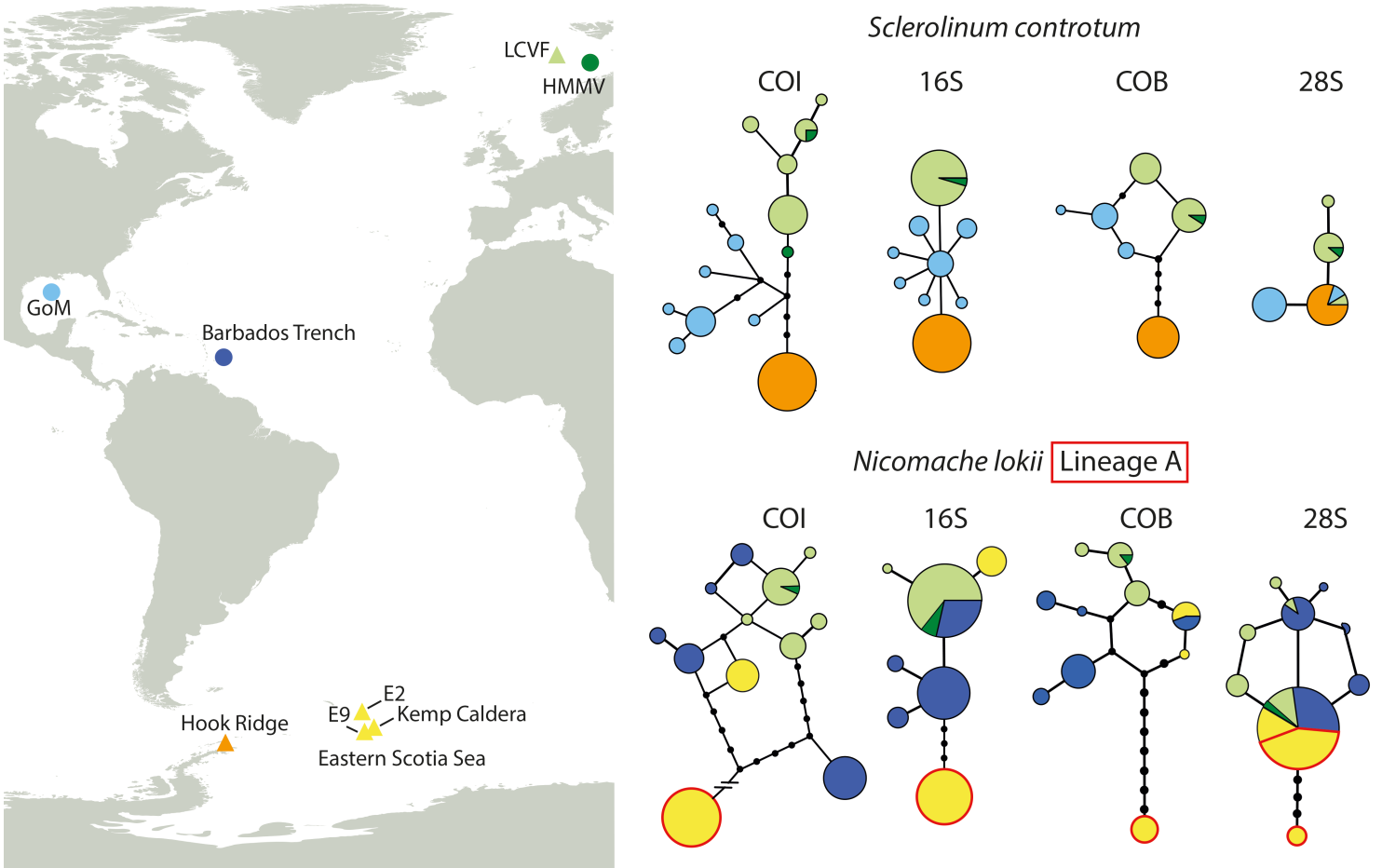

Figure 3.4. Map of sampling localities and TCS haplotype networks for *Sclerolinum contortum* and *Nicomache lokii*. Abbreviations: GoM – Gulf of Mexico, HMMV – Håkon Mosby Mud Volcano, LCVF – Loki's Castle Vent Field. Circles on the haplotype networks are proportional to the number of specimens with that haplotype, each step in the network represents one mutation and black circles represent missing haplotypes. In the networks for *N. lokii*, Lineage A in the Antarctic is highlighted with a red outline. Figure adapted from **Paper IV**.

Interestingly, most ampharetids in CBEs show quite restricted geographic ranges, although there is some variability within the family (**Paper II**). One of the ampharetid species with the widest range is *Amphisamytha galapagensis*, which is distributed in an area spanning more than 6400 km (Stiller et al., 2013). The difference in geographic ranges between the ampharetids and *Sclerolinum contortum*/*Nicomache lokii* may be related to dispersal potential or habitat specificity. Most ampharetid species are habitat specific (discussed below), and this implies that there are fewer suitable habitat patches available, which may lead to more limited geographic ranges. All ampharetid larvae documented have been lecithotrophic (Rouse, 2000), but direct evidence of the larval biology of CBE-adapted ampharetids is missing, making inferences about dispersal potential difficult. It should, however, be noted that the geographic ranges of some ampharetids may be underestimated due to insufficient sampling of many geographic regions.

3.3 Biogeography of the Loki's Castle Vent Field

The fauna of LCVF was initially suggested to be more closely related to fauna of Pacific vents than that of the Atlantic vents, based on the presence of taxa belonging to genera common at Pacific vents such as *Amphisamytha* sp. and *Nicomache lokii* (Pedersen et al., 2010). The description of the two ampharetid species from LCVF showed that these do in fact belong to the genera *Pavelius* and *Paramytha* (new genus, **Paper I**). *Pavelius* was a monotypic genus until recently, with the only species described from cold seeps in the North-West Pacific (Kuznetsov & Levenstein, 1988). Presently, there are five known species, with representatives in the Pacific, Atlantic and the Indian Ocean, of which two are not yet formally described (reviewed in **Paper II**). Apart from *Pavelius smileyi* from the LCVF, all species in this genus inhabit cold seeps. *Pavelius* is closely related to the genus *Grassleia*, which is known from cold seeps and sedimented vents in the East Pacific (reviewed in **Paper II**), and was recently recorded from a whale fall in the SW Atlantic (Sumida et al., 2016). The genus *Paramytha* is presently represented by two species, *Paramytha schanderi* from LCVF

and *Paramytha ossicola* from an organic fall in the Atlantic (**Paper I**). The closely related genus *Decemunciger* (discussed in the section on taxonomy and diversity above), has one species described from wood falls in the NW-Atlantic and one hitherto undescribed species recorded from wood falls in the NE-Pacific (Zottoli, 1982; Bernardino et al., 2017). Thus, it appears that *Paramytha schanderi* belongs to a globally distributed clade, of which most species inhabit organic falls.

Given the putatively global distribution of both *Pavelius* and *Paramytha*/*Decemunciger*, it is not possible to assign any geographic affinity of the ampharetid species at LCVF. However, the extensive geographic distributions of *Sclerolinum contortum* and *Nicomache lokii* links the Arctic CBEs (both LCVF and HMMV) with seeps in the Atlantic/Gulf of Mexico and with hydrothermal vents in the Antarctic (**Paper IV**). The degree and direction of geneflow between the Arctic CBEs and those further south is difficult to assess at present, due to the likely existence of unsampled populations between the presently sampled localities. Still, the presence of two such widespread species in the Arctic Ocean contrasts with the general impression of the deep basins of the Nordic Seas as very isolated, and with high degrees of endemism (Svavarsson et al., 1993; Stuart & Rex, 2009). It is interesting to note, however, that based on the taxa studied in this thesis, the annelid fauna of LCVF seems more related to the fauna of seeps and organic falls, than to that of bare rock vents. The sedimentary influence at LCVF makes the vent fluids more similar to seep fluids (Baumberger et al., 2016), which may contribute to the more seep-like annelid fauna, especially in the low temperature, diffuse flow area of the vent. In the biogeographic analysis by Kiel (2016) sedimented vents showed a higher connectivity to bare-rock vents than to cold seeps in general, but this analysis was based on molluscs, and it is possible that the pattern is different for annelids. The evolutionary connection between a sedimented vent and organic falls showed here in the *Paramytha*/*Decemunciger* clade is also interesting, and to my knowledge such a connection has not been shown before. A comprehensive study of the fauna of LCVF

in a biogeographic/phylogeographic context is needed to further explore the links between this locality and other CBEs around the world.

3.4 Environmental conditions and habitat specificity

The review of habitat-use of ampharetids in CBEs revealed that many species are very flexible in their microhabitat when it comes to fluid flux, temperature and substratum (**Paper II**). For example, *Amphisamytha carldarei* is found in the warmest zone together with *Paralvinella sulfincola*, but also in diffuse flow areas among *Riftia pachyptila*, and even in areas of diminished flow and dead tubeworms (McHugh & Tunnicliffe, 1994). Most seep-specific species are found in the sediments, while seep/vent generalists and vent specific species are found on all kinds of substrata, including sediment, bare rocks, structure forming animals such as bivalves or tubeworms, or even attached to the carapace of crabs (reviewed in **Paper II**). Ampharetids found at organic falls can either be inhabiting the enriched sediments around the fall, such as *Decemunciger*, *Endecamera* or *Grassleia* (Zottoli, 1982; Sumida et al., 2016), or sitting in the fall itself, like *Paramytha ossicola,* which occupies holes inside decaying bones (Queirós et al., 2017).

Despite this apparent flexibility in terms of substratum and temperature, most ampharetids are restricted to one type of CBEs. Out of 24 species included in the review in **Paper II**, only four are recorded from multiple CBEs (both vents and seeps). Looking at the depth ranges of species, the species recorded from multiple habitats are among the species with the widest depth ranges, which could indicate that differences in depth may be limiting some species to a single habitat. It is also possible that trophic specialization or biological interactions such as competition may be affecting the habitat specificity of ampharetids (discussed in **Paper II**), but at present the ecology of this group is too poorly understood to evaluate these hypotheses. Considering that the sampling of CBEs is still patchy, we will probably find more examples of ampharetids inhabiting multiple CBEs in the future.

Since *Sclerolinum contortum* and *Nicomache lokii* are found in slightly different habitats, we were able to hypothesize about which factors may be shaping their habitat preferences (**Paper IV**). In the Antarctic *S. contortum* is found at sedimented hydrothermal vents on Hook Ridge in the Bransfield Strait, while it is absent at the E2 and E9 vent sites in the Scotia Sea, which is occupied by *N. lokii*. Hook Ridge is characterized by diffuse flow at low temperatures and relatively low levels of sulphide (Aquilina et al., 2013), and a study of the environmental conditions *S. contortum* inhabits at this site indicated that it does not inhabit temperatures above 20°C (Sahling et al., 2005). It could be that the ability of *S. contortum* to take advantage of sulphide below the sediment surface allows it to inhabit this site, despite the low fluid flux, while *N. lokii* is excluded. On the other hand, *S. contortum* may be excluded from the E2 and E9 vents in the Scotia Sea, which have higher temperature venting. The presence of *N. lokii* on the chimney walls at LCVF, and putatively at vents on the Mid Cayman Rise and the MAR (**Paper IV**), also fits well with the hypothesis that this species is adapted to higher temperature than *S. contortum*. The ability of *S. contortum* to colonize sunken wood may also be a reflection of the ability of this species to utilize low levels of sulphide. These observations support previous findings that environmental factors varying across different CBEs, such as fluid flux, may be important in determining the faunal composition of these habitats (Portail et al., 2015).

3.5 Conclusions and future perspectives

This thesis has contributed to a better understanding of the biogeographic ranges, habitat-use and evolutionary history of annelids in CBEs. I have also attempted to re-evaluate the biogeographic position of Arctic CBEs based on the taxa studied in this thesis. The main conclusions of this thesis are as follows:

- The two ampharetid species at LCVF were described as *Pavelius smileyi* sp. nov. and *Paramytha schanderi* gen. et sp. nov. **(Paper I)**.

- The phylogeny and ancestral habitat reconstruction in **Paper II** shows that the colonization of CBEs has happened at least four times independently in Ampharetidae.

- **Paper II** further indicates that habitat shifts are relatively common in Ampharetidae, and habitat transitions are inferred both from seeps to vents and vents to seeps. At least two of the three habitat transitions inferred involves sedimented vents, indicating a potential evolutionary role of sedimented vents in linking bare rock vents and cold seeps. A novel link between sedimented vents and organic falls was also demonstrated.

- Both *Sclerolinum contortum* and *Nicomache lokii* are distributed from the Arctic to the Antarctic, which is the widest known geographic range of animals from CBEs **(Paper III and IV)**. This corroborates findings by other authors indicating that wide geographic ranges might not be unusual for annelids from CBEs.

- The ampharetid species from LCVF belong to globally distributed clades and have no clear geographic affinities (**Papers I** and **II**). However, the wide distributions of *Sclerolinum contortum* and *Nicomache lokii* indicates a higher degree of connectivity between Arctic and Atlantic CBEs, and even the Antarctic, than previously recognized (**Paper IV**).

- The review of habitat-use of ampharetids from CBEs in **Paper II** shows that many species are flexible in terms of substratum, temperature and fluid flux, but depth and biological interactions may play a role in determining the habitat specificity and distributions of species. Observations on the environmental conditions inhabited by *Sclerolinum contortum* and *Nicomache lokii* in **Paper IV** indicates that *S. contortum* may be limited by high temperatures, while *N. lokii* seems to require a higher level of

fluid flux. These findings support the notion that environmental factors varying across habitats are important in shaping the faunal composition of CBEs.

In general, the results presented in this thesis shows that there is still much to be learned about the animals inhabiting CBEs. For the ampharetids there is clearly a lot of undescribed diversity in CBEs around the world, and in addition to increased sampling there is a need for integrative taxonomic work on the group to describe new species and resolve the known taxonomic issues. As a globally distributed and common taxon in all kinds of CBEs, the ampharetids represent a promising model group for evolutionary and biogeographical studies. The results presented here suggest a slightly different evolutionary history in Ampharetidae, compared to what has been shown for symbiotrophic taxa, and an increased focus on heterotrophic groups may give new insights into evolutionary processes in CBEs. The large geographical distributions shown for *Sclerolinum contortum* and *Nicomache lokii*, and their presence in a wide range of reducing habitats, illustrate the importance of comparisons across habitats and geographic regions. This is usually not possible without extensive international collaborations, and this thesis has greatly benefited from such collaborations. Hopefully future collaborative projects will enable a better understanding of large scale patterns and processes in CBEs.

4. References

Adams, DK, Arellano, SM, & Govenar, B. (2012). Larval dispersal: vent life in the water column. *Oceanography,* 25(1): 256–268. http://dx.doi.org/10.5670/oceanog.2012.24

Aquilina, A, Connelly, DP, Copley, JT, Green, DRH, Hawkes, JA, Hepburn, LE, Huvenne, VAI, Marsh, L, Mills, RA, & Tyler, PA. (2013). Geochemical and Visual Indicators of Hydrothermal Fluid Flow through a Sediment-Hosted Volcanic Ridge in the Central Bransfield Basin (Antarctica). *PLOS ONE,* 8(1): e54686. https://doi.org/10.1371/journal.pone.0054686

Audzijonyte, A, & Vrijenhoek, RC. (2010a). Three nuclear genes for phylogenetic, SNP and population genetic studies of molluscs and other invertebrates. *Molecular Ecology Resources,* 10(1): 200–204. http://doi.org/10.1111/j.1755-0998.2009.02737.x

Audzijonyte, A, & Vrijenhoek, RC. (2010b). When gaps really are gaps: statistical phylogeography of hydrothermal vent invertebrates. *Evolution,* 64(8): 2369–2384. http://doi.org/10.1111/j.1558-5646.2010.00987.x

Baco, AR, & Smith, CR. (2003). High species richness in deep-sea chemoautotrophic whale skeleton communities. *Marine Ecology Progress Series,* 260: 109–114. http://doi.org/10.3354/meps260109

Ballard, JWO, & Whitlock, MC. (2004). The incomplete natural history of mitochondria. *Molecular Ecology,* 13(4): 729–744. http://dx.doi.org/10.1046/j.1365-294X.2003.02063.x

Barley, AJ, Brown, JM, & Thomson, RC. (2017). Impact of Model Violations on the Inference of Species Boundaries Under the Multispecies Coalescent. *Systematic Biology*. http://dx.doi.org/10.1093/sysbio/syx073

Baumberger, T, Früh-Green, GL, Thorseth, IH, Lilley, MD, Hamelin, C, Bernasconi, SM, Okland, IE, & Pedersen, RB. (2016). Fluid composition of the sediment-influenced Loki's Castle vent field at the ultra-slow spreading Arctic Mid-Ocean Ridge. *Geochimica et Cosmochimica Acta,* 187: 156–178. http://dx.doi.org/10.1016/j.gca.2016.05.017

Bazin, E, Glémin, S, & Galtier, N. (2006). Population Size Does Not Influence Mitochondrial Genetic Diversity in Animals. *Science,* 312(5773): 570–572. http://doi.org/10.1126/science.1122033

Belinky, F, Szitenberg, A, Goldfarb, I, Feldstein, T, Wörheide, G, Ilan, M, & Huchon, D. (2012). ALG11 – A new variable DNA marker for sponge phylogeny: Comparison of phylogenetic performances with the 18S rDNA and the COI gene. *Molecular Phylogenetics and Evolution,* 63(3): 702–713. https://doi.org/10.1016/j.ympev.2012.02.008

Bell, JB, Woulds, C, Brown, LE, Sweeting, CJ, Reid, WDK, Little, CTS, & Glover, AG. (2016). Macrofaunal Ecology of Sedimented Hydrothermal Vents in the Bransfield Strait, Antarctica. *Frontiers in Marine Science,* 3: 32. https://doi.org/10.3389/fmars.2016.00032

Bernardino, AF, Levin, LA, Thurber, AR, & Smith, CR. (2012). Comparative Composition, Diversity and Trophic Ecology of Sediment Macrofauna at Vents, Seeps and Organic Falls. *PLoS ONE,* 7(4): e33515. http://doi.org/10.1371/journal.pone.0033515

Bernardino, AF, Li, Y, Smith, CR, & Halanych, KM. (2017). Multiple introns in a deep-sea Annelid (*Decemunciger*: Ampharetidae) mitochondrial genome. *Scientific Reports,* 7(1): 4295. https://doi.org/10.1038/s41598-017-04094-w

Bienhold, C, Ristova, PP, Wenzhofer, F, Dittmar, T, & Boetius, A. (2013). How Deep-Sea Wood Falls Sustain Chemosynthetic Life. *Plos One,* 8(1): e53590. http://doi.org/10.1371/journal.pone.0053590

Black, MB, Halanych, KM, Maas, PAY, Hoeh, WR, Hashimoto, J, Desbruyères, D, Lutz, RA, & Vrijenhoek, RC. (1997). Molecular systematics of vestimentiferan tubeworms from hydrothermal vents and cold-water seeps. *Marine Biology,* 130(2): 141–149. http://doi.org/10.1007/s002270050233

Blaimer, BB, Lloyd, MW, Guillory, WX, & Brady, SG. (2016). Sequence Capture and Phylogenetic Utility of Genomic Ultraconserved Elements Obtained from Pinned Insect Specimens. *PLOS ONE,* 11(8): e0161531. https://doi.org/10.1371/journal.pone.0161531

Blake, JA. (1985). Polychaeta from the vicinity of deep-sea geothermal vents in the eastern Pacific. I. Euphrosinidae, Phyllodocidae, Hesionidae, Nereididae, Glyceridae, Dorvilleidae, Orbiniidae, and Maldanidae. *Bulletin of the Biological Society of Washington,* 6: 67–101.

Blake, JA, & Hilbig, B. (1990). Polychaeta from the Vicinity of Deep-sea Hydrothermal Vents in the Eastern Pacific. ll. New Species and Records from the Juan de Fuca and Explorer Ridge Systems. *Pacific Science,* 44(3): 219–253.

Błażewicz-Paszkowycz, M, & Bamber, RN. (2011). Tanaidomorph Tanaidacea (Crustacea: Peracarida) from mud-volcano and seep sites on the Norwegian Margin. *Zootaxa,* 3061: 1–35. http://doi.org/10.5281/zenodo.278931

Borda, E, Kudenov, JD, Chevaldonné, P, Blake, JA, Desbruyères, D, Fabri, M-C, Hourdez, S, Pleijel, F, Shank, TM, & Wilson, NG. (2013). Cryptic species of *Archinome* (Annelida: Amphinomida) from vents and seeps. *Proceedings of the Royal Society B: Biological Sciences,* 280(1770): 20131876. http://doi.org/10.1098/rspb.2013.1876

Camargo, A, Avila, LJ, Morando, M, & Sites, JW, Jr. (2012). Accuracy and Precision of Species Trees: Effects of Locus, Individual, and Base Pair Sampling on Inference of Species Trees in Lizards of the *Liolaemus darwinii* Group (Squamata, Liolaemidae). *Systematic Biology,* 61(2): 272–288. http://doi.org/10.1093/sysbio/syr105

Cavanaugh, CM, Gardiner, SL, Jones, ML, Jannasch, HW, & Waterbury, JB. (1981). Prokaryotic Cells in the Hydrothermal Vent Tube Worm *Riftia pachyptila* Jones: Possible Chemoautotrophic Symbionts. *Science,* 213(4505): 340–342. http://doi.org/10.1126/science.213.4505.340

Childress, JJ, & Fisher, CR. (1992). The biology of hydrotermal vent animals: physiology, biochemistry and autotrophic symbioses. *Oceanography and Marine Biology - An Annual Review,* 30: 337–441.

Clement, M, Posada, D, & Crandall, KA. (2000). TCS: a computer program to estimate gene genealogies. *Molecular Ecology,* 9(10): 1657–1659. http://doi.org/10.1046/j.1365-294x.2000.01020.x

Cole, CS, James, RH, Connelly, DP, & Hathorne, EC. (2014). Rare earth elements as indicators of hydrothermal processes within the East Scotia subduction zone system. *Geochimica et Cosmochimica Acta,* 140(Supplement C): 20–38. https://doi.org/10.1016/j.gca.2014.05.018

Connelly, DP, Copley, JT, Murton, BJ, Stansfield, K, Tyler, PA, German, CR, Van Dover, CL, Amon, D, Furlong, M, Grindlay, N, Hayman, N, Hühnerbach, V, Judge, M, Le Bas, T, McPhail, S, Meier, A, Nakamura, K-i, Nye, V, Pebody, M, Pedersen, RB, Plouviez, S, Sands, C, Searle, RC, Stevenson, P, Taws, S, & Wilcox, S. (2012). Hydrothermal vent

fields and chemosynthetic biota on the world's deepest seafloor spreading centre. *Nature Communications,* 3: 620. http://doi.org/10.1038/ncomms1636

Copley, JT, Marsh, L, Glover, AG, Hühnerbach, V, Nye, VE, Reid, WDK, Sweeting, CJ, Wigham, BD, & Wiklund, H. (2016). Ecology and biogeography of megafauna and macrofauna at the first known deep-sea hydrothermal vents on the ultraslow-spreading Southwest Indian Ridge. *Scientific Reports,* 6: 39158. http://dx.doi.org/10.1038/srep39158

Cordes, EE, Hourdez, S, Predmore, B, Redding, ML, & Fisher, CR. (2005). Succession of hydrocarbon seep communities associated with the long-lived foundation species *Lamellibrachia luymesi*. *Marine Ecology Progress Series,* 305: 17–29. http://doi.org/10.3354/meps305017

Cordes, EE, Cunha, MR, Galéron, J, Mora, C, Olu-Le Roy, K, Sibuet, M, Van Gaever, S, Vanreusel, A, & Levin, LA. (2010). The influence of geological, geochemical, and biogenic habitat heterogeneity on seep biodiversity. *Marine Ecology,* 31(1): 51–65. http://doi.org/10.1111/j.1439-0485.2009.00334.x

Corl, A, & Ellegren, H. (2013). Sampling strategies for species trees: The effects on phylogenetic inference of the number of genes, number of individuals, and whether loci are mitochondrial, sex-linked, or autosomal. *Molecular Phylogenetics and Evolution,* 67(2): 358–366. http://doi.org/10.1016/j.ympev.2013.02.002

Corliss, JB, Dymond, J, Gordon, LI, Edmond, JM, von Herzen, RP, Ballard, RD, Green, K, Williams, D, Bainbridge, A, Crane, K, & van Andel, TH. (1979). Submarine Thermal Sprirngs on the Galápagos Rift. *Science,* 203(4385): 1073–1083. http://doi.org/10.1126/science.203.4385.1073

Cowart, DA, Huang, C, Arnaud-Haond, S, Carney, SL, Fisher, CR, & Schaeffer, SW. (2013). Restriction to large-scale gene flow vs. regional panmixia among cold seep *Escarpia* spp. (Polychaeta, Siboglinidae). *Molecular Ecology,* 22(16): 4147–4162. http://doi.org/10.1111/mec.12379

Coykendall, DK, Johnson, SB, Karl, SA, Lutz, RA, & Vrijenhoek, RC. (2011). Genetic diversity and demographic instability in *Riftia pachyptila* tubeworms from eastern Pacific hydrothermal vents. *BMC Evolutionary Biology,* 11(1). https://doi.org/10.1186/1471-2148-11-96

Cunha, MR, Matos, FL, Génio, L, Hilário, A, Moura, CJ, Ravara, A, & Rodrigues, CF. (2013). Are Organic Falls Bridging Reduced Environments in the Deep Sea? - Results from Colonization Experiments in the Gulf of Cádiz. *PLoS ONE,* 8(10): e76688. http://doi.org/10.1371/journal.pone.0076688

De Queiroz, K. (2007). Species concepts and species delimitation. *Systematic Biology,* 56(6): 879–886. https://doi.org/10.1080/10635150701701083

Decker, C, Olu, K, Cunha, RL, & Arnaud-Haond, S. (2012). Phylogeny and Diversification Patterns among Vesicomyid Bivalves. *PLoS ONE,* 7(4): e33359. http://doi.org/10.1371/journal.pone.0033359

Degnan, JH, & Rosenberg, NA. (2009). Gene tree discordance, phylogenetic inference and the multispecies coalescent. *Trends in Ecology & Evolution,* 24(6): 332–340. https://doi.org/10.1016/j.tree.2009.01.009

Desbruyeres, D, & Laubier, L. (1980). *Alvinella pompejana* gen. sp. nov., Ampharetidae aberrant des sources hydrothermales de la ride Est-Pacifique. *Oceanologica Acta,* 3(3): 267–274.

Distel, DL, Baco, AR, Chuang, E, Morrill, W, Cavanaugh, C, & Smith, CR. (2000). Marine ecology - Do mussels take wooden steps to deep-sea vents? *Nature,* 403(6771): 725–726. http://doi.org/10.1038/35001667

Edmonds, HN, Michael, PJ, Baker, ET, Connelly, DP, Snow, JE, Langmuir, CH, Dick, HJB, Mühe, R, German, CR, & Graham, DW. (2003). Discovery of abundant hydrothermal venting on the ultraslow-spreading Gakkel ridge in the Arctic Ocean. *Nature,* 421: 252–256. http://dx.doi.org/10.1038/nature01351

Eichinger, I, Hourdez, S, & Bright, M. (2013). Morphology, microanatomy and sequence data of *Sclerolinum contortum* (Siboglindae, Annelida) of the Gulf of Mexico. *Organisms, Diversity & Evolution,* 13(3): 311–329. http://doi.org/10.1007/s13127-012-0121-3

Excoffier, L, & Lischer, H. (2010). Arlequin suite ver 3.5: a new series of programs to perform population genetics analyses under Linux and Windows. *Molecular Ecology Resources,* 10: 564–567. http://doi.org/10.1111/j.1755-0998.2010.02847.x

Faure, B, Schaeffer, SW, & Fisher, CR. (2015). Species Distribution and Population Connectivity of Deep-Sea Mussels at Hydrocarbon Seeps in the Gulf of Mexico. *PLOS ONE,* 10(4): e0118460. http://doi.org/10.1371/journal.pone.0118460

Fontanillas, E, Galzitskaya, OV, Lecompte, O, Lobanov, MY, Tanguy, A, Mary, J, Girguis, PR, Hourdez, S, & Jollivet, D. (2017). Proteome evolution of deep-sea hydrothermal vent alvinellid polychaetes supports the ancestry of thermophily and subsequent adaptation to cold in some lineages. *Genome Biology and Evolution,* 9(2): 279–296. https://doi.org/10.1093/gbe/evw298

Fricke, H, Giere, O, Stetter, K, Alfredsson, GA, Kristjansson, JK, & Stoffers, P. (1989). Hydrothermal vent communities at the shallow subpolar Mid-Atlantic ridge. *Marine Biology,* 102: 425–429. https://doi.org/10.1007/BF00428495

Gaudron, SM, Pradillon, F, Pailleret, M, Duperron, S, Le Bris, N, & Gaill, F. (2010). Colonization of organic substrates deployed in deep-sea reducing habitats by symbiotic species and associated fauna. *Marine Environmental Research,* 70(1): 1–12. https://doi.org/10.1016/j.marenvres.2010.02.002

Gebruk, AV, Krylova, EM, Lein, AY, Vinogradov, GM, Anderson, E, Pimenov, NV, Cherkashev, GA, & Crane, K. (2003). Methane seep community of the Håkon Mosby mud volcano (the Norwegian Sea): composition and trophic aspects. *Sarsia,* 88(6): 394–403. http://doi.org/10.1080/00364820310003190

Gérard, K, Guilloton, E, Arnaud-Haond, S, Aurelle, D, Bastrop, R, Chevaldonné, P, Derycke, S, Hanel, R, Lapègue, S, Lejeusne, C, Mousset, S, Ramšak, A, Remerie, T, Viard, F, Féral, J-P, & Chenuil, A. (2013). PCR survey of 50 introns in animals: Cross-amplification of homologous EPIC loci in eight non-bilaterian, protostome and deuterostome phyla. *Marine Genomics,* 12(Supplement C): 1–8. https://doi.org/10.1016/j.margen.2013.10.001

German, CR, & Parson, LM. (1998). Distributions of hydrothermal activity along the Mid-Atlantic Ridge: interplay of magmatic and tectonic controls. *Earth and Planetary Science Letters,* 160(3): 327–341. https://doi.org/10.1016/S0012-821X(98)00093-4

Ginsburg, GD, Milkov, AV, Soloviev, VA, Egorov, AV, Cherkashev, GA, Vogt, PR, Crane, K, Lorenson, TD, & Khutorskoy, MD. (1999). Gas hydrate accumulation at the Håkon Mosby Mud Volcano. *Geo-Marine Letters,* 19(1): 57–67. https://doi.org/10.1007/s003670050093

Glover, AG, Källström, B, Smith, CR, & Dahlgren, TG. (2005). World-wide whale worms? A new species of *Osedax* from the shallow north Atlantic. *Proceedings of the Royal*

Society B: Biological Sciences, 272(1581): 2587–2592. http://doi.org/10.1098/rspb.2005.3275

Goffredi, SK, Johnson, S, Tunnicliffe, V, Caress, D, Clague, D, Escobar, E, Lundsten, L, Paduan, JB, Rouse, G, Salcedo, DL, Soto, LA, Spelz-Madero, R, Zierenberg, R, & Vrijenhoek, R. (2017). Hydrothermal vent fields discovered in the southern Gulf of California clarify role of habitat in augmenting regional diversity. *Proceedings of the Royal Society B: Biological Sciences,* 284(1859). http://doi.org/10.1098/rspb.2017.0817

Govenar, B, Fisher, CR, & Shank, TM. (2015). Variation in the diets of hydrothermal vent gastropods. *Deep Sea Research Part II: Topical Studies in Oceanography,* 121: 193–201. https://doi.org/10.1016/j.dsr2.2015.06.021

Hansen, B, & Østerhus, S. (2000). North Atlantic–Nordic Seas exchanges. *Progress in Oceanography,* 45(2): 109–208. https://doi.org/10.1016/S0079-6611(99)00052-X

Harrison, RG, & Larson, EL. (2014). Hybridization, Introgression, and the Nature of Species Boundaries. *Journal of Heredity,* 105(S1): 795–809. http://dx.doi.org/10.1093/jhered/esu033

Heled, J, & Drummond, AJ. (2010). Bayesian Inference of Species Trees from Multilocus Data. *Molecular Biology and Evolution,* 27(3): 570–580. http://doi.org/10.1093/molbev/msp274

Hestetun, JT, Vacelet, J, Boury-Esnault, N, Borchiellini, C, Kelly, M, Ríos, P, Cristobo, J, & Rapp, HT. (2016). The systematics of carnivorous sponges. *Molecular Phylogenetics and Evolution,* 94(Part A): 327–345. https://doi.org/10.1016/j.ympev.2015.08.022

Hey, J. (2010). Isolation with Migration Models for More Than Two Populations. *Molecular Biology and Evolution,* 27(4): 905–920. http://doi.org/10.1093/molbev/msp296

Hilario, A, Cunha, MR, Génio, L, Marçal, AR, Ravara, A, Rodrigues, CF, & Wiklund, H. (2015). First clues on the ecology of whale falls in the deep Atlantic Ocean: results from an experiment using cow carcasses. *Marine Ecology,* 36: 82–90. http://doi.org/10.1111/maec.12246

Hjartarson, Á, Erlendsson, Ö, & Blischke, A. (2017). The Greenland–Iceland–Faroe Ridge Complex. *Geological Society, London, Special Publications,* 447: 127–148. http://doi.org/10.1144/SP447.14

Hurtado, LA, Lutz, RA, & Vrijenhoek, RC. (2004). Distinct patterns of genetic differentiation among annelids of eastern Pacific hydrothermal vents. *Molecular Ecology,* 13(9): 2603-2615. http://doi.org/10.1111/j.1365-294X.2004.02287.x

Ivanov, AV, & Selivanova, RV. (1992). *Sclerolinum javanicum* sp. n., a new pogonophoran living on rotten wood. A contribution to the classification of Pogonophora. *Biologiya Morya (Vladivostok),* 1–2: 27–33.

Jang, S-J, Park, E, Lee, W-K, Johnson, SB, Vrijenhoek, RC, & Won, Y-J. (2016). Population subdivision of hydrothermal vent polychaete *Alvinella pompejana* across equatorial and Easter Microplate boundaries. *BMC Evolutionary Biology,* 16: 235. http://doi.org/10.1186/s12862-016-0807-9

Jannasch, HW, & Wirsen, CO. (1979). Chemosynthetic Primary Production at East Pacific Sea Floor Spreading Centers. *Bioscience,* 29(10): 592–598. http://doi.org/10.2307/1307765

Jarman, SN, Ward, RD, & Elliott, NG. (2002). Oligonucleotide Primers for PCR Amplification of Coelomate Introns. *Marine Biotechnology,* 4(4): 347–355. http://doi.org/10.1007/s10126-002-0029-6

Jennings, RM, & Etter, RJ. (2011). Exon-primed, intron-crossing (EPIC) loci for five nuclear genes in deep-sea protobranch bivalves: primer design, PCR protocols and locus utility. *Molecular Ecology Resources,* 11(6): 1102–1112. http://doi.org/10.1111/j.1755-0998.2011.03038.x

Jirkov, IA. (2011). Discussion of taxonomic characters and classification of Ampharetidae (Polychaeta). *Italian Journal of Zoology,* 78(sup1): 78–94. https://doi.org/10.1080/11250003.2011.617216

Jollivet, D, Faugeres, J-C, Griboulard, R, Desbruyers, D, & Blanc, G. (1990). Composition and spatial organization of a cold seep community on the South Barbados accretionary prism: Tectonic, geochemical and sedimentary context. *Progress in Oceanography,* 24(1): 25–45. https://doi.org/10.1016/0079-6611(90)90017-V

Jollivet, D, Comtet, T, Chevaldonné, P, Desbruyères, D, & Dixon, DR. (1998). Unexpected relationships between dispersal strategies and speciation within the association *Bathymodiolus* (Bivalvia) - *Branchipolynoe* (Polychaeta) inferred from the rDNA neutral ITS2 marker. *Cahiers de Biologie Marine,* 39: 359–362.

Jones, G. (2017). Algorithmic improvements to species delimitation and phylogeny estimation under the multispecies coalescent. *Journal of Mathematical Biology,* 74: 447–467. http://doi.org/10.1007/s00285-016-1034-0

Kelley, DS, Karson, JA, Früh-Green, GL, Yoerger, DR, Shank, TM, Butterfield, DA, Hayes, JM, Schrenk, MO, Olson, EJ, Proskurowski, G, Jakuba, M, Bradley, A, Larson, B, Ludwig, K, Glickson, D, Buckman, K, Bradley, AS, Brazelton, WJ, Roe, K, Elend, MJ, Delacour, A, Bernasconi, SM, Lilley, MD, Baross, JA, Summons, RE, & Sylva, SP. (2005). A Serpentinite-Hosted Ecosystem: The Lost City Hydrothermal Field. *Science,* 307(5714): 1428–1434. http://doi.org/10.1126/science.1102556

Kiel, S. (2016). A biogeographic network reveals evolutionary links between deep-sea hydrothermal vent and methane seep faunas. *Proceedings of the Royal Society B: Biological Sciences,* 283(1844). http://dx.doi.org/10.1098/rspb.2016.2337

Kiel, S. (2017). Reply to Smith *et al*.: Network analysis reveals connectivity patterns in the continuum of reducing ecosystems. *Proceedings of the Royal Society B: Biological Sciences,* 284(1863). http://doi.org/10.1098/rspb.2017.1644

Kojima, S, Segawa, R, Hashimoto, J, & Ohta, S. (1997). Molecular phylogeny of vestimentiferans collected around Japan, revealed by the nucleotide sequences of mitochondrial DNA. *Marine Biology,* 127: 507–513. https://doi.org/10.1007/s002270050039

Kongsrud, JA, & Rapp, HT. (2012). *Nicomache* (*Loxochona*) *lokii* sp nov (Annelida: Polychaeta: Maldanidae) from the Loki's Castle vent field: an important structure builder in an Arctic vent system. *Polar Biology,* 35(2): 161–170. http://doi.org/10.1007/s00300-011-1048-4

Kubatko, LS, Degnan, JH, & Collins, T. (2007). Inconsistency of Phylogenetic Estimates from Concatenated Data under Coalescence. *Systematic Biology,* 56(1): 17–24. http://dx.doi.org/10.1080/10635150601146041

Kumar, S, Stecher, G, & Tamura, K. (2016). MEGA7: Molecular Evolutionary Genetics Analysis Version 7.0 for Bigger Datasets. *Molecular Biology and Evolution,* 33(7): 1870–1874. http://doi.org/10.1093/molbev/msw054

Kuznetsov, AP, & Levenstein, RY. (1988). *Pavelius uschakovi* gen. et sp. n. (Polychaeta, Ampharetidae) from Paramushir Gas Hydrate Spring in the Okhotsk Sea. *Zoologichesky Zhurnal,* 67(6): 819–825.

LaBonte, AL, Brown, KM, & Tryon, MD. (2007). Monitoring periodic and episodic flow events at Monterey Bay seeps using a new optical flow meter. *Journal of Geophysical Research: Solid Earth,* 112(B2): B02105. http://doi.org/10.1029/2006JB004410

Levesque, C, Juniper, SK, & Marcus, J. (2003). Food resource partitioning and competition among alvinellid polychaetes of Juan de Fuca Ridge hydrothermal vents. *Marine Ecology Progress Series,* 246: 173–182. http://doi.org/10.3354/meps246173

Levin, LA. (2005). Ecology of cold seep sediments: interactions of fauna with flow, chemistry and microbes. *Oceanography and Marine Biology Annual Review,* 43: 1–46.

Levin, LA, & Mendoza, GF. (2007). Community structure and nutrition of deep methane-seep macrobenthos from the North Pacific (Aleutian) Margin and the Gulf of Mexico (Florida Escarpment). *Marine Ecology,* 28(1): 131–151. http://dx.doi.org/10.1111/j.1439-0485.2006.00131.x

Levin, LA, Mendoza, GF, Gonzalez, JP, Thurber, AR, & Cordes, EE. (2010). Diversity of bathyal macrofauna on the northeastern Pacific margin: the influence of methane seeps and oxygen minimum zones. *Marine Ecology,* 31(1): 94–110. http://doi.org/10.1111/j.1439-0485.2009.00335.x

Levin, LA, Orphan, VJ, Rouse, GW, Rathburn, AE, Ussler, W, Cook, GS, Goffredi, SK, Perez, EM, Waren, A, Grupe, BM, Chadwick, G, & Strickrott, B. (2012). A hydrothermal seep on the Costa Rica margin: middle ground in a continuum of reducing ecosystems. *Proceedings of the Royal Society B: Biological Sciences,* 279(1738): 2580-2588. http://doi.org/10.1098/rspb.2012.0205

Levin, LA, Mendoza, GF, Grupe, BM, Gonzalez, JP, Jellison, B, Rouse, G, Thurber, AR, & Waren, A. (2015). Biodiversity on the Rocks: Macrofauna Inhabiting Authigenic Carbonate at Costa Rica Methane Seeps. *PLOS ONE,* 10(7): e0131080. http://doi.org/10.1371/journal.pone.0131080

Li, Y, Kocot, KM, Whelan, NV, Santos, SR, Waits, DS, Thornhill, DJ, & Halanych, KM. (2016). Phylogenomics of tubeworms (Siboglinidae, Annelida) and comparative performance of different reconstruction methods. *Zoologica Scripta,* 46: 200–213. http://doi.org/10.1111/zsc.12201

Librado, P, & Rozas, J. (2009). DnaSP v5: a software for comprehensive analysis of DNA polymorphism data. *Bioinformatics,* 25(11): 1451–1452. http://doi.org/10.1093/bioinformatics/btp187

Lonsdale, P. (1977). Clustering of suspension-feeding macrobenthos near abyssal hydrothermal vents at oceanic spreading centers. *Deep-Sea Research,* 24(9): 857–863. http://doi.org/10.1016/0146-6291(77)90478-7

Lorion, J, Kiel, S, Faure, B, Kawato, M, Ho, SYW, Marshall, B, Tsuchida, S, Miyazaki, J, & Fujiwara, Y. (2013). Adaptive radiation of chemosymbiotic deep-sea mussels. *Proceedings of the Royal Society B: Biological Sciences,* 280(1770): 20131243. http://doi.org/10.1098/rspb.2013.1243

Luther, GW, III, Rozan, TF, Taillefert, M, Nuzzio, DB, Di Meo, C, Shank, TM, Lutz, RA, & Cary, SC. (2001). Chemical speciation drives hydrothermal vent ecology. *Nature,* 410: 813–816. http://doi.org/10.1038/35071069

Marsh, AG, Mullineaux, LS, Young, CM, & Manahan, DT. (2001). Larval dispersal potential of the tubeworm *Riftia pachyptila* at deep-sea hydrothermal vents. *Nature,* 411: 77–80. http://doi.org/10.1038/35075063

McHugh, D, & Tunnicliffe, V. (1994). Ecology and reproductive biology of the hydrothermal vent polychaete *Amphisamytha galapagensis* (Ampharetidae). *Marine Ecology Progress Series,* 106(1–2): 111–120. http://doi.org/10.3354/meps106111

McMullin, ER, Bergquist, DC, & Fisher, CR. (2007). Metazoans in extreme environments: adaptations of hydrothermal vent and hydrocarbon seep fauna. *Gravitational and Space Research,* 13(2):13–23.

Micheli, F, Peterson, CH, Mullineaux, LS, Fisher, CR, Mills, SW, Sancho, G, Johnson, GA, & Lenihan, HS. (2002). Predation structures communities at deep-sea hydrothermal vents. *Ecological Monographs,* 72(3): 365–382. http://dx.doi.org/10.1890/0012-9615(2002)072[0365:PSCADS]2.0.CO;2

Mitarai, S, Watanabe, H, Nakajima, Y, Shchepetkin, AF, & McWilliams, JC. (2016). Quantifying dispersal from hydrothermal vent fields in the western Pacific Ocean. *Proceedings of the National Academy of Sciences,* 113(11): 2976–2981. http://doi.org/10.1073/pnas.1518395113

Miura, T. (1991). *Nicomache otai*, new species (Polychaeta: Maldanidae) collected from the Hatsushima cold-seep in Sagami Bay. *Proceedings of the Biological Society of Washington,* 104: 159–165.

Moalic, Y, Desbruyères, D, Duarte, CM, Rozenfeld, AF, Bachraty, C, & Arnaud-Haond, S. (2012). Biogeography Revisited with Network Theory: Retracing the History of Hydrothermal Vent Communities. *Systematic Biology,* 61(1): 127–127. http://doi.org/10.1093/sysbio/syr088

Nakamura, K, & Takai, K. (2014). Theoretical constraints of physical and chemical properties of hydrothermal fluids on variations in chemolithotrophic microbial communities in seafloor hydrothermal systems. *Progress in Earth and Planetary Science,* 1(1): 5. http://doi.org/10.1186/2197-4284-1-5

Olsen, BR, Økland, IE, Thorseth, IH, Pedersen, RB, & Rapp, HT. (2016). *Environmental challenges related to offshore mining and gas hydrate extraction*. Rapport M-532. Miljødirektoratet.

Parapar, J, Helgason, GV, Jirkov, I, & Moreira, J. (2012). Polychaetes of the genus *Ampharete* (Polychaeta: Ampharetidae) collected in Icelandic waters during the BIOICE project. *Helgoland marine research,* 66(3): 331–344. https://doi.org/10.1007/s10152-011-0274-z

Paull, CK, Hecker, B, Commeau, R, Freemanlynde, RP, Neumann, C, Corso, WP, Golubic, S, Hook, JE, Sikes, E, & Curray, J. (1984). Biological Communities at the Florida Escarpment Resemble Hydrothermal Vent Taxa. *Science,* 226(4677): 965–967. http://doi.org/10.1126/science.226.4677.965

Peakall, R, & Smouse, PE. (2012). GenAlEx 6.5: genetic analysis in Excel. Population genetic software for teaching and research—an update. *Bioinformatics,* 28(19): 2537–2539. http://doi.org/10.1093/bioinformatics/bts460

Pedersen, RB, Rapp, HT, Thorseth, IH, Lilley, MD, Barriga, F, Baumberger, T, Flesland, K, Fonseca, R, Fruh-Green, GL, & Jorgensen, SL. (2010). Discovery of a black smoker vent field and vent fauna at the Arctic Mid-Ocean Ridge. *Nature Communications,* 1: 126. http://doi.org/10.1038/ncomms1124

Perez-Garcia, C, Feseker, T, Mienert, J, & Berndt, C. (2009). The Håkon Mosby mud volcano: 330 000 years of focused fluid flow activity at the SW Barents Sea slope. *Marine Geology,* 262(1–4): 105–115. https://doi.org/10.1016/j.margeo.2009.03.022

Plouviez, S, Shank, TM, Faure, B, Daguin-Thiebaut, C, Viard, F, Lallier, FH, & Jollivet, D. (2009). Comparative phylogeography among hydrothermal vent species along the East Pacific Rise reveals vicariant processes and population expansion in the South. *Molecular Ecology,* 18(18): 3903–3917. http://doi.org/10.1111/j.1365-294X.2009.04325.x

Portail, M, Olu, K, Escobar-Briones, E, Caprais, JC, Menot, L, Waeles, M, Cruaud, P, Sarradin, PM, Godfroy, A, & Sarrazin, J. (2015). Comparative study of vent and seep macrofaunal communities in the Guaymas Basin. *Biogeosciences,* 12(18): 5455–5479. http://doi.org/10.5194/bg-12-5455-2015

Portail, M, Olu, K, Dubois, SF, Escobar-Briones, E, Gelinas, Y, Menot, L, & Sarrazin, J. (2016). Food-Web Complexity in Guaymas Basin Hydrothermal Vents and Cold Seeps. *PLoS ONE,* 11(9): e0162263. https://doi.org/10.1371/journal.pone.0162263

Pradillon, F, Shillito, B, Young, CM, & Gaill, F. (2001). Deep-sea ecology: Developmental arrest in vent worm embryos. *Nature,* 413(6857): 698–699. http://doi.org/10.1038/35099674

Queirós, JP, Ravara, A, Eilertsen, MH, Kongsrud, JA, & Hilário, A. (2017). *Paramytha ossicola* sp. nov. (Polychaeta, Ampharetidae) from mammal bones: reproductive biology and population structure. *Deep Sea Research Part II Topical Studies in Oceanography,* 137: 349–358. http://doi.org/10.1016/j.dsr2.2016.08.017

Rau, GH, & Hedges, JI. (1979). Carbon-13 Depletion in a Hydrothermal Vent Mussel: Suggestion of a Chemosynthetic Food Source. *Science,* 203(4381): 648–649. http://doi.org/10.1126/science.203.4381.648

Ravaux, J, Hamel, G, Zbinden, M, Tasiemski, AA, Boutet, I, Léger, N, Tanguy, A, Jollivet, D, & Shillito, B. (2013). Thermal Limit for Metazoan Life in Question: In Vivo Heat Tolerance of the Pompeii Worm. *PLOS ONE,* 8(5): e64074. http://doi.org/10.1371/journal.pone.0064074

Reuscher, M, Fiege, D, & Wehe, T. (2009). Four new species of Ampharetidae (Annelida: Polychaeta) from Pacific hot vents and cold seeps, with a key and synoptic table of characters for all genera. *Zootaxa,* 2191: 1–40.

Reuscher, M, Fiege, D, & Wehe, T. (2012). Terebellomorph polychaetes from hydrothermal vents and cold seeps with the description of two new species of Terebellidae (Annelida: Polychaeta) representing the first records of the family from deep-sea vents. *Journal of the Marine Biological Association of the United Kingdom,* 92(05): 997–1012. https://doi.org/10.1017/S0025315411000658

Reuscher, MG, & Fiege, D. (2016). Ampharetidae (Annelida: Polychaeta) from cold seeps off Pakistan and hydrothermal vents off Taiwan, with the description of three new species. *Zootaxa,* 4139(2): 197–208. http://doi.org/10.11646/zootaxa.4139.2.4

Rex, MA, Etter, RJ, Morris, JS, Crouse, J, McClain, CR, Johnson, NA, Stuart, CT, Deming, JW, Thies, R, & Avery, R. (2006). Global bathymetric patterns of standing stock and body size in the deep-sea benthos. *Marine Ecology Progress Series,* 317: 1–8. http://doi.org/10.3354/meps317001

Richter, S, Schwarz, F, Hering, L, Böggemann, M, & Bleidorn, C. (2015). The Utility of Genome Skimming for Phylogenomic Analyses as Demonstrated for Glycerid Relationships (Annelida, Glyceridae). *Genome Biology and Evolution,* 7(12): 3443–3462. http://dx.doi.org/10.1093/gbe/evv224

Rogers, AD, Tyler, PA, Connelly, DP, Copley, JT, James, R, Larter, RD, Linse, K, Mills, RA, Garabato, AN, Pancost, RD, Pearce, DA, Polunin, NVC, German, CR, Shank, T, Boersch-

Supan, PH, Alker, BJ, Aquilina, A, Bennett, SA, Clarke, A, Dinley, RJJ, Graham, AGC, Green, DRH, Hawkes, JA, Hepburn, L, Hilario, A, Huvenne, VAI, Marsh, L, Ramirez-Llodra, E, Reid, WDK, Roterman, CN, Sweeting, CJ, Thatje, S, & Zwirglmaier, K. (2012). The Discovery of New Deep-Sea Hydrothermal Vent Communities in the Southern Ocean and Implications for Biogeography. *PLoS Biology,* 10(1): e1001234. http://doi.org/10.1371/journal.pbio.1001234

Rona, PA, Klinkhammer, G, Nelsen, TA, Trefry, JH, & Elderfield, H. (1986). Black smokers, massive sulphides and vent biota at the Mid-Atlantic Ridge. *Nature,* 321: 33–37. http://dx.doi.org/10.1038/321033a0

Roterman, CN, Copley, JT, Linse, KT, Tyler, PA, & Rogers, AD. (2013). The biogeography of the yeti crabs (Kiwaidae) with notes on the phylogeny of the Chirostyloidea (Decapoda: Anomura). *Proceedings of the Royal Society B: Biological Sciences,* 280(1764): 20130718. http://doi.org/10.1098/rspb.2013.0718

Rouse, GW. (2000). Bias? What bias? The evolution of downstream larval-feeding in animals. *Zoologica Scripta,* 29(3): 213–236. http://doi.org/10.1046/j.1463-6409.2000.00040.x

Rouse, GW, Goffredi, SK, & Vrijenhoek, RC. (2004). *Osedax*: Bone-Eating Marine Worms with Dwarf Males. *Science,* 305(5684): 668–671. http://doi.org/10.1126/science.1098650

Sahling, H, Wallmann, K, Dählmann, A, Schmaljohann, R, & Petersen, S. (2005). The physicochemical habitat of *Sclerolinum* sp. at Hook Ridge hydrothermal vent, Bransfield Strait, Antarctica. *Limnology and Oceanography,* 50(2): 598–606. http://doi.org/10.4319/lo.2005.50.2.0598

Salazar-Vallejo, SI, & Hutchings, P. (2012). A review of characters useful in delineating ampharetid genera (Polychaeta). *Zootaxa,* 3402(1): 45–53.

Schander, C, Rapp, HT, Halanych, KM, Kongsrud, JA, & Sneli, J-A. (2010a). A case of co-occurrence between *Sclerolinum* pogonophoran (Siboglinidae: Annelida) and *Xylophaga* (Bivalvia) from a north-east Atlantic wood-fall. *Marine Biodiversity Records,* 3: e43. http://doi.org/10.1017/S1755267210000394

Schander, C, Rapp, HT, Kongsrud, JA, Bakken, T, Berge, J, Cochrane, S, Oug, E, Byrkjedal, I, Todt, C, Cedhagen, T, Fosshagen, A, Gebruk, A, Larsen, K, Levin, L, Obst, M, Pleijel, F, Stöhr, S, Warén, A, Mikkelsen, NT, Hadler-Jacobsen, S, Keuning, R, Petersen, KH, Thorseth, IH, & Pedersen, RB. (2010b). The fauna of hydrothermal vents on the Mohn Ridge (North Atlantic). *Marine Biology Research,* 6(2): 155–171. http://doi.org/10.1080/17451000903147450

Schulze, A, & Halanych, KM. (2003). Siboglinid evolution shaped by habitat preference and sulfide tolerance. *Hydrobiologia,* 496(1): 199–205. https://doi.org/10.1023/A:1026192715095

Sen, A, Becker, EL, Podowski, EL, Wickes, LN, Ma, S, Mullaugh, KM, Hourdez, S, Luther, GW, & Fisher, CR. (2013). Distribution of mega fauna on sulfide edifices on the Eastern Lau Spreading Center and Valu Fa Ridge. *Deep Sea Research Part I: Oceanographic Research Papers,* 72(Supplement C): 48–60. https://doi.org/10.1016/j.dsr.2012.11.003

Sen, A, Podowski, EL, Becker, EL, Shearer, EA, Gartman, A, Yücel, M, Hourdez, S, Luther Iii, GW, & Fisher, CR. (2014). Community succession in hydrothermal vent habitats of the Eastern Lau Spreading Center and Valu Fa Ridge, Tonga. *Limnology and Oceanography,* 59(5): 1510–1528. http://doi.org/10.4319/lo.2014.59.5.1510

Sibuet, M, & Olu, K. (1998). Biogeography, biodiversity and fluid dependence of deep-sea cold-seep communities at active and passive margins. *Deep Sea Research Part II*

Topical Studies in Oceanography, 45(1-3): 517–567. http://doi.org/10.1016/s0967-0645(97)00074-x

Smirnov, RV. (2000). Two new species of Pogonophora from the arctic mud volcano off northwestern Norway. *Sarsia,* 85(2): 141–150. http://doi.org/10.1080/00364827.2000.10414563

Smith, CK, Kukert, H, Wheatcroft, RA, Jumars, PA, & Deming, JW. (1989). Vent fauna on whale remains. *Nature,* 341: 27–28. http://doi.org/10.3354/meps07972

Smith, CR, Baco, AR, & Glover, AG. (2002). Faunal succession on replicate deep-sea whale falls: time scales and vent-seep affinities. *Cahiers de Biologie Marine,* 43(3–4): 293–298.

Smith, CR, & Baco, AR. (2003). Ecology of whale falls at the deep-sea floor. *Oceanography and Marine Biology: an Annual Review,* 41: 311–354.

Smith, CR, Glover, AG, Treude, T, Higgs, ND, & Amon, DJ. (2015). Whale-fall ecosystems: recent insights into ecology, paleoecology, and evolution. *Annual Review of Marine Science,* 7: 571–596. https://doi.org/10.1146/annurev-marine-010213-135144

Smith, CR, Amon, DJ, Higgs, ND, Glover, AG, & Young, EL. (2017). Data are inadequate to test whale falls as chemosynthetic stepping-stones using network analysis: faunal overlaps do support a stepping-stone role. *Proceedings of the Royal Society B: Biological Sciences,* 284(1863). http://doi.org/10.1098/rspb.2017.1281

Stecher, J, Tunnicliffe, V, & Türkay, M. (2003). Population characteristics of abundant bivalves (Mollusca, Vesicomyidae) at a sulphide-rich seafloor site near Lihir Island, Papua New Guinea. *Canadian Journal of Zoology,* 81(11): 1815–1824. https://doi.org/10.1139/z03-180

Steen, IH, Dahle, H, Stokke, R, Roalkvam, I, Daae, F-L, Rapp, HT, Pedersen, RB, & Thorseth, IH. (2015). Novel Barite Chimneys at the Loki's Castle Vent Field Shed Light on Key Factors Shaping Microbial Communities and Functions in Hydrothermal Systems. *Frontiers in Microbiology,* 6: 4248. http://doi.org/10.3389/fmicb.2015.01510

Stewart, FJ, & Cavanaugh, CM. (2006). Bacterial endosymbioses in *Solemya* (Mollusca: Bivalvia)—Model systems for studies of symbiont–host adaptation. *Antonie Van Leeuwenhoek,* 90(4): 343–360. http://doi.org/10.1007/s10482-006-9086-6

Stiller, J, Rousset, V, Pleijel, F, Chevaldonné, P, Vrijenhoek, RC, & Rouse, GW. (2013). Phylogeny, biogeography and systematics of hydrothermal vent and methane seep *Amphisamytha* (Ampharetidae, Annelida), with descriptions of three new species. *Systematics and biodiversity,* 11(1): 35–65. http://dx.doi.org/10.1016/j.dsr2.2016.08.015

Stuart, CT, & Rex, MA. (2009). Bathymetric patterns of deep - sea gastropod species diversity in 10 basins of the Atlantic Ocean and Norwegian Sea. *Marine Ecology – an Evolutionary Perspective,* 30(2): 164–180. http://doi.org/10.1111/j.1439-0485.2008.00269.x

Sukumaran, J, & Knowles, LL. (2017). Multispecies coalescent delimits structure, not species. *Proceedings of the National Academy of Sciences,* 114(7): 1607–1612. http://doi.org/10.1073/pnas.1607921114

Sumida, PYG, Alfaro-Lucas, JM, Shimabukuro, M, Kitazato, H, Perez, JAA, Soares-Gomes, A, Toyofuku, T, Lima, AOS, Ara, K, & Fujiwara, Y. (2016). Deep-sea whale fall fauna from the Atlantic resembles that of the Pacific Ocean. *Scientific Reports,* 6: 22139. http://doi.org/10.1038/srep22139

Svavarsson, J, Stromberg, JO, & Brattegard, T. (1993). The deep-sea Asellote (Isopoda, Crustacea) fauna of the northern seas - species composition, distributional patters and origin. *Journal of Biogeography,* 20(5): 537–555. http://doi.org/10.2307/2845725

Tandberg, AH, Rapp, HT, Schander, C, Vader, W, Sweetman, AK, & Berge, J. (2012). Exitomelita sigynae gen. et sp nov.: a new amphipod from the Arctic Loki Castle vent field with potential gill ectosymbionts. *Polar Biology,* 35(5): 705–716. http://doi.org/10.1007/s00300-011-1115-x

Tandberg, AH, Rapp, HT, Schander, C, & Vader, W. (2013). A new species of *Exitomelita* (Amphipoda: Melitidae) from a deep-water wood fall in the northern Norwegian Sea. *Journal of Natural History,* 47(25–28). http://doi.org/10.1080/00222933.2012.725778

Tarasov, VG, Gebruk, AV, Mironov, AN, & Moskalev, LI. (2005). Deep-sea and shallow-water hydrothermal vent communities: Two different phenomena? *Chemical Geology,* 224(1–3): 5–39. http://doi.org/10.1016/j.chemgeo.2005.07.021

Teixeira, S, Cambon-Bonavita, M-A, Serrão, EA, Desbruyéres, D, & Arnaud-Haond, S. (2011). Recent population expansion and connectivity in the hydrothermal shrimp *Rimicaris exoculata* along the Mid-Atlantic Ridge. *Journal of Biogeography,* 38(3): 564–574. http://10.1111/j.1365-2699.2010.02408.x

Teixeira, S, Olu, K, Decker, C, Cunha, RL, Fuchs, S, Hourdez, S, Serrão, EA, & Arnaud-Haond, S. (2013). High connectivity across the fragmented chemosynthetic ecosystems of the deep Atlantic Equatorial Belt: efficient dispersal mechanisms or questionable endemism? *Molecular Ecology,* 22(18): 4663–4680. http://doi.org/10.1111/mec.12419

Thornhill, DJ, Struck, TH, Ebbe, B, Lee, RW, Mendoza, GF, Levin, LA, & Halanych, KM. (2012). Adaptive radiation in extremophilic Dorvilleidae (Annelida): diversification of a single colonizer or multiple independent lineages? *Ecology and evolution,* 2(8): 1958–1970. http://doi.org/10.1002/ece3.314

Thubaut, J, Puillandre, N, Faure, B, Cruaud, C, & Samadi, S. (2013). The contrasted evolutionary fates of deep-sea chemosynthetic mussels (Bivalvia, Bathymodiolinae). *Ecology and Evolution,* 3(14): 4748–4766. http://doi.org/10.1002/ece3.749

Thurber, AR, Levin, LA, Rowden, AA, Sommer, S, Linke, P, & Kröger, K. (2013). Microbes, macrofauna, and methane: A novel seep community fueled by aerobic methanotrophy. *Limnology and Oceanography,* 58(5): 1640–1656. http://doi.org/10.4319/lo.2013.58.5.1640

Tobler, M, Passow, CN, Greenway, R, Kelley, JL, & Shaw, JH. (2016). The Evolutionary Ecology of Animals Inhabiting Hydrogen Sulfide–Rich Environments. *Annual Review of Ecology, Evolution, and Systematics,* 47(1): 239–262. http://doi.org/10.1146/annurev-ecolsys-121415-032418

Treude, T, Smith, CR, Wenzhoefer, F, Carney, E, Bernardino, AF, Hannides, AK, Krueger, M, & Boetius, A. (2009). Biogeochemistry of a deep-sea whale fall: sulfate reduction, sulfide efflux and methanogenesis. *Marine Ecology Progress Series,* 382: 1–21. http://doi.org/10.3354/meps07972

Tunnicliffe, V, Juniper, SK, & Sibuet, M. (2003). Reducing environments of the deep-sea floor. In P. A. Tyler (Ed.), *Ecosystems of the deep oceans* (pp. 81–110). Amsterdam: Elsevier Science.

Turnipseed, M, Knick, KE, Lipcius, RN, Dreyer, J, & Van Dover, CL. (2003). Diversity in mussel beds at deep-sea hydrothermal vents and cold seeps. *Ecology Letters,* 6(6): 518–523. http://doi.org/10.1046/j.1461-0248.2003.00465.x

Van Dover, CL. (1995). Ecology of Mid-Atlantic Ridge hydrothermal vents. *Geological Society, London, Special Publications,* 87(1): 257–294. https://doi.org/10.1144/GSL.SP.1995.087.01.21

Van Dover, CL. (2000). *The ecology of deep-sea hydrothermal vents*. Princeton: Princeton University Press.

Van Dover, CL, Humphris, SE, Fornari, D, Cavanaugh, CM, Collier, R, Goffredi, SK, Hashimoto, J, Lilley, MD, Reysenbach, AL, Shank, TM, Von Damm, KL, Banta, A, Gallant, RM, Gotz, D, Green, D, Hall, J, Harmer, TL, Hurtado, LA, Johnson, P, McKiness, ZP, Meredith, C, Olson, E, Pan, IL, Turnipseed, M, Won, Y, Young, CR, & Vrijenhoek, RC. (2001). Biogeography and ecological setting of Indian Ocean hydrothermal vents. *Science,* 294(5543): 818–823. http://doi.org/10.1126/science.1064574

Van Dover, CL, German, CR, Speer, KG, Parson, LM, & Vrijenhoek, RC. (2002). Evolution and biogeography of deep-sea vent and seep invertebrates. *Science,* 295(5558): 1253–1257. http://doi.org/10.1126/science.1067361

Van Gaever, S, Raes, M, Pasotti, F, & Vanreusel, A. (2010). Spatial scale and habitat-dependent diversity patterns in nematode communities in three seepage related sites along the Norwegian Sea margin. *Marine Ecology,* 31(1): 66–77. http://dx.doi.org/10.1111/j.1439-0485.2009.00314.x

Vrijenhoek, RC. (2009). Cryptic species, phenotypic plasticity, and complex life histories: Assessing deep-sea faunal diversity with molecular markers. *Deep Sea Research Part II Topical Studies in Oceanography,* 56(19): 1713–1723. https://doi.org/10.1016/j.dsr2.2009.05.016

Vrijenhoek, RC, Johnson, SB, & Rouse, GW. (2009). A remarkable diversity of bone-eating worms (*Osedax*; Siboglinidae; Annelida). *BMC Biology,* 7(1): 74. https://doi.org/10.1186/1741-7007-7-74

Vrijenhoek, RC. (2010). Genetic diversity and connectivity of deep-sea hydrothermal vent metapopulations. *Molecular Ecology,* 19(20): 4391–4411. http://doi.org/10.1111/j.1365-294X.2010.04789.x

Watanabe, H, Fujikura, K, Kojima, S, Miyazaki, J-I, & Fujiwara, Y. (2010). Japan: Vents and Seeps in Close Proximity. In S. Kiel (Ed.), *The Vent and Seep Biota* (pp. 379–401). Netherlands: Springer.

Weersing, K, & Toonen, RJ. (2009). Population genetics, larval dispersal, and connectivity in marine systems. *Marine Ecology Progress Series,* 393: 1–12. http://doi.org/10.3354/meps08287

Weigert, A, Helm, C, Meyer, M, Nickel, B, Arendt, D, Hausdorf, B, Santos, SR, Halanych, KM, Purschke, G, Bleidorn, C, & Struck, TH. (2014). Illuminating the Base of the Annelid Tree Using Transcriptomics. *Molecular Biology and Evolution,* 31(6): 1391. http://dx.doi.org/10.1093/molbev/msu080

Wolff, T. (2005). Composition and endemism of the deep-sea hydrothermal vent fauna. *Cahiers de Biologie Marine,* 46(2): 97–104.

Won, Y, Young, CR, Lutz, RA, & Vrijenhoek, RC. (2003). Dispersal barriers and isolation among deep-sea mussel populations (Mytilidae: *Bathymodiolus*) from eastern Pacific hydrothermal vents. *Molecular Ecology,* 12(1): 169–184. http://doi.org/10.1046/j.1365-294X.2003.01726.x

Zottoli, RA. (1982). Two new genera of deep sea polychaete worms of the family Ampharetidae and the role of one species in deep sea ecosystems. *Proceedings of the Biological Society of Washington,* 95(1): 48–57.

Zottoli, RA. (1983). *Amphisamytha galapagensis*, a new species of ampharetid polychaete from the vicinity of abyssal hydrothermal vents in the Galapagos Rift, and the role of this species in rift ecosystems. *Proceedings of the Biological Society of Washington,* 96(3): 379–391.

Publications

I

Deep-Sea Research II 137 (2017) 232–245

Contents lists available at ScienceDirect

Deep-Sea Research II

journal homepage: www.elsevier.com/locate/dsr2

New species of Ampharetidae (Annelida: Polychaeta) from the Arctic Loki Castle vent field

Jon A. Kongsrud [a,*], Mari H. Eilertsen [b,c], Tom Alvestad [a], Katrine Kongshavn [a], Hans Tore Rapp [b,c,d]

[a] Department of Natural History, University Museum of Bergen, P.O. Box 7800, N-5020 Bergen, Norway
[b] Department of Biology, University of Bergen, Norway
[c] Centre for Geobiology, University of Bergen, Norway
[d] Uni Research, Uni Environment, Bergen, Norway

ARTICLE INFO

Available online 4 September 2016

Keywords:
Vent fauna
Norwegian Sea
Arctic Mid Ocean Ridge
Black smokers
Molecular phylogeny
Paramytha
new genus
Pavelius

ABSTRACT

Ampharetid polychaetes adapted to live in chemosynthetic environments are well known from the deep Pacific and Atlantic Oceans, but to date no such species have been reported from the Arctic Ocean. Here, we describe two new species, *Paramytha schanderi* gen. et sp. nov. and *Pavelius smileyi* sp. nov., from the Arctic Loki's Castle vent field on the Knipovich Ridge north–east of the island of Jan Mayen. The new species are both tube-builders, and are found in a sedimentary area at the NE flank of the vent field, characterized by low-temperature venting and barite chimneys. The new genus, *Paramytha*, is characterized by a prostomium without lobes or glandular ridges, smooth buccal tentacles, four pairs of cirriform branchiae arranged as 2+1+1 without median gap dorsally on segments II–IV, absence of chaetae (paleae) on segment II, and absence of modified segments. *P. smileyi* sp. nov. is placed in the previously monotypic genus *Pavelius*, primarily based on the presence of a rounded prostomium without lobes and four pairs of branchiae arranged in a single transverse row without median gap dorsally on segment III. *Pavelius smileyi* sp. nov. differs from the type species, *Pavelius uschakovi*, in the number of thoracic and abdominal chaetigers, and the absence of chaetae (paleae) on segment II. The phylogenetic position of the two new species from Loki's Castle is further explored by use of molecular data. New sequences of mitochondrial (16S rDNA and cytochrome c oxidase subunit 1, COI) and nuclear (18S rDNA) markers have been produced for both species from Loki's Castle, as well as for specimens identified as *Paramytha* sp. from Setùbal Canyon off Portugal, and for the following species: *Pavelius uschakovi*, *Grassleia* cf. *hydrothermalis*, *Sosane wireni*, *Amphicteis ninonae* and *Samythella neglecta*. Results from phylogenetic analysis, including 22 species and 12 genera of Ampharetidae, recovered *Paramytha* gen. nov. as monophyletic with maximum support, and a close relationship between the genera *Pavelius* and *Grassleia* which together form a well supported monophyletic clade.

1. Introduction

The family Ampharetidae is the second largest family within the order Terebellida with more than 300 species and 100 genera described (Jirkov, 2011). The family has a world-wide distribution and is well represented in deep-sea environments, often as one of the more dominant families of polychaetes in soft bottom habitats (Rouse and Pleijel, 2001). Ampharetid polychaetes are also well known from chemosynthetic environments such as hydrothermal vents and cold seeps (Reuscher et al., 2009; Stiller et al., 2013; Thurber et al., 2013), as well as from organic falls (Zottoli, 1982; Bennet et al., 1994; Queiros et al., 2017). To date, there are no records of ampharetids considered as obligate to chemosynthetic environments from the Arctic or the Antarctic. However, recent identification of fauna samples from the Arctic Loki's Castle hydrothermal vent field at 2350 m depth on the Mohn–Knipovich ridge north–east of Jan Mayen has documented a total of 14 species of polychaetes, including two ampharetids. Unlike the more shallow water hydrothermal vent sites in the Arctic (Fricke et al., 1989; Schander at al., 2010), the fauna at Loki's Castle has been shown to be endemic and highly adapted to the chemosynthetic environment (Pedersen et al., 2010; Tandberg et al., 2012). Until now, only the two dominating polychaetes, the siboglinid *Sclerolinum contortum* Smirnov, 2000 and the maldanid *Nicomache lokii* Kongsrud and Rapp, 2012 have been reported (Pedersen

* Corresponding author.
E-mail address: Jon.Kongsrud@uib.no (J.A. Kongsrud).

http://dx.doi.org/10.1016/j.dsr2.2016.08.015

Table 1
PCR and sequencing primers.

Marker	Primer name	Sequence 5′-3′	Direction	Source
COI	LCO1490	GGTCAACAAATCATAAAGATATTGG	Forward	Folmer et al. (1994)
	HCO2198	TAAACTTCAGGGTGACCAAAAATCA	Reverse	–
16S	16Sar-L	CGCCTGTTTATCAAAAACAT	Forward	Palumbi et al. (1991)
	16Sbr-H	CCGGTCTGAACTCAGATCACGT	Reverse	–
18S	18e	CTGGTTGATCCTGCCAGT	Forward	Hillis and Dixon (1991)
	18L	GAATTACCGCGGCTGCTGGCACC	Reverse	Halanych et al. (1995)
	18F509	CCCCGTAATTGGAATGAGTACA	Forward	Struck et al. (2002)
	18R	GTCCCCTTCCGCAATTYCTTTAAG	Reverse	Passamaneck et al. (2004)
	18F997	TTCGAAGACGATCAGATACCG	Forward	Struck et al. (2002)
	18R1843	GGATCCAAGCTTGATCCTTCTGCAGGTTCACCTAC	Reverse	Struck et al. (2005), modified from Cohen et al. (1998)

et al., 2010; Kongsrud and Rapp, 2012), and several of the remaining species are considered new to science.

In the present study, we formally describe two new species of Ampharetidae from the Loki's Castle vent field. The most abundant one belongs to the subfamily Ampharetinae, but based on morphological characteristics the species could not be further identified to any hitherto described genera, and consequently a new genus has been proposed. The other ampharetid species found at Loki's Castle is described as a new species of *Pavelius* Kuznetsov and Levenstein, 1988, a genus originally described from cold seeps in the Sea of Okothsk, NW Pacific. The genus *Pavelius* was considered a junior synonym to *Phyllocomus* Grube, 1877 by Jirkov (2011), but is here recognized as a valid genus, now containing two species. An emended diagnosis of the genus *Pavelius* is provided.

The phylogenetic relationships of the new species from Loki Castle with other ampaharetids have been further explored by use of molecular data. DNA sequences of mitochondrial (16S rDNA and cytochrome c oxidase subunit 1, COI) and nuclear (18S rDNA) markers were produced for the two new species described herein, as well as for six other species, including specimens identified as *Paramytha* sp. from Setùbal Canyon, Portugal (see Queiros et al. (2017)), and *Pavelius uschakovi* Kuznetsov and Levenstein, 1988. A concatenated phylogenetic analysis, including additional data from GenBank for 14 ampharetids, is presented.

2. Material and methods

2.1. Sample collection and morphological analysis

All samples were collected from the Loki's Castle vent field (Fig. 1) using the "Bathysaurus" XL remotely operated vehicle (ROV) provided by Argus Remote Systems during cruises with the R/V *G. O. Sars* in July 2008, August 2009, and July 2010. The fauna samples were sorted into main groups on board and fixed in either 96% ethanol or 6% buffered formaldehyde.

In the laboratory, specimens were examined by use of a Leica MZ Stereomicroscope and a Leica DM 6000 B compound microscope. A Leica M205C stereo microscope was used to make digital photos of specimens. The Leica LAS software was used to make compound images with the 'Z-stack' option. SEM micrographs were taken using a ZEISS Supra 55VP SEM on dried and gold/palladium coated material in the Laboratory for Electron Microscopy, University of Bergen. Final editing of plates and drawings were prepared in Adobe Photoshop and Illustrator version CS5. All examined specimens, including types, have been deposited in the Department of Natural History, University Museum of Bergen, Norway (ZMBN).

2.2. Taxon sampling for the molecular phylogenetic analysis

New DNA-sequences were produced for four specimens of *Pavelius smileyi* sp. nov. and three specimens of *Paramytha schanderi* gen. et sp. nov, in addition to four specimens identified as *Paramytha* sp. collected from mammal bones in the Setùbal Canyon off Portugal (see Queiros et al. (2017)), and for one specimen of each of the following species: *Pavelius uschakovi* Kuznetsov and Levenstein, 1988, *Grassleia* cf. *hydrothermalis* Solis-Weiss, 1993, *Samythella neglecta* Wollebaek, 1912, *Amphicteis ninonae* Jirkov, 1985 and *Sosane wireni* (Hessle, 1917) (Table 2). DNA voucher specimens are located at the Department of Natural History, University Museum of Bergen, apart from the *Grassleia* specimen, which is housed at the Scripps Oceanography Benthic Invertebrate Collection (SIO-BIC). Available sequences of *Amphisamytha* spp. and other ampharetids from non-chemosynthetic habitats were downloaded from GenBank, as well as species from Alvinellidae and Terebellidae as outgroups. In total 33 terminals, representing 22 species and 12 genera of ampharetids were included in the analysis.

2.3. DNA extraction, amplification and sequencing

The mitochondrial genetic markers cytochrome c oxidase subunit I (COI) and 16S rRNA (two primers each, see Table 1), and the nuclear marker 18S rRNA (six primers in three pairs, see Table 1) were chosen for the phylogenetic analysis.

DNA was extracted using the QIAGEN DNeasy Blood and Tissue Kit, following the manufacturer's protocol (spin-column protocol). The PCR reaction contained 2.5 µL CoralLoad buffer from QIAGEN, 1 µL MgCl (QIAGEN, 25 mM), 2 µL dNTP (TaKaRa, 2.5 mM of each dNTP), 1 µL of each of the primers (10 µM solution), 0.15 mL TaKaRa HS Taq, 1 or 2 µL DNA extract and ddH2O to make the total reaction volume 25 µL. PCR cycling profiles were as follows: COI – 5 min at 95 °C, 5 cycles with 45 s at 95 °C, 45 s at 45 °C, and 1 min at 72 °C, followed by 35 cycles of 45 s at 95 °C, 45 s at 51 °C, and 1 min at 72 °C, and finally 10 min at 72 °C. 16S – 5 min at 95 °C, 35 cycles with 30 s at 95 °C, 30 s at 50 °C, and 1.5 min at 72 °C, and finally 10 min at 72 °C. 18S – 3 min at 94 °C, 35 cycles with 1 min at 94 °C, 1.5 min at 42 °C, and 2 min at 72 °C, and finally 7 min at 72 °C.

Quality and quantity of PCR products was assessed by gel electrophoresis imaging using a FastRuler DNA Ladder (Life Technologies) and GeneSnap and GeneTools (SynGene) for image capture and band quantification. Successful PCRs were purified using Exonuclease 1 (EXO, 10 U mL–1) and Shrimp Alkaline Phosphatase (SAP, 10 U mL–1, USB Europe, Germany) in 10 µL reactions (0.1 mL EXO, 1 µL SAP, 0.9 µL ddH2O, and 8 µL PCR product). Samples were incubated at 37 °C for 15 min followed by an inactivation step at 80 °C for 15 min. The purified PCR products were sequenced using BigDye v3.1 (Life Technologies) and run on

Table 2
Specimens used for phylogenetic analyses with museum voucher number, sampling location and GenBank accession numbers of sequences included in present study.

Species	Voucher	Location	COI	16S	18S
Terebellidae					
Polycirrus carolinensis Day, 1973	SIO-BIC A1101	Curlew Bank, Belize	JX423769	JX423681	JX423651
Terebella lapidaria Linnaeus, 1767	SIO-BIC A1102	Plymouth, UK	JX423771	JX423683	JX423653
Alvinellidae					
Alvinella caudata Desbruyères and Laubier, 1986	SIO-BIC A1092	German Flats, E.P.R.	JX423737	JX423669	JX423641
Ampharetidae, Mellininnae					
Mellinna albicincta Mackie and Pleijel, 1995	SIO-BIC A1113	Trondheimsfjord, Norway	JX423767	JX423679	JX423649
Ampharetidae, Ampharetinae					
Ampharete finmarchica (Sars, 1865)	SIO-BIC A1100	Hornsunddjupet, Svalbard	JX423738	JX423670	JX423642
Ampharete octocirrata (Sars, 1835)	SIO-BIC A1109	Trondheimsfjord, Norway	JX423770	JX423682	JX423652
Amphicteis ninonae Jirkov, 1985	ZMBN 95441	Norwegian Sea	KX497038	KX513562	–
Amphisamytha julianeae Stiller et al., 2013	–	North Fiji Basin, W. Pacific	JX423763	JX423676	JX423647
Amphisamytha bioculata (Moore, 1906)	SIO-BIC A2524	San Nicholas Is., CA, USA	JX423685	JX423654	JX423634
Amphisamytha caldarei Stiller et al., 2013	SIO-BIC A2576-7	South Cleft, Juan de Fuca	JX423726	JX423664	JX423638
Amphisamytha fauchaldi Solís-Weiss and Hernández-Alcántara, 1994	SIO-BIC A2563	Hydrate Ridge, OR, USA	JX423699	JX423658	JX423636
Amphisamytha galapagensis Zottoli, 1983	–	German Flats, E.P.R.	JX423711	JX423662	JX423637
Amphisamytha jacksoni Stiller et al., 2013	–	South Cleft, Juan de Fuca	JX423758	JX423675	JX423646
Amphisamytha lutzi (Desbruyères and Laubier, 1996)	SIO-BIC A2530	Rainbow, Mid-Atlantic Ridge	JX423736	JX423667	JX423639
Amphisamytha vanuatuensis Reuscher et al., 2009	–	Lau Back-Arc Basin, W. Pacific	JX423741	JX423673	JX423645
Anobothrus gracilis Malmgren, 1866	SIO-BIC A1106	Trondheimsfjord, Norway	JX423739	JX423671	JX423643
Eclysippe vanelli (Fauvel, 1936)	SIO-BIC A1108	Trondheimsfjord, Norway	JX423766	JX423678	JX423648
Grassleia cf. *hydrothermalis* Solís-Weiss, 1993	SIO-BIC A6137	Pinkie's Vent, Gulf of California	KX497032	KX513552	KX513568
Paramytha schanderi gen. et sp. nov.	ZMBN 87801	Loki's Castle vent field	–	KX513556	KX513572
Paramytha schanderi gen. et sp. nov.	ZMBN 87820	Loki's Castle vent field	KX497035	KX513555	KX513571
Paramytha schanderi gen. et sp. nov.	ZMBN 87821	Loki's Castle vent field	–	KX513559	KX513575
Paramytha sp.	ZMBN 107232	Setùbal Canyon, Portugal	–	KX513547	KX513563
Paramytha sp.	ZMBN 207233	Setùbal Canyon, Portugal	–	KX513548	KX513564
Paramytha sp.	ZMBN 107234	Setùbal Canyon, Portugal	–	KX513549	KX513565
Paramytha sp.	ZMBN 107236	Setùbal Canyon, Portugal	–	KX513550	KX513566
Pavelius smileyi sp. nov.	ZMBN 87807	Loki's Castle vent field	KX497034	KX513554	KX513570
Pavelius smileyi sp. nov.	ZMBN 87809	Loki's Castle vent field	–	KX513557	KX513573
Pavelius smileyi sp. nov.	ZMBN 87810	Loki's Castle vent field	KX497036	KX513558	KX513574
Pavelius smileyi sp. nov.	ZMBN 87825	Loki's Castle vent field	KX497037	KX513560	KX513576
Pavelius uschakovi Kuznetsov and Levenstein, 1988	ZMBN 108241	Okhotsk Sea, Russia	KX497033	KX513553	KX513569
Samythella neglecta Wollbaek, 1912	ZMBN 99276	Norwegian Sea	–	KX513551	KX513567
Sosane wahrbergi (Eliason, 1955)	SIO-BIC A1118	Gullmarsfjorden, Sweden	JX423768	JX423680	JX423650
Sosane wireni (Hessle, 1917)	ZMBN 95447	Lysefjorden, Norway	KX497039	KX513561	KX513577

an Automatic Sequencer 3730XL at the sequencing facility of the Institute of Molecular Biology, University of Bergen.

2.4. Alignments and phylogenetic analysis

Sequences were assembled using Geneious (Biomatters Ltd.), checked for potential contamination using BLAST (Altschul et al., 1990) and have been deposited in GenBank (Table 2).

COI sequences were aligned using MUSCLE (Edgar, 2004), and 16S and 18S sequences were aligned using MAFFT (Katoh and Standley, 2013) with the Q-INS-i method. Blocks of ambigous data were identified and excluded from the 16S and 18S alignments using Gblocks with relaxed settings (Kück et al., 2010; Talavera and Castresana, 2007; for settings see Table 3). Saturation was tested for the first, second and third codon positions of the COI gene by plotting pairwise uncorrected p-distances against total substitutions (transitions+transversions), but no saturation was detected. Pairwise genetic distances for COI and 16S were calculated in Geneious (Biomatters Ltd). For 16S distances were calculated on the alignment after trimming with Gblocks. The best-fitting model of evolution for each gene was found using JModelTest 2.1.4 (Darriba et al., 2012; Guindon and Gascuel, 2003). For all genes the GTR+I+G model was considered the best fit according to the Akaike Information Criterion, but due to statistical concerns regarding the coestimation of the gamma and invariant-site parameters (discussed in the RAxML manual; Stamatakis, 2008) the GTR+G model was chosen instead.

Table 3
Settings for Gblocks analysis of 16S and 18S alignment.

	16S	18S
Minimum number of sequences for conserved positions	17	17
Minimum number of sequences for flank positions	17 (28)	17 (27)
Maximum number of contigs at non-conserved positions	10 (8)	10 (8)
Minimum length of block	5 (10)	5 (10)
Allowed gap positions	all (none)	all (none)
Original number of positions	880	1969
Number of positions in Gblocks alignment	622	1842

Single gene and concatenated datasets (with missing data coded as "?") were analyzed in MrBayes (Huelsenbeck and Ronquist, 2001; Ronquist and Huelsenbeck, 2003) with two parallel runs of 5 million generations for the single gene datasets and 10 million generations for the concatenated dataset. Convergence of runs was checked using Tracer v1.5 (Rambaut and Drummond, 2009) and the burn-in was set to 10%. Consensus phylograms were generated in MrBayes, annotated and converted to graphics in Figtree 1.3.1 (Rambaut, 2012), and final adjustments were made in Adobe Illustrator CS6.

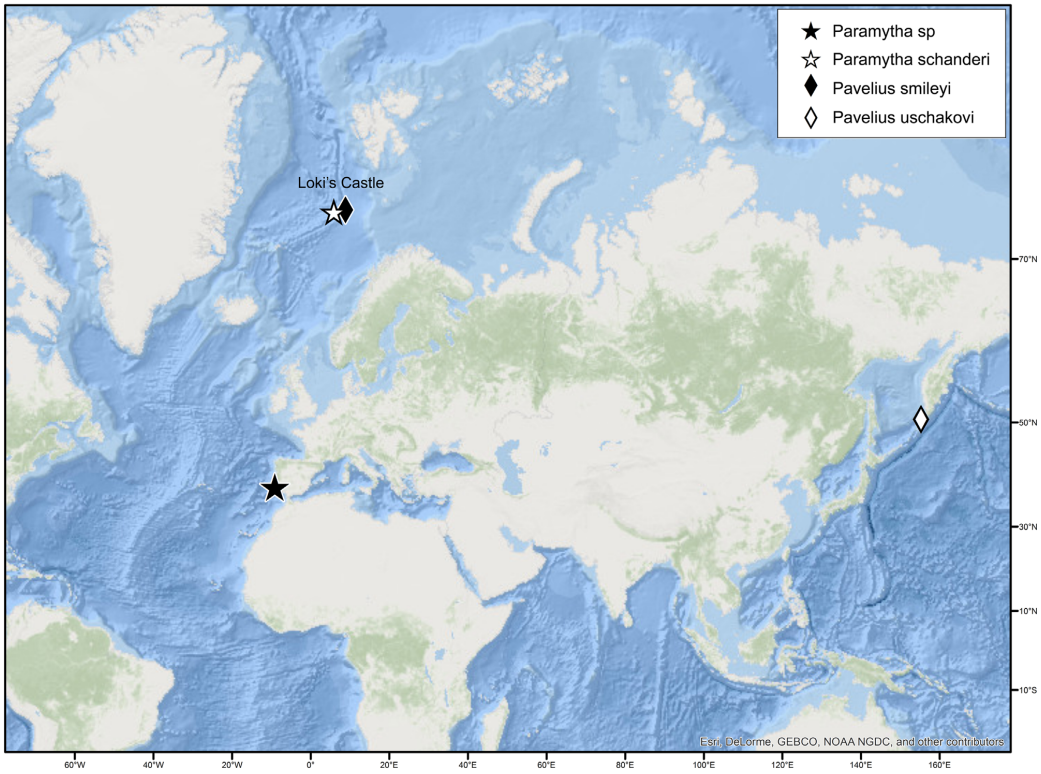

Fig. 1. Map showing records of species referred to *Paramytha* gen. nov. and *Pavelius* Kuznetsov and Levenstein, 1988. Exact localities: Loki's Castle hydrothermal vent field, 73°33'N 08°09'E, 2350 m depth; Off Island Paramushir (Kuril islands), south-eastern part of the Sea of Okhotsk, 50°30.88'N 155°18.14'E, 800 m depth, cold seeps; Setúbal Canyon, NE Atlantic off Portugal, 38°16.850N 09°06.680'W, 1000 m depth, mammal bones.

3. Results

3.1. Molecular phylogenetic analyses

We were not able to amplify COI for all species (see Table 2), but 16S and 18S was successfully sequenced for all specimens except *Amphicteis ninonae*, for which amplification of 18S failed. The Gblocks analysis excluded 258 positions from the 16S alignment and 127 positions from the 18S alignment (Table 3).

COI intraspecific genetic distances for *Pavelius smileyi* sp. nov. was $<0.3\%$, while the closest related species, *Grassleia* cf. *hydrothermalis*, differed by 13.1%. The single COI sequence of *Paramytha schanderi* gen. et sp. nov. was 14.6% different from the closest species, *Ampharete octocirrata*. For the entire COI dataset, the lowest interspecific distance was 12.6% between *Amphisamytha fauchaldi* and *Amphisamytha lutzi*. For 16S the sequences of *Paramytha schanderi* gen. et sp. nov. diverged by 0.4–1.1%, while the distance to the closest species (*Paramytha* sp.) ranged between 17.6% and 19.4%. The sequences of *Paramytha* sp. diverged by 0–0.4%. The 16S sequences of *Pavelius smileyi* sp. nov. diverged by 0–0.4%, and the distance to the closest species, *Pavelius uschakovi*, was 15%. In the entire 16S dataset, the closest interspecific distance was 9.7% between *Amphisamytha lutzi* and *Amphisamytha caldarei*.

The single gene trees and the combined tree all recovered *Pavelius smileyi* sp. nov., *Paramytha schanderi* gen. et sp. nov. and *Paramytha* sp. as monophyletic with maximum support, and *Paramytha schanderi* gen. et sp. nov. and *Paramytha* sp. as sister species (Fig. 2; Supplementary Material, Figs S1–S3). The concatenated tree recovers Ampharetidae as paraphyletic with high support, with *Melinna albicincta* (Ampharetidae, Melinninae) as sister to *Alvinella caudata* (Alvinellidae)+Ampharetinae, and with both *Paramytha* gen. nov. and *Pavelius* recovered well within the subfamily Ampharetinae. *Paramytha* gen. nov. shows no close connection to any of the other genera included in the analysis. In the combined tree *Pavelius smileyi* sp. nov. is recovered in a well-supported clade together with *Pavelius uschakovi* and *Grassleia* cf. *hydrothermalis*., but the internal relationships between these tree species are not resolved. It is interesting to note that *Ampharete finmarchica* and *Ampharete octocirrata* are not recovered together, and neither are *Sosane wireni* and *Sosane wahrbergi*.

3.2. Systematics

Family Ampharetidae Malmgren, 1866.
Subfamily Ampharetinae Malmgren, 1866.

3.2.1. Genus *Paramytha* gen. nov

Type species: *P. schanderi* sp. nov.
Additional species: *Paramytha* sp. (Queiros et al., 2017).

3.2.1.1. Diagnosis. Prostomium rectangular with thickened anterior margin, without lobes or glandular ridges. Buccal tentacles smooth. Four pairs of cirriform branchiae arranged as 2+1+1 on segments II–IV respectively; two anterior pairs in transverse row

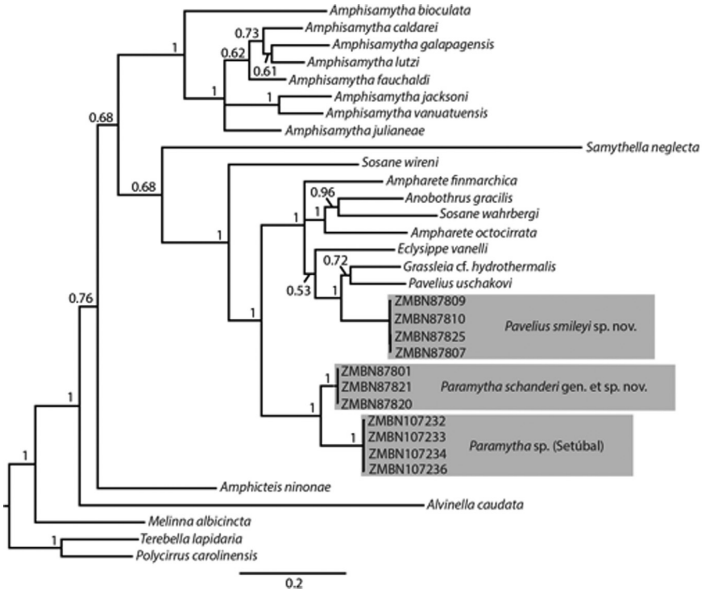

Fig. 2. Phylogenetic tree inferred from analysis of combined dataset (COI, 16S and 18S) in MrBayes. Node labels are posterior probabilities (PP) and nodes with less than 0.5 PP have been collapsed.

without median gap. Chaetae on segment II (paleae) absent. Number of thoracic and abdominal chaetigers interspecifically variable. Modified segments absent. Abdominal neuropodia gradually increasing in size forming pinnules from about 4th abdominal chaetiger. Anal cirri absent.

3.2.1.2. Etymology. The generic name is based on the stem "amytha" as commonly used in ampharetid nomenclature. Gender female.

3.2.1.3. Remarks. The generic diagnosis is based on the type species and on specimens identified as *Paramytha* sp. collected from the Setúbal Canyon off the coast of Portugal in 1000 m depth, dwelling on mammal bones (Queiros et al., 2017). *Paramytha* sp. is morphologically similar to *P. schanderi* gen. et sp. nov. in most respects, but differs most noticeably in the number of thoracic and abdominal chaetigers. In *P. schanderi* gen et sp. nov., 15 thoracic and up to 20 abdominal chaetigers are present compared to 20 thoracic and up to 12 abdominal chaetigers in specimens identified as *Paramytha* sp. from Setúbal Canyon. The inclusion of the specimens from Setúbal Canyon as a separate species in *Paramytha* is supported by molecular data (see Section 3.1).

Paramytha gen. nov. appears to be related to *Phyllocomus* Grube, 1877 and *Orochi* Reuscher et al., 2015, and these genera share the presence of a prostomium without lobes and glandular ridges, four pairs of branchiae, absence of chaetae on segment II (paleae), and absence of modified segments. However, the shape of the prostomium here described for *Paramytha* gen. nov., being rectangular with a thickened anterior margin is distinctly different from the spade-like prostomium described for *Orochi* and *Phyllocomus* (Reuscher et al., 2015). *Orochi* and *Phyllocomus* differ further from *Paramytha* gen. nov. by the presence of a high membrane connecting the branchiae. *Phyllocomus* differ from *Paramytha* gen. nov. and *Orochi* in the presence of strongly modified branchiae, and *Orochi* differs from *Paramytha* gen. nov., and all other ampharetids, in that the neuropodia of the last thoracic chaetiger are of the same shape as abdominal pinnules (Reuscher et al., 2015). The segmental arrangement of the four pairs of branchiae in *Paramytha* as 2+1+1 on segment II–IV is characteristic, and differs from the more common arrangement in the ampharetids, including *Orochi* and *Phyllocomus*, where the branchiae are located on only 1 or 2 segments (see e.g. Holthe (1986), Reuscher et al. (2009, 2015)). Within Ampharetinae, *Decemunciger* Zottoli, 1982 seems to be the only other genus with four pairs of cirriform branchiae arranged segmentally as 2+1+1, and with only a small median gap between the two groups of branchiae (Zottoli, 1982). Segmental arrangement of branchiae is also seen in some species referred to *Amage* Malmgren, 1866 and *Grubianella* McIntosh, 1885, but in these genera the two groups of branchiae are well separated by a wide median gap (e.g. Holthe, 1986; Schüller and Jirkov, 2013). *Decemunciger* is also similar to *Paramytha* gen. nov. by the lack of chaetae on segment II (paleae) and presence of smooth buccal tentacles (Zottoli, 1982). However, *Decemunciger* differs from *Paramytha* gen. nov by the presence of a lobed prostomium (Zottoli, 1982).

Based on the morphological characteristics we conclude that *P. schanderi* gen. et sp. nov. and the related species from Setúbal Canyon off Portugal cannot be placed in any previously described genus, hence a new genus is proposed.

3.2.2. Paramytha schanderi sp. nov

Figs. 3–5 and 9.

3.2.2.1. Type locality. Loki Castle vent field, 73°33'N 08°09'E, 2350 m depth.

3.2.2.2. Type material. Type locality, from sedimentary area with low-temperature diffuse venting with barite chimneys, R/V "G.O. Sars" H2DEEP cruise 2009 sample ROV-8, 07 August 2009, fixed in 96% ethanol, holotype (ZMBN 87798), 7 paratypes in 96% ethanol (ZMBN 87800, 87802, 87803, 87815, 87821, 87823, 87824) and 1 paratype mounted for SEM (ZMBN 87799).

Fig. 3. *Paramytha schanderi* gen. et sp. nov. (A) holotype (ZMBN 87798), lateral view; (B) paratype (ZMBN 87800), partly in tube; (C) paratype (ZMBN 87799-1), stained in methyl blue, ventral and partly lateral view; (D) Same, dorsal view. Scale bars: 1.0 mm.

3.2.2.3. Additional material. Type locality: R/V "G.O. Sars" BIODEEP cruise 2008, sample ROV-11, 14 July 2008, fixed in 96% ethanol: 4 spms (ZMBN 87817–87820). R/V "G.O. Sars" CGB DEEP cruise 2010: Sample ROV-05, 16 July 2010, fixed in 96% ethanol: 2 specimens, both partly damaged (ZMBN 87814), 1 complete specimen (ZMBN 87827); Sample ROV-09, 18 July 2010, fixed in 96% ethanol: 6 spms (ZMBN 87797, 87801, 87804–87806, 87816).

3.2.2.4. Diagnosis. A *Paramytha* with 15 thoracic and up to 20 abdominal chaetigers.

3.2.2.5. Description. Holotype, complete female with 15 thoracic and 19 abdominal chaetigers, 10 mm long and 1.5 mm wide in thorax (Fig. 3A). Other complete specimens are up to 18 mm long and 2.2 mm wide in thorax, with 15 thoracic and 18–20 abdominal chaetigers. Color in ethanol pale. All specimens examined with buccal tentacles partly or fully extended. Prostomium and peristomium fused, not sub-divided in lobes, almost rectangular in shape with wide anterior, thickened margin (Fig. 4A–D). Prostomium without glandular ridges; possible nuchal organs as small depressions dorsally on posterior part of prostomium. Eyespots absent. Buccal tentacles smooth, cylindrical, longitudinally grooved, some with swollen base (may be related to fixation) (Fig. 3A); buccal tentacles inserted on large tentacular membrane (Fig. 4B). Four pairs of branchiae; branchiae about 1/3–1/4 of body length, cylindrical (Fig. 3A). Branchiostyles loosely attached to branchiophores, often lost. Branchiophores as distinct lobes firmly attached to body wall (Fig. 4A–D). Branchial arrangement 2+1+1 dorsally on segments II–IV, respectively (Figs. 4A–D, 9A). Two anterior pairs arranged closely together in transverse row without median gap; 3rd pair with distinct median gap; 4th pair, in lateral position dorsally to notopodia on segment IV (chaetiger 2). Innermost branchiae of anterior pairs originating from segment II, outermost branchiae of anterior pairs originating from segment III. Third pair originating from segment IV and posterior pair

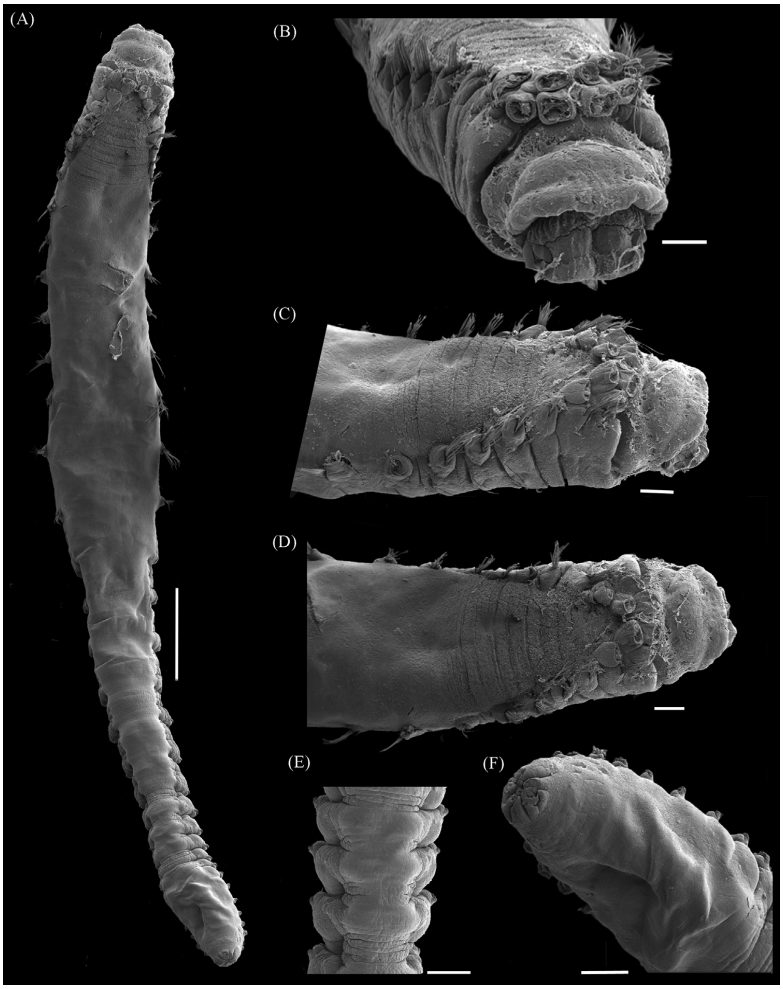

Fig. 4. *Paramytha schanderi* gen. et sp. nov. SEM micrographs of paratype (ZMBN 87799-2), branchiae and buccal tentacles lost: (A) complete specimen, dorsal view; (B) head and anterior part of body, frontal view; (C) same, dorso-lateral view; (D) same, dorsal view; (E) abdominal chaetigers 7–10, dorsal view. (F) posterior part of body and pygidium, dorsal view. Scale bars: (A) 1.0 mm; (B–F) 0.2 mm.

originating from segment V (Fig. 9A). Nephridial papillae not observed. Body cylindrical with thorax and abdomen of similar length (Figs. 3C–D, 4A). Segments II–IV appear as fused (Fig. 4C), but all three segments discernible when stained in methyl blue (Fig. 3C); segmentation indistinct dorsally in mid-body segments (Fig. 4A). Segment II without chaetae (paleae). A total of 15 thoracic segments with notopodia and capillary chaetae, starting on segment III (Fig. 4A); last 12 chaetigers of thorax with neuropodial tori bearing single row of uncini. Notopodia as rounded lobes, anterior 7 distinctly set off from body, remaining notopodia less developed and close to body wall (Fig. 3A). Notopodia of anterior two chaetigers less developed than notopodia in chaetigers 3–7 (Fig. 4C). Anterior 2–3 notopodia in dorsal position, lateral to group of branchiae; notopodia of chaetiger 4–7 gradually shifting to more lateral position; remaining notopodia in lateral position (Figs. 3A, 4A, C). Notochaetae arranged in vertical rows with alternating short and long chaetae; all notochaetae hirsute, with narrow brim (Fig. 5A–B). Neuropodial tori oval in shape in anterior uncingerous segments, becoming smaller and more rounded in posterior part of thorax. Thoracic uncini with 15–20 teeth arranged in 3–4 horizontal arcs above main rostrum and basal prow (Fig. 5C). Abdomen muscular with distinct ventral longitudinal groove, interrupted with small transverse segmental ridges (Fig. 3C). Abdominal neuropodia gradually increase in size forming pinnules from about 4th abdominal chaetiger, without papillae or cirri. Abdominal neuropodia with dorsal thickened ridge (Fig. 4E). Abdominal uncini with numerous teeth arranged in 5 horizontal arcs above rostrum and basal prow (Fig. 5D–E). Anal opening terminal, surrounded with small papillae or tissue-folds (Fig. 4F); anal cirri absent. Tube flexible, up to about 50 mm in length, with inner thin transparent organic layer, incrusted with fine-particulate material, pieces of polychaete tubes and small shell fragments (Fig. 3B). Head and thorax generally deeply dyed in methyl blue except branchial region, parapods and nuchal organs (Fig. 3C–D). Posterior part of body without distinct staining pattern.

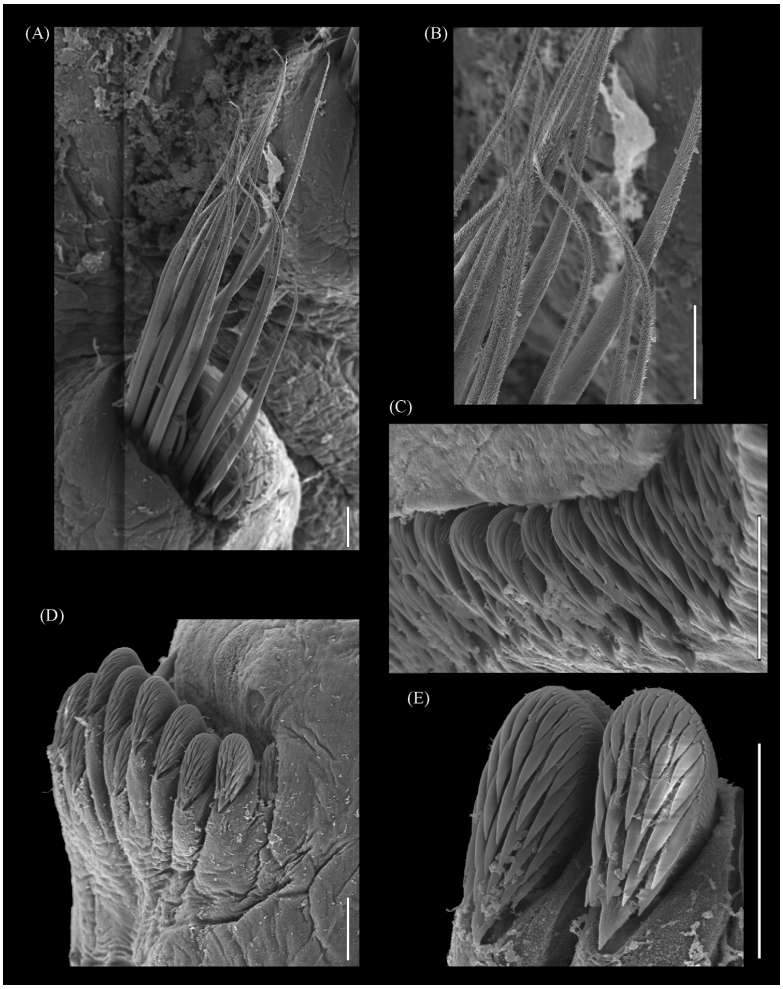

Fig. 5. *Paramytha schanderi* gen. et sp. nov. SEM micrographs of paratype (ZMBN 87799-2). (A) capillary chaetae; (B) same, close up of distal ends; (C) thoracic uncini; (D) abdominal uncini; (E) same, close up. Scale bars: (A–B, D) 20 μm; (C, E) 10 μm.

3.2.2.6. Reproduction. Gonochoric, without sexual dimorphism. Females with oocytes in thoracic and anterior abdominal chaetigers, visible through body wall; oocytes of different sizes, up to about 20 μm in diameter. One female with oocytes in tube (ZMBN 87827). Several males observed with clusters of sperm in anterior part of body.

3.2.2.7. Etymology. The species in named in honor of our late colleague and dear friend Professor Christoffer Schander.

3.2.3. Genus Pavelius Kuznetsov and Levenstein, 1988, emended

Type species: *Pavelius uschakovi* Kuznetsov and Levenstein, 1988: 819–824.

3.2.3.1. Diagnosis, emended. Prostomium rounded, without lobes or glandular ridges. Buccal tentacles smooth. Chaetae on segment II (paleae) present or absent, if present, similar to notochaeta, but smaller. Four pairs of branchiae, arranged in a single transverse row on segment III. Males with large nephridial papillae on chaetiger 4. Number of thoracic and abdominal chaetigers interspecifically variable, 14–15 thoracic and up to 24 abdominal chaetigers. Modified segments absent. Neuropodia enlarged as pinnules from abdominal chaetiger 2 or 3. Anal cirri absent.

3.2.3.2. Remarks. The generic diagnosis has been emended to include the new species described herein, specifically related to the number of thoracic chaetigers, presence/absence of chaetae on segment II (paleae) and the presence of two types of neuropodia, tori and pinnules. In addition, new information about the type species, *P. uschakovi*, has been provided by Jirkov (2011, pers. comm.), based on re-examination of specimens from type locality: The prostomium is without lobes, nephridial papillae on chaetigers 4 are only present in males and thus represent a dimorphism, the abdominal region have up to 24 chaetigers, and the neuropodia are enlarged as pinnules from the 3rd abdominal chaetiger.

Fig. 6. *Pavelius smileyi* sp. nov. (A) paratype (ZMBN 87810), complete specimen stained in methyl blue, lateral view. (B) holotype (ZMBN 87807), lateral view; (C) paratype (ZMBN 87810), head region in frontal view; (D) paratype (ZMBN 87812), with posterior part of body in tube. Scale bars: 2.0 mm.

Grassleia hydrothermalis Solis-Weiss, 1993, described from chemosynthetic environments in the deep E Pacific, also have a rounded prostomium without lobes and glandular ridges, and four pairs of branchiae arranged in a single transverse row without median gap. *G. hydrothermalis*, however, differs from the species of *Pavelius* by the absence of neurochaetae on the 5th chaetiger (segment 6), probably unique within the Ampharetidae, as well as the presence of a very short abdomen with only 7 chaetigers compared to more than 20 in species of *Pavelius* (see Solis-Weiss (1993)). We consider these genera to be closely allied, which is supported by the molecular analysis (Fig. 2).

3.2.4. *Pavelius smileyi sp. nov*

Figs. 6–9.

3.2.4.1. Type locality. Loki Castle vent field, Arctic mid-ocean ridge, 73°33'N 08°09'E, 2350 m depth.

3.2.4.2. Type material. Type locality from sedimentary area with low-temperature diffuse venting with barite chimneys, R/V "G.O. Sars" H2DEEP cruise 2009 sample ROV-8, 07 August 2009, fixed in 96% ethanol, holotype (ZMBN 87807) and 1 paratype (ZMBN 87809). R/V "G.O. Sars" CGB DEEP cruise 2010: Sample ROV-04, 15 July 2010, fixed in 6% formaldehyde and preserved in 80% ethanol: 1 paratype (ZMBN 87808-1), 2 paratypes (ZMBN 87812), 1 paratype mounted for SEM (ZMBN 87808-2), 1 paratype fixed in 96% ethanol (ZMBN 87826); sample ROV-05, 16 July 2010, fixed in 96% ethanol: 1 paratype (ZMBN 87810); sample ROV-06, July 2010, fixed in 96% ethanol: 1 paratype (ZMBN 87825).

3.2.4.3. Diagnosis. A *Pavelius* with 14 thoracic and up to 21 abdominal chaetigers; chaetae on segment II (paleae) absent.

3.2.4.4. Description. Holotype, complete male, with 14 thoracic and 20 abdominal chaetigers, 26 mm long and 3.0 mm wide in thorax (Fig. 6B). Other complete specimens are up to 28 mm in length and

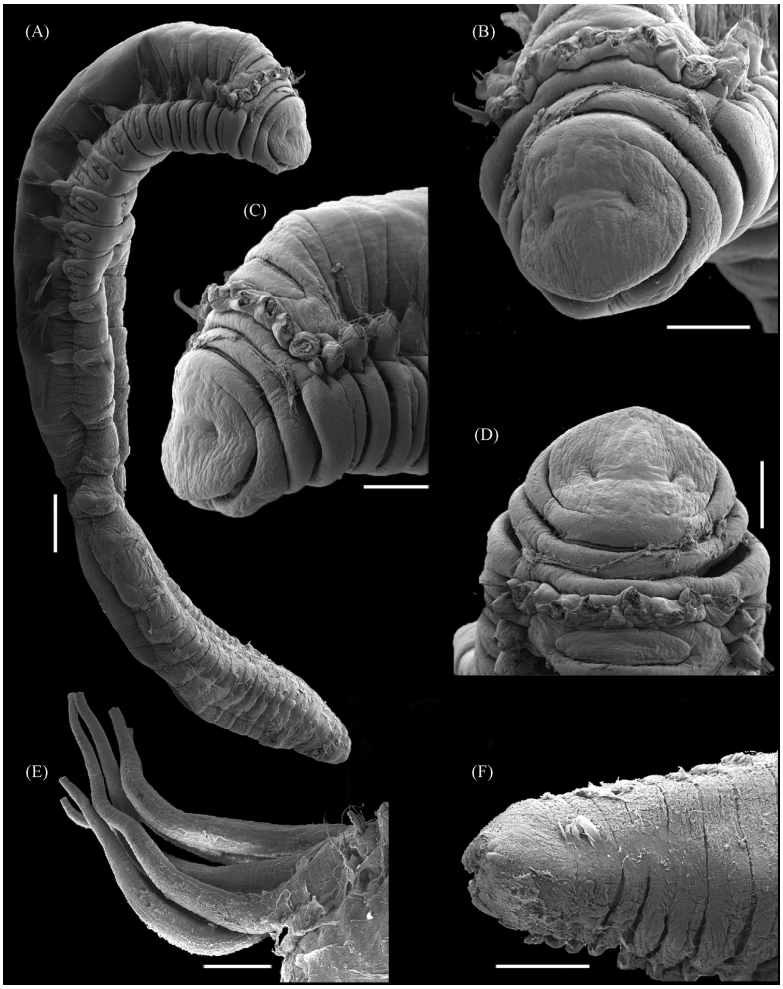

Fig. 7. *Pavelius smileyi* sp. nov. SEM micrographs: (A) complete specimen, lateral view; (B) head and anterior part of body, frontal view; (C) same, lateral view; (D) same, dorsal view; (E) details of branchiae; (F) posterior part of body and pygidium, dorsal view. (A–D) paratype, ZMBN 87808; (E–F) paratype, ZMBN 87811. Scale bars: (A) 1.0 mm; (B–F) 0.5 mm.

3.1 mm wide in thorax, with 14 thoracic and 20–21 abdominal chaetigers. Color in ethanol pale to brownish (Fig. 6B–D). Examined specimens with buccal tentacles withdrawn, or only partly extended. Prostomium broadly rounded, fused with peristomium dorsally, without lobes and glandular ridges (Fig. 7A–D). Paired nuchal organs as short, ciliated slits, centrally placed on prostomium (Fig. 7B). Eyes absent. Buccal tentacles smooth, cylindrical, longitudinally grooved. Segment I with distinct segmental borders (Fig. 7C–D). Four pairs of branchiae arranged close together in transverse row without median gap, dorsally on segment III (chaetiger 1) (Fig. 7A–D); branchiostyles relatively short, less than 1/5 of body length, tapering distally (Fig. 6A–D). Branchiophores as distinct lobes, fused at base, firmly attached to body wall (Fig. 7B–D). Second outermost branchiae originating from segment II, outermost branchiae originating from segment III, innermost branchiae originating from segment IV, second innermost branchiae originating from segment V (Fig. 9B). Distinct oval-shaped patch posterior to row of branchiae on segment 4 (chaetiger 2), covering half width of segment, with distinct anterior papillae arising slightly posterior and between the two branchial groups (Fig. 7D). Males with nephridial papillae as short lobes on chaetiger 4, posterior to notopodia. Body cylindrical, tapering posteriorly, with thorax and abdomen of similar length (Figs. 6A–B; 7A). Segment II without chaetae (paleae). A total of 14 thoracic segments with notopodia and capillary chaetae, starting on segment III (Fig. 7A); last 11 with neuropodial tori bearing single row of uncini. Notopodia as rounded lobes, up to three times longer than wide, gradually increasing in size from 1st to 3rd chaetigers (Fig. 7A, C). Notochaeta as hirsute capillaries (Fig. 8A–B), arranged in vertical rows; capillaries from anterior row generally thinner and shorter than from more posterior rows (Fig. 8A). Thoracic neuropodial tori oval in shape (Fig. 7A; 8A). Thoracic uncini with about 8 teeth arranged in 2–3 vertical rows above main rostrum and basal prow (Fig. 8C). First abdominal segment with

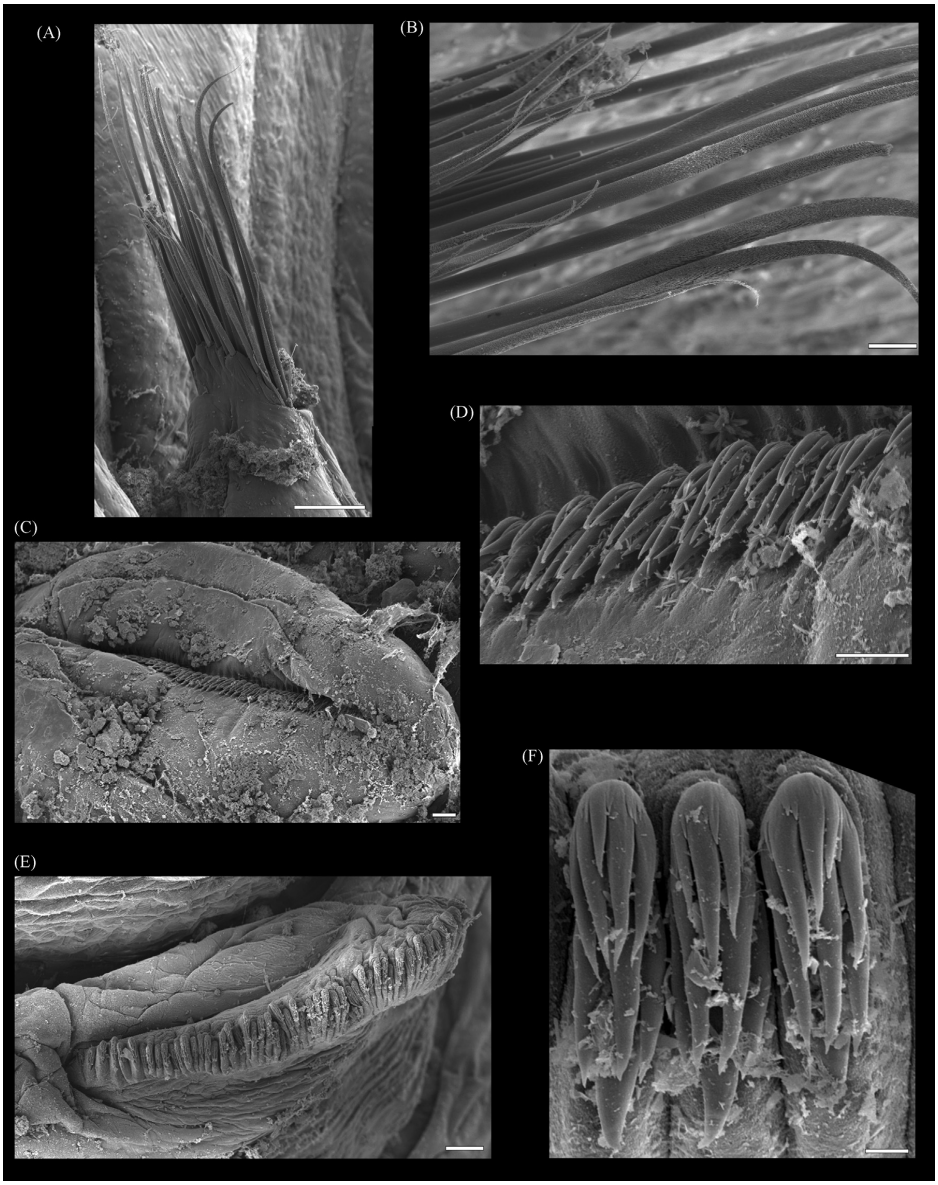

Fig. 8. *Pavelius smileyi* sp. nov. SEM micrographs of paratype (ZMBN 87808): (A) capillary chaetae; (B) details of capillary chaetae; (C) thoracic tori with uncini; (D) details of thoracic uncini; (E) abdominal neuropodia with uncini; (F) details of abdominal uncini. Scale bars: (A) 0.1 mm; (B–C, E) 20 μm; (D) 10 μm; (F) 2 μm.

neuropodia as thoracic type (tori); remaining abdominal neuropodia as weakly developed pinnules (Fig. 8E), without papillae or cirri. Abdominal uncini with up to 12–15 teeth above main rostrum, alternating in 4 vertical rows (Fig. 8F). Anal opening terminal, surrounded by small papillae or tissue-folds (Fig. 7F); anal cirri absent. Tube with thin organic layer incrusted with thick layer of fine mud (Fig. 6D). Head region (except nuchal organs), thoracic ventral glandular pads and basal part of notopodia deeply stained in methyl blue (Fig. 6A).

3.2.4.5. Reproduction: gonochoric. Females with oocytes and males with clusters of sperm in anterior part of body, observed by dissection. Large nephridial papilla on chaetiger 4 present in males.

3.2.4.6. Etymology. The species name refers to the "happy" appearance of the worm.

3.2.4.7. Remarks. The genus *Pavelius* includes at present two species, *P. uschakovi* and *Pavelius smileyi* sp. nov., both described from

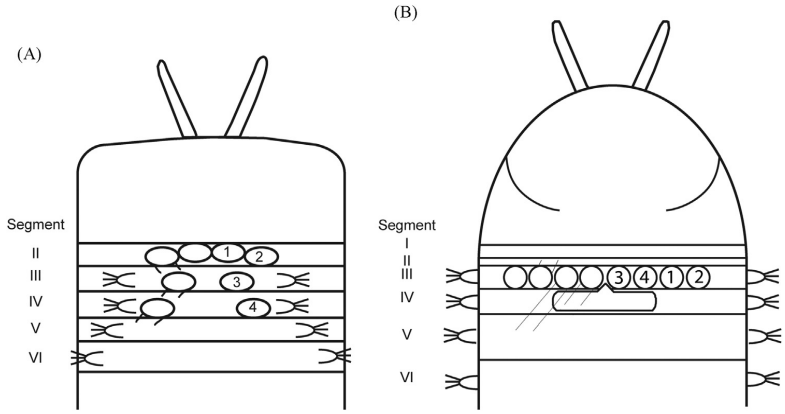

Fig. 9. Schematic illustrations of important taxonomical characters related to the anterior part of the body. (A) *Paramytha schanderi* gen. et sp. nov.; (B) *Pavelius smileyi* sp. nov.

chemosynthetic environments. *Pavelius smileyi* differs from *P. uschakovi* in the presence of 14 thoracic and up to 21 abdominal chaetigers rather than 15 thoracic and up to 24 abdominal chaetigers (Kuznetsov and Levenstein 1988; Jirkov, pers. comm.). *P. uschakovi* also have, in contrast to *Pavelius smileyi*, a few, small and thin chaetae (paleae) on segment II.

4. Discussion

The taxonomy of the family Ampharetidae is complex, with a high number of genera of which many are poorly characterized (see Reuscher et al. (2009), Jirkov (2011)). Traditionally, number of thoracic chaetigers and presence or absence of chaetae (paleae) on segment II, have been considered as important characters to define genera in the family (Holthe, 1986). However, in a number of genera, e.g. *Ampharete* Malmgren, 1866, *Anobothrus* Levinsen, 1884, *Amage* Malmgren, 1866 and *Amphisamytha* Hessle, 1917, some variation in these characters has been described (Jirkov, 2009; Imajima et al., 2012; Schüller and Jirkov, 2013; Stiller et al., 2013; Reuscher et al., 2015). In the present study, we document interspecific variation in number of thoracic chaetigers in both *Paramytha* gen. nov. and *Pavelius*, and the presence or absence of chaetae (paleae) on segment II in *Pavelius*, thus supporting that number of thoracic chaetigers and the presence or absence of chaetae on segment II are of limited value in defining genera of Ampharetidae.

Jirkov (2009, 2011) emphasized the shape of the prostomium as an important character to delimitate genera in the subfamily Ampharetinae. The prostomium in both *Paramytha* gen. nov. and *Pavelius* may be described as unilobed without glandular ridges, as in a number of other genera in the subfamily Ampharetinae (see Jirkov (2011), Reuscher et al. (2015)). We are not able to assign the characteristic prostomium in *Paramytha* gen. nov., being rectangular in shape with a thickened anterior margin, to any of the "typical" prostomial types in the subfamily as described by Jirkov (2011). The presence of a wide, rounded prostomium with distinct nuchal organs seems to be characteristic for the genera *Pavelius* and *Grassleia*. However, the use of prostomial shape to delimitate genera of ampharetids might be problematic as the shape to some degree will depend on whether the buccal tentacles are withdrawn or extended (see Day, 1964). At present, we consider the characteristic and unusual arrangement of the branchiae to be a key character defining *Paramytha* (see Section 3.2.1.3) and *Pavelius* (see Section 3.2.3.2).

Molecular data is presently only available for a selection of species (and genera) of ampharetids and thus the molecular phylogeny presented here provides limited information about relationships among the currently recognized genera of the family. However, the molecular data clearly support the inclusion of *Pavelius smileyi* sp. nov. in *Pavelius*, and also the expected relationship between *Pavelius* and *Grassleia* (see Section 3.2.3.2). *Paramytha* gen. nov. forms a well supported monophyletic group within the subfamily Ampharetinae, but no clear sister relationship with other genera were identified. Based on morphological data, *Paramytha* gen. nov. is here considered to be related to the genera *Phyllocomus* and *Orochi*, and perhaps *Decemunciger* (see Section 3.2.1.3). At present, molecular data is not available to test this hypothesis.

Ampharetid polychaetes are among the more common families recorded from hydrothermal vents and cold seeps with 17 species representing 8 different genera considered as exclusively adapted to live in these chemosynthetic environments (Kuznetsov and Levenstein, 1988; Solis-Weiss, 1993; Reuscher et al., 2009, 2012; Stiller et al., 2013; present study). The genera *Amage* (with about 25 species), *Glyphanostomum* (five species) and *Anobothrus* (about 20 species) are each only represented by a single species adapted to chemosynthetic environments, and most species in these genera are found in other marine environments. The genus *Amphisamytha* includes seven species adapted to vent and seep habitats and two additional species known from shallow waters in the Pacific. The genera *Pavelius* (two species), *Grassleia* (one species) and *Paramytha* gen. nov. (two species) are only known from chemosynthetic environments. Morphological and molecular data (see Fig. 2) indicate that adaptation to live in chemosynthetic environment has evolved several times within the ampharetids.

In the initial exploration of the fauna from the Loki's Castle vent field it has been speculated that the fauna has more in common with the North Pacific than with the fauna in the Atlantic south of the Faroe-Iceland-Greenland ridge (Pedersen et al., 2010, Kongsrud and Rapp, 2012). The close relationship of *Pavelius smileyi* sp. nov. with *P. uschakovi* from the NW Pacific, and also *Grassleia* cf. *hydrothermalis* from the NE Pacific (see Section 3.2.3.2) supports the connection between the Arctic and Pacific deep-sea chemosynthetic faunas. *P. schanderi* gen. et sp. nov., on the other hand, is related to a bone-living species of *Paramytha* from off the Coast of Portugal at 1000 m depth (Queiros et al., 2017). The recently recorded maldanid *Nicomache* sp. from the mid-Cayman Ridge in the Caribbean (Plouviez et al., 2015) is very similar to *Nicomache*

lokii (Kongsrud and Rapp, 2012) in the mitochondrial marker COI (< 1.5%, Genbank accession numbers: *Nicomache* sp: KJ566962; *N. lokii*: FR877579, FR877578), and clearly demonstrates a connection between Atlantic and Arctic chemosynthetic faunas. A similar case has been demonstrated for the siboglinid *Sclerolinum contortum* Smirnov, 2000, which based on molecular data has been shown to be widespread in chemosynthetic environments both in the Arctic (including Loki's Castle), the Gulf of Mexico and in the Antarctic (Georgieva et al., 2015). These highly contrasting links to other known vent and seep faunas, from both the Atlantic and Pacific Oceans, call for a more comprehensive study aiming to investigate the genetic connectivity and phylogeographic history of polychaetes inhabiting chemosynthetic habitats at a large geographic scale.

Acknowledgments

We thank the crew, scientists and students onboard the R/V G. O. Sars during the cruises 2008–2015 and the operators of the ROV Bathysaurus and Ægir6000 for their assistance at sea. Thanks to Greg Rouse and Josefin Stiller at the Scripps Institution of Oceanography for the use of the *Grassleia* specimen, to Bob Vrijenhoek (Monterey Bay Aquarium Research Institute) for allowing GR the opportunity to collect the *Grassleia*, and to Igor Jirkov, Moscow State University for the *P. uschakovi* specimen. Thanks also to Solveig Thorkildsen and Adriana Alvizu for help with the molecular work, which was performed at the Biodiversity Laboratories, University of Bergen. We thank the staff at the Laboratory for Electron Microscopy, University of Bergen for assisting with SEM images. Thanks are also due to Marina Cunha and two anonymous referees for helpful comments on the manuscript. This work has been supported by the NFR through Centre for Geobiology (project number 179560), the Norwegian Academy of Science and Letters and The Norwegian Deep Sea Program (the taxonomy fund), and the Norwegian Taxonomy Initiative (project 'Polychaete diversity in the Norwegian Sea - from coast to the deep sea' – PolyNor: project number 70184227) through the Norwegian Biodiversity Information Centre. DNA-barcode data generated in this project is part of the Norwegian Barcode of Life (NorBOL) project funded by the Research Council of Norway and the Norwegian Biodiversity Information Centre.

Appendix A. Supporting information

Supplementary data associated with this article can be found in the online version at http://dx.doi.org/10.1016/j.dsr2.2016.08.015.

References

Altschul, S.F., Gish, W., Miller, W., Myers, E.W., Lipman, D.J., 1990. Basic local alignment search tool. J. Mol. Biol. 215, 403–410.
Bennet, B.A., Smith, C.R., Glaser, B., Maybaum, H.L., 1994. Faunal community structure of a chemoautotrophic assemblage on whale bones in the deep northeast Pacific Ocean. Mar. Ecol. Prog. Ser. 108, 205–223.
Cohen, B.L., Gawthrop, A., Cavalier-Smith, T., 1998. Molecular phylogeny of brachiopods and phoronids based on nuclear-encoded small subunit ribosomal RNA gene sequences. Philos. Trans. R. Soc. B 353, 2039–2061.
Darriba, D., Taboada, G.L., Doallo, R., Posada, D., 2012. jModelTest 2: more models, new heuristics and parallel computing 9, 772.
Day, J.H., 1964. A review of the family Ampharetidae (Polychaeta). Ann. S. Afr. Mus. 48 (4), 97–120.
Edgar, R.C., 2004. MUSCLE: multiple sequence alignment with high accuracy and high throughput. Nucleic Acids Res. 32, 1792–1797.
Folmer, O., Black, M., Hoeh, W., Lutz, R., Vrijenhoek, R., 1994. DNA primers for amplification of mitochondrial cytochrome c oxidase subunit I from diverse metazoan invertebrates. Mol. Mar. Biol. Biotechnol. 3, 294–299.
Fricke, H., Giere, O., Stetter, K., Alfredsson, G.A., Kristjansson, J.K., Stoffers, P., Svavarsson, J., 1989. Hydrothermal vent communities at the shallow subpolar Mid-Atlantic Ridge. Mar. Biol. 102, 425–429.
Georgieva, M.N., Wiklund, H., Bell, J.B., Eilertsen, M.H., Mills, R.A., Little, C.T.S., Glover, A.G., 2015. A chemosynthetic weed: the tubeworm *Sclerolinum contortum* is a bipolar, cosmopolitan species. BMC Evol. Biol. 15. http://dx.doi.org/10.1186/s12862-015-0559-y.
Guindon, S., Gascuel, O., 2003. A simple, fast and accurate method to estimate large phylogenies by maximum-likelihood. Syst. Biol. 52, 696–704.
Grube, A.E., 1877. Anneliden - Ausbeute S.M.S. Gazelle. Monatsbericht der Koniglich Preussischer Akademie der Wissenschaften zu Berlin, 1877, 509–554, available online at ⟨http://biodiversitylibrary.org/page/35723826⟩.
Halanych, K.M., Bacheller, J.D., Aguinaldo, A.M., Liva, S.M., Hillis, D.M., Lake, J.A., 1995. Evidence from 18S ribosomal DNA that the lophophorates are protostome animals. Science 267, 1641–1643.
Hessle, C., 1917. Zur Kenntnis der terebellomorphen Polychaeten. Zoologiska bidrag från Uppsala 5: 39–258.
Hillis, D.M., Dixon, M.T., 1991. Ribosomal DNA: molecular evolution and phylogenetic inference. Q. Rev. Biol. 66, 411–453.
Holthe, T., 1986. Polychaeta terebellomorpha. Mar. Invertebr. Scand. 7, 1–192.
Huelsenbeck, J.P., Ronquist, F., 2001. MRBAYES: Bayesian inference of phylogeny. Bioinformatics 17, 754–755.
Imajima, M., Reuscher, M.G., Fiege, D., 2012. Ampharetidae (Annelida: Polychaeta) from Japan. Part I: The genus *Ampharete* Malmgren, 1866, along with a discussion of several taxonomic characters of the family and the introduction of a new identification tool. Zootaxa 3490, 75–88.
Jirkov, I.A., 1985. *Amphicteis ninonae* sp.n. (Polychaeta, Ampharetidae) from the northern waters. Zool. Zhurnal 64 (12), 1894–1898.
Jirkov, I.A., 2009. Revision of Ampharetidae (Polychaeta) with modified thoracic notopodia. Invertebr. Zool. 5 (2), 111–132 [text date 2008].
Jirkov, I.A., 2011. Discussion of taxonomic characters and classification of Ampharetidae (Polychaeta). Ital. J. Zool. 78 (Suppl. 1), S78–S94. http://dx.doi.org/10.1080/11250003.2011.617216.
Katoh, K., Standley, D.M., 2013. MAFFT multiple sequence alignment software version 7: improvements in performance and usability. Mol. Biol. Evol. 30, 772–780.
Kongsrud, J.A., Rapp, H.T., 2012. *Nicomache (Loxochona) lokii* sp. nov. (Annelida: Polychaeta: Maldanidae) from the Loki's Castle vent field: an important structure builder in an Arctic vent system. Polar Biol. 35 (2), 161–170. http://dx.doi.org/10.1007/s00300-011-1048-4.
Kuznetsov, A.P., Levenstein, R.Y., 1988. *Pavelius uschakovi* gen. et sp. n. (Polychaeta, Ampharetidae) from Paramushir gas hydrate spring in the Okhotsk Sea. Zool. Zhurnal 67 (6), 819–825.
Kück, P., Meusemann, K., Dambach, J., Thormann, B., von Reumont, B.M., Wägele, J.W., Misof, B., 2010. Parametric and non-parametric masking of randomness in sequence alignments can be improved and leads to better resolved trees. Front. Zool. 7, 10.
Levinsen, G.M.R., 1884. Systematisk-geografisk Oversigt over de nordiske Annulata, Gephyrea, Chaetognathi og Balanoglossi. Vidensk. Medd. dansk naturh. Foren. Köbenhavn 1883, 92–350.
Malmgren, A.J., 1866. Nordiska Hafs-Annulater. Öfversigt af Königlich Vetenskapsakademiens förhandlingar, Stockholm, 22 (5), 355–410.
McIntosh, W.C., 1885. Report on the Annelida Polychaeta collected by H.M.S. Challenger during the years 1873-1876. Report on the Scientific Results of the Voyage of H.M.S.Challenger during the years 1872-76, Ser. Zoology 12, 1–554.
Palumbi, S., Martin, A., Roman, S., McMillan, W.O., Stice, L., Grabowski, G., 1991. The Simple Fool's Guide to PCR. Department of Zoology, University of Hawaii, Honolulu, Special Publication.
Passamaneck, Y.J., Schander, C., Halanych, K.M., 2004. Investigation of molluscan phylogeny using large-subunit and small-subunit nuclear rRNA sequences. Mol. Phylogenet. Evol. 32, 25–38.
Pedersen, R.B., Rapp, H.T., Thorseth, I.H., Lilley, M., Barriga, F., Baumberger, T., Flesland, K., Bernasconi-Green, G., Flesland, K., Jørgensen, S.L., 2010. Discovery of a black smoker field and vent fauna at the Arctic Mid-Ocean Ridge. Nat. Commun. 1. http://dx.doi.org/10.1038/ncomms1124.
Plouviez, S., Jacobson, A., Wu, A.M., Van Dover, C.L., 2015. Characterization of vent fauna at the Mid-Cayman Spreading Center. Deep Sea Res. I 97, 124–133.
Queiros, J.P., Ravara, A., Eilertsen, M.H., Kongsrud, J.A., Hilário, A., 2017. *Paramytha osdomus* sp. nov. (Polychaeta, Ampharetidae) from mammal bones: reproductive biology and population structure. Deep-sea Res. II 137, 349–358. http://dx.doi.org/10.1016/j.dsr2.2016.08.015.
Rambaut, A., 2012. FigTree. Version 1.4.0., University of Edinburgh, Edinburgh, UK. Available at: ⟨http://tree.bio.ed.ac.uk/software/figtree⟩ (last accessed May 2014).
Rambaut, A., Drummond, A.J., 2009. Tracer v1.5, p. Available from ⟨http://beast.bio.ed.ac.uk/Tracer⟩.
Reuscher, M., Fiege, D., Wehe, T., 2009. Four new species of Ampharetidae (Annelida: Polychaeta) from Pacific hot vents and cold seeps, with a key and synoptic table of characters for all genera. Zootaxa 2191, 1–40.
Reuscher, M., Fiege, D., Wehe, T., 2012. Terebellomorph polychaetes from hydrothermal vents and cold seeps with the description of two new species of Terebellidae (Annelida: Polychaeta) representing the first records of the family from deep-sea vents. J. Mar. Biol. Assoc. 92 (5), 997–1012. http://dx.doi.org/10.1017/s0025315411000658.
Reuscher, M., Fiege, D., Imajima, M., 2015. Ampharetidae (Annelida: Polychaeta) from Japanese waters. Part IV. Miscellaneous genera. J. Mar. Biol. Assoc. 95 (6), 1105–1125. http://dx.doi.org/10.1017/S0025315415000545.

Ronquist, F., Huelsenbeck, J.P., 2003. MRBAYES 3: Bayesian phylogenetic inference under mixed models. Bioinformatics 19, 1572–1574.
Rouse, G.W., Pleijel, F., 2001. Polychaetes. Oxford University Press, p. 354.
Schander, C., Rapp, H.T., Kongsrud, J.A., Bakken, T., Berge, J., Cochrane, S., Oug, E., Byrkjedal, I., Cedhagen, T., Fosshagen, A., Gebruk, A., Larsen, K., Nygren, A., Obst, M., Plejel, F., Stöhr, S., Todt, C., Warén, A., Handler-Jacobsen, S., Kuening, R., Levin, L., Mikkelsen, N.T., Petersen, K.K., Thorseth, I.H., Pedersen, R.B., 2010. The fauna of the hydrothermal vents on the Mohn Ridge (North Atlantic). Mar. Biol. Res. 6, 155–171.
Schüller, M., Jirkov, I.A., 2013. New Ampharetidae (Polychaeta) from the deep Southern Ocean and shallow Patagonian waters. Zootaxa 3692 (1), 204–237 ⟨http://biotaxa.org/Zootaxa/article/view/zootaxa.3692.1.11⟩.
Solis-Weiss, V., 1993. *Grassleia hydrothermalis*, a new genus and species of Ampharetidae (Annelida: Polychaeta) from the hydrothermal vents off the Oregon coast (U.S.A.) at Gorda Ridge. Proc. Biol. Soc. Wash. 106 (4), 661–665.
Smirnov, R.V., 2000. Two new species of Pogonophora from the Arctic mud volcano off northwestern Norway. Sarsia 85, 141–150.
Stamatakis, A., 2008. The RAxML 7.0.3 Manual. The Exelixis Lab, LMU Munich, Available from: ⟨http://sco.h-its.org/exelixis/pubs/PRIB2008.pdf⟩.
Stiller, J., Rousset, V., Pleijel, F., Chevaldonné, P., Vrijenhoek, R.C., Rouse, G.W., 2013. Phylogeny, biogeography and systematics of hydrothermal vent and methane seep *Amphisamytha* (Ampharetidae, Annelida), with description of three new species. Syst. Biodivers. 11 (1), 35–65.
Struck, T., Hessling, R., Purschke, G., 2002. The phylogenetic position of the Aeolosomatidae and Parergodrilidae, two enigmatic oligochaete-like taxa of the "Polychaeta", based on molecular data from 18SrDNA sequences. J. Zool. Syst. Evolut. Res. 40, 155–163.
Struck, T.H., Purschke, G., Halanych, K.M., 2005. A scaleless scale worm: molecular evidence for the phylogenetic placement of *Pisione remota* (Pisionidae, Annelida). Mar. Biol. Res. 1, 243–253.
Talavera, G., Castresana, J., 2007. Improvement of phylogenies after removing divergent and ambiguously aligned blocks from protein sequence alignments. Syst. Biol. 56, 564–577.
Tandberg, A.H.S., Rapp, H.T., Schander, C., Vader, W., Sweetman, A.K., Berge, J., 2012. *Exitomelita sigynae* gen. et sp. nov.: a new amphipod from the Arctic Loki Castle vent field with potential gill ectosymbionts. Polar Biol. 35 (5), 705–716.
Thurber, A.R., Levin, L.A., Rowden, A.A., Sommer, S., Linke, P., Kröger, K., 2013. Microbes, macrofauna, and methane: a novel seep community fueled by aerobic methanotrophy. Limnol. Oceanogr. 58 (5), 1640–1656.
Wollebaek, A., 1912. Nordeuropaeiske annulata Polychaeta I. Ammocharidae, Amphictenidae, Ampharetidae, Terebellidae og Serpulidae. Skrifter utgit av Videnskapsselskapet i Kristiania. I, Matematisk-naturvidenskabelig klasse (1911) 18, 1–144.
Zottoli, R.A., 1982. Two new genera of deep-sea polychaete worms of the family Ampharetidae and the role of one species in deep-sea ecosystems. Proc. Biol. Soc. Wash. 95 (1), 48–57.

II

Eilertsen et al. BMC Evolutionary Biology (2017) 17:222
DOI 10.1186/s12862-017-1065-1

BMC Evolutionary Biology

RESEARCH ARTICLE Open Access

Do ampharetids take sedimented steps between vents and seeps? Phylogeny and habitat-use of Ampharetidae (Annelida, Terebelliformia) in chemosynthesis-based ecosystems

Mari H. Eilertsen[1,2*], Jon A. Kongsrud[3], Tom Alvestad[3], Josefin Stiller[4], Greg W. Rouse[4] and Hans T. Rapp[1,2,5]

Abstract

Background: A range of higher animal taxa are shared across various chemosynthesis-based ecosystems (CBEs), which demonstrates the evolutionary link between these habitats, but on a global scale the number of species inhabiting multiple CBEs is low. The factors shaping the distributions and habitat specificity of animals within CBEs are poorly understood, but geographic proximity of habitats, depth and substratum have been suggested as important. Biogeographic studies have indicated that intermediate habitats such as sedimented vents play an important part in the diversification of taxa within CBEs, but this has not been assessed in a phylogenetic framework. Ampharetid annelids are one of the most commonly encountered animal groups in CBEs, making them a good model taxon to study the evolution of habitat use in heterotrophic animals. Here we present a review of the habitat use of ampharetid species in CBEs, and a multi-gene phylogeny of Ampharetidae, with increased taxon sampling compared to previous studies.

Results: The review of microhabitats showed that many ampharetid species have a wide niche in terms of temperature and substratum. Depth may be limiting some species to a certain habitat, and trophic ecology and/or competition are identified as other potentially relevant factors. The phylogeny revealed that ampharetids have adapted into CBEs at least four times independently, with subsequent diversification, and shifts between ecosystems have happened in each of these clades. Evolutionary transitions are found to occur both from seep to vent and vent to seep, and the results indicate a role of sedimented vents in the transition between bare-rock vents and seeps.

Conclusion: The high number of ampharetid species recently described from CBEs, and the putative new species included in the present phylogeny, indicates that there is considerable diversity still to be discovered. This study provides a molecular framework for future studies to build upon and identifies some ecological and evolutionary hypotheses to be tested as new data is produced.

Keywords: Ampharetidae, Annelida, Chemosynthesis-based ecosystems, Deep-sea, Evolutionary stepping-stones, Phylogeny, Sedimented vents, Specialization

* Correspondence: mari.eilertsen@uib.no
[1]Department of Biology, University of Bergen, Bergen, Norway
[2]K.G. Jebsen Centre for Deep-Sea Research, University of Bergen, Bergen, Norway
Full list of author information is available at the end of the article

Background

In the deep-sea, there is no sunlight to fuel photosynthetic primary production. Energy to sustain life is therefore either derived from organic matter falling from surface waters, or from chemosynthetic primary production. Chemosynthetic bacteria and archaea, which utilize energy from reduced chemical compounds (e.g. hydrogen sulfide or methane) instead of sunlight, are found both free-living and as symbionts of macrofauna [1]. Compared to the surrounding food-limited deep-sea, chemosynthesis-based ecosystems (CBEs) are teeming with macrofauna, and specialized organisms can reach extremely high population densities (e.g. [2]).

Three main categories of deep-sea CBEs are defined based on the process that forms the reduced chemical compounds: hydrothermal vents, cold seeps and organic falls [3]. However, there are some habitats that have been considered intermediates between vents and seeps, such as sedimented vents [4] and hydrothermal seeps [5], and recent work has suggested that CBEs form a continuum of environmental conditions [5–7]. Some animal clades are shared across vents, seeps and falls, which demonstrates the evolutionary link between these habitats [8], but on a global scale the number of shared species is low [3, 4, 9]. In addition to the geochemical differences between CBEs, the distinctiveness of the fauna is affected by the geographic proximity of habitats [6, 10], and differences in depth [10, 11] and substratum [6, 7]. In the Guaymas Basin, where sedimented vents and seeps are found in close geographic proximity and at similar depth, the macrofaunal community composition is not determined by the type of ecosystem, but rather by environmental parameters that vary across ecosystems [6]. Similarly, no clear distinction was found between sedimented vents in Okinawa Trough and seeps at similar depths in Sagami Bay [10]. Recently, a biogeographic analysis demonstrated the importance of sedimented vents in linking vent and seep faunas on a global scale, and also indicated that sedimented vents might have been central in the evolution of taxa within CBEs [7].

Over the last decades, a number of phylogenetic studies have elucidated the evolutionary histories of fauna from CBEs, but these have mostly focused on the dominant symbiotrophic taxa such as vesicomyid and bathymodiolin bivalves [12–16] and siboglinid annelids [17–19]. The hypothesis that vent and seep mussels (Bathymodiolinae) evolved from wood-dwelling ancestors [20] has been followed by studies on other taxa, with either organic falls or seeps functioning as stepping-stones into the vent habitat [14, 15, 18, 21, 22]. However, the role of sedimented vents as an evolutionary stepping-stone has not previously been assessed in a phylogenetic framework.

Ampharetidae is a commonly occurring taxon at hydrothermal vents [23–26], cold seeps [2, 24, 26] and organic falls [27, 28] and can be a dominant part of the macrofaunal community [2, 4]. There are several species described from sedimented vents and one species is also recorded from the Costa Rica hydrothermal seep [23–25]. Although some species of ampharetids encountered in CBEs are also found in the surrounding deep-sea [29], many species are exclusively known from CBEs and are considered to be specialists [23–27]. Ampharetids are deposit feeders, and gut content, fatty acid and isotope analyses indicate that specialized ampharetids in CBEs are feeding on chemosynthetic bacteria [2, 30–32]. Most ampharetids are habitat-specific, and even when hydrothermal vents and cold seeps are found in close geographic proximity, the same species of ampharetids are usually not found in both habitats [25]. The almost ubiquitous presence of ampharetids in various CBEs makes them a good model taxon to study the evolution of habitat-use in heterotrophic animals.

Although Ampharetidae is one of the most common groups within CBEs, only two molecular phylogenies have been published to date, both with a limited taxon sampling of the family [23, 25]. The first study by Stiller et al. [25] focused on the genus *Amphisamytha,* which has 7 recognized species from vent and seep habitats. The second phylogeny by Kongsrud et al. [23] included five additional species from CBEs belonging to the genera *Pavelius*, *Paramytha* and *Grassleia* and indicated that adaptation into CBEs has happened multiple times independently in Ampharetidae, but still with limited taxon sampling of non-CBE ampharetids. In this paper, we expanded upon previous efforts and present a multi-gene phylogeny with increased taxon sampling of species both from CBEs and other habitats. In addition, we performed a review of the habitat-use of CBE-specialized ampharetids. With this we aimed to: 1) assess the effect of environmental factors such as substratum, temperature and depth on the habitat-specificity and distributions of ampharetids in CBEs; 2) test the hypothesis of multiple evolutionary origins of ampharetids in CBEs; and 3) infer the frequency and direction of habitat-shifts in the evolutionary history of Ampharetidae, with special attention paid to the role of intermediate habitats such as sedimented vents and hydrothermal seeps.

Methods

Review of habitat use

For the review we only included species of Ampharetidae obligate to CBEs. Although molecular data indicates that Alvinellidae should be considered a subfamily of Ampharetidae ([25], present study), species in this group were not included in the review due to their unique and very specialized ecology [33]. Because of the difficulty in validating records of species that are not formally described (recorded as genus sp. nov.), we further limited the review to species that are formally described, plus the undescribed species included in the present phylogeny (23 species in total). Details of the habitat where the specimens were collected are often not included in published papers, therefore cruise reports

were also studied when these were available [34]. For each record, we collected data on: habitat (hydrothermal vent, sedimented vent, inactive vent, hydrothermal seep, cold seep or organic fall), temperature, water/fluid chemistry, depth, substratum and geographical locality. All literature included in the review can be found in Additional file 1.

Molecular work

Taxon sampling

The focus of this paper is on species of Ampharetidae from CBEs, but we also included a broad taxonomic sampling of Ampharetidae from non-CB habitats. In total 101 specimens of Ampharetidae were included in the molecular dataset, of which 38 specimens were from CBEs. Twenty-one ampharetid genera (including both subfamily Ampharetinae and Melinninae) were represented in the dataset, which comprises approximately one third of the currently recognized genera in Ampharetidae [35] (see Additional file 2 for specimen list with metadata). Four hitherto undescribed species of Ampharetidae from CBEs were included; *Anobothrus* sp. A from the Snake Pit vent field on the Mid-Atlantic Ridge, *Anobothrus* sp. B and *Pavelius* sp. B from methane seeps on the Hikurangi Margin off New Zealand [2] and *Pavelius* sp. A from mud volcanoes in the Gulf of Cadiz off Portugal [36]. As outgroup, we chose *Pista cristata* (Terebellidae) and we also included representatives of 'Alvinellidae' (*Paralvinella* spp.). DNA voucher specimens are deposited at the Department of Natural History, University Museum of Bergen (ZMBN), the Scripps Oceanography Benthic Invertebrate Collection (SIO-BIC) or the German Center for Marine Biodiversity Research, Senckenberg (DZMB).

DNA extraction, amplification and sequencing

Four genetic markers were selected for this study, the mitochondrial cytochrome oxidase subunit I (COI) and 16S ribosomal DNA (16S), and the nuclear 18S and 28S ribosomal DNA (18S and 28S). Tissue for DNA extraction was, when possible, taken from branchiae or the posterior part of the worm, but in some cases the animals were so small that it was necessary to use the whole animal. In these cases, additional specimens from the same sample act as DNA-vouchers. Most of the molecular work was performed at the Biodiversity Laboratories, University of Bergen, except amplification and sequencing of 28S from *Amphisamytha* spp., which was done at the Scripps Institution of Oceanography. DNA extraction and amplification of COI, 16S and 18S was performed as described in [23]. Partial sequences of 28S were obtained using the primers Po28R4 (5′-3′ GTTCACCATCTTTGGGGTCCCAAC, [37]) and 28F5 (5′-3′ CAAGTACCGTGAGGGAAAGTTG, [38]). For *Amphisamytha* spp. the PCR reactions consisted of 12.5 μl (μl) Conquest PCR Master Mix, 1 μl of each of the primers, 50–100 ng DNA and ddH_2O to make the final reaction volume 25 μl. For the remaining specimens, the PCR reactions were set up as in [23]. The PCR cycling profile for 28S for all specimens was as follows: 3 min at 94 °C, 7 cycles with 30 s at 94 °C, 30 s at 55 °C and 2 min at 72 °C, 35 cycles with 30 s at 94 °C, 30 s at 52 °C, and 2 min at 72 °C, and finally 10 min at 72 °C. Quality and quantity of PCR products was assessed by gel electrophoresis imaging using a FastRuler DNA Ladder (Life Technologies) and GeneSnap and GeneTools (SynGene) for image capture and band quantification. In cases where the standard PCR protocol did not yield satisfying product a new PCR was performed with 1 μl dimethyl sulphoxide (DMSO) added. If gel electrophoresis showed multiple bands, the total PCR product was run on a new gel and the desired band was extracted from the gel using MinElute Gel Extraction Kit (QIAGEN) following the manufacturer's protocol. PCR products of *Amphisamytha* spp. were cleaned using ExoSAP-IT (Affymetrix, Inc., Cleveland, OH, USA) and sequenced by Retrogen Inc. (San Diego, CA, USA), while for the remaining specimens purification and sequencing was performed as in [23].

Phylogenetic analyses

Forward and reverse sequences were assembled in Geneious (Biomatters Ltd.), checked for contamination using BLAST [39] and have been deposited in GenBank (see Additional file 2 for accession numbers). Additional sequences of Ampharetidae were downloaded from GenBank and included in the analyses (see Additional file 2). Three sets of alignments were made, one with the complete dataset, and two with subsets of taxa corresponding to clades identified in initial analyses (Clade A and Clade C, see Results) and with *Melinna cristata* as outgroup. The alignments of Clade A and C were made to reduce the proportion of ambiguously aligned regions, allowing a higher number of positions to be included, and also to save computation time for species tree reconstruction with STACEY (see below).

COI sequences were aligned in Geneious using MUSCLE [40], and 16S, 18S and 28S sequences were aligned using the MAFFT online server [41] and the option for automatic selection of alignment algorithm [42, 43]. The alignments were inspected and minor corrections were made manually in Geneious. Blocks of ambiguous data were identified and excluded from the 16S, 18S and 28S alignments using the Gblocks online server [44] with relaxed settings [45, 46]. Substitution saturation for the first, second and third codon position of COI was assessed in DAMBE6 [47] using the Xia method [48, 49]. The third codon position showed strong signs of saturations in all alignments, so this position was excluded in the following analyses. Concatenated matrices of all genes were generated using Sequence Matrix [50] with missing data coded as question marks (?). The best partition scheme and the best fitting model of evolution for each partition for the combined analyses were

found using Partition Finder v2.1.1 with the greedy algorithm and PhyML ([51–53] see Additional file 3 for models). The I + G model for rate heterogeneity was suggested for some partitions, but due to statistical concerns regarding the co-estimation of the alpha and invariant-site parameters (discussed in the RAxML manual [54]) we chose to use only the + G model instead for all analyses. The best partition scheme was found to be five partitions with each gene and the first and second codon position of COI as separate partitions.

Single genes and a concatenated matrix of all genes for the complete dataset were analysed by maximum likelihood using RAxML v8.1.22 [55] implemented in raxmlGUI v1.3.1 [56], and by Bayesian inference in MrBayes v3.2.2 [57]. For the single-gene datasets identical sequences were removed prior to analysis. All maximum likelihood analyses were done under the GTRGAMMA model with 200 thorough bootstrap analyses for single gene analyses and 1000 for the concatenated dataset. In the MrBayes analyses partitions and substitution models were defined as suggested by Partition Finder, but since the TIM, TVM and TRN substitution models are not available in MrBayes these were replaced by the GTR model. Three parallel runs were performed for each MrBayes analysis with 5 million generations for single gene analyses and 10 million for concatenated analyses. MrBayes analyses were run on the Lifeportal server at the University of Oslo [58].

Due to computational constraints, we performed species tree analysis for Clade A and Clade C separately under the multi-species coalescent model (MSC) using STACEY v1.2.2 [59, 60] in BEAST2 v 2.4.4 [61]. STACEY implements species delimitation and species tree estimation within the same MCMC run, and therefore does not require any a priori species assignments [60]. All specimens were defined as separate species (leaving delimitation to the analysis), and the outgroup was set by defining the ingroup as monophyletic. Site and clock models were unlinked for all partitions, while the tree model was linked for all the mitochondrial partitions, and unlinked for the other partitions. Initially, analyses were run with substitution models as suggested by Partition Finder, but these analyses would not reach convergence, so the model was simplified by setting all site models as HKY + G. Gamma category count was set to 4 and gamma shape was estimated. Ploidy was set to 1 for the mitochondrial markers and 2 for the nuclear markers. The uncorrelated lognormal relaxed clock was selected as clock model for all partitions and the prior for clock rate was set as a lognormal distribution with M = 0 and S = 1. The relative death rate was fixed to 0.5, the prior for the species growth rate was given a lognormal distribution with a mean (M) of 4.6 and standard deviation (S) of 2, and popPriorScale was modeled with a lognormal distribution with M = −7 and S = 2. The remaining priors were left at the default. Six independent analyses were run for clade A and two for clade C with 1×10^8 generations and sampling every 10,000 generations. BEAST2 analyses were run on the CIPRES Science Gateway [62]. The log files were examined in Tracer v1.5 to check for convergence (ESS > 200 for all parameters of the combined analyses [63]). Analyses were combined and burn-in (10% for each analysis) was removed using LogCombiner v2.4.4 and maximum clade credibility trees were generated in TreeAnnotator v2.4.4. Both of these programs are part of the BEAST2 package [61]. All trees were converted to graphics using FigTree v1.4.0 [64] and final adjustments were made in Adobe Illustrator v16.0.4 (Adobe Systems, San Jose, CA, USA). Similarity matrices from the species delimitation analyses were calculated using the software SpeciesDelimitationAnalyser [65] and an R-script created by Graham Jones included in the supplementary information for DISSECT [66]. Heatmaps were generated using the R package pheatmap [67].

To generate species trees for Clade A and C with each tip representing a species, new analyses were run in STACEY with species defined according to the species delimitation results from the first analyses, i.e. all clusters with pp. > 0.8 were designated as separate species. All the other settings and priors were the same as in the first analyses, the results were combined, and consensus trees generated as described above. Ancestral states were reconstructed using parsimony in Mesquite v 3.11 [68].

Results

Distributions and habitat use

All the compiled data on habitat use with references and taxonomic authorities can be found in Additional file 1. In total, 24 species of Ampharetidae, representing eight genera, are known exclusively from CBEs, including the four putative new species included in the phylogeny presented herein, but excluding Alvinellidae (Table 1). *Eclysippe yonaguniensis* was originally described from a station with "low CO_2 seepage" [24], but this was in fact a reference station unaffected by CO_2 (M. Reuscher pers. comm.). *Eclysippe yonaguniensis* is therefore not considered as obligate to CBEs and consequently excluded from this review. *Amage benhami* is recorded from cold seeps on Hydrate Ridge (Cascadia Margin, NE Pacific) and from the Ross Sea (Antarctic) [26, 69], but it is unclear if the latter locality could have been a cold seep. There are indications that there are cold seeps in the Ross Sea [70], and for the purpose of this review we considered *A. benhami* a seep-specialist. *Grassleia* sp. A from the Guaymas Basin ([23], this study), is similar to *Grassleia hydrothermalis*, but there are some subtle morphological differences from the original description. Due to these differences, and the geographical distance to the type locality of *G. hydrothermalis*, we decided to designate these specimens as a separate species, but this needs to be reassessed when sequence data of *G. hydrothermalis* from the type locality becomes available.

Table 1 Summary of data on the microhabitat of Ampharetidae in CBEs. Species are ordered by habitat

	Habitat	Distribution	Type locality	Depth (m)	DR (m)	Temp.	Substratum				
							Sed.	Hard	Bivalve	Tube-worm	Crab
Amphisamytha fauchaldi	SV, HS, S	EP: Hydrate R. to Costa Rica	Guaymas B.	603–2860	2257	A-30 °C[a]	–	–	x	x	–
Amphisamytha vanuatuensis	V, S	WP: Lihir B., North Fiji B., Lau B.	Edison Seamt. (Lihir B.)	1114–2719	1605	A-14 °C	x	–	x	x	x
Grassleia hydrothermalis	V, S	EP: Gorda R., Hydrate R.	Escanaba T. (Gorda R.)	595–3271	2676	–	x	–	–	–	–
Grassleia sp. A	S	EP: Guaymas B.	–	1572	0	–	x	–	–	–	–
Anobothrus apaleatus	IV, S	EP: Southern East Pacific Rise, Hydrate R.	Central Axial High	524–2219	1695	A	x	x	–	–	–
Amphisamytha carldarei	V	EP: Juan de Fuca R.	Main Endeavour	2187–2415	228	A-40 °C	x	x	–	x	x
Amphisamytha galapagensis	V	EP: East Pacific Rise	Galapagos R.	2335–2725	390	A-23 °C	–	x	x	–	–
Amphisamytha jacksoni	V	EP: East Pacific Rise, 11°N to 38°S	31°S	2235–2515	280	–	–	–	–	–	–
Amphisamytha julianeae	V	WP: North Fiji B.	White Lady	1980	0	–	–	–	–	–	–
Amphisamytha lutzi	V	At: Mid-Atlantic R.	Lucky Strike	1622–4080	2458	5–14 °C	x	x	x	–	–
Anobothrus sp. A	V	At: Mid-Atlantic R. (Snake Pit)	–	3481–3522	41	–	x	x	–	–	–
Glyphanostomum bilabiatum	SV	WP: Okinawa T.	Yonaguni Knoll IV	1365–1385	20	–	x	–	–	–	–
Paramytha schanderi	SV	Ar: Arctic Mid-Ocean R.	Lokis Castle	2350	0	20 °C	–	–	–	x	–
Pavelius smileyi	SV	Ar: Arctic Mid-Ocean R.	Lokis Castle	2350	0	20 °C	–	–	–	x	–
Anobothrus sp. B	S	WP: Hikurangi M.	–	650–1100	450	A	x	–	–	–	–
Glyphanostomum holthei	S	EP: Aleutian Trench	Edge	4743–4947	204	A	x	–	x	–	–
Amage benhami	S	EP: Hydrate R., Ant: Ross Sea	Hydrate R.	293–625	332	A	x	–	–	–	–
Pavelius makranensis	S	IO: Makran accretionary prism	Flare 2	1015–1038	23	A	x	–	–	–	–
Pavelius sp. A	S	At: Gulf of Cadiz	–	650–1100	450	A	x	–	–	–	–
Pavelius sp. B	S	WP: Hikurangi M.	–	1300	0	A	x	–	–	–	–
Pavelius uschakovi	S	WP: Sea of Okhotsk	Sea of Okhotsk	765–810	45	A	x	–	–	–	–
Decemunciger apalea	F	At: North-West Atlantic (Woods Hole, TOTO)	Woods Hole	1830–3506	1676	A	x	–	–	–	–
Endecamera palea	F	At: Carribean Sea	St Croix	3995	0	A	x	–	–	–	–
Paramytha ossicola	F	At: Setubal Canyon	Setubal Canyon	1000	0	A	–	x	–	–	–

Abbreviations (habitat): *V* hydrothermal vent (bare-rock), *SV* sedimented hydrothermal vent, *IV* inactive vent, *HS* hydrothermal seep, *S* seep, *F* organic fall. *Abbreviations* (distributions): *EP* East Pacific, *WP* West Pacific, *At* Atlantic, *Ar* Arctic, *IO* Indian Ocean, *TOTO* Tongue of the Ocean (Bahama Islands), *B* Basin, *M* Margin, *R* Ridge, *T* Trough. Temperatures are shown as highest and lowest recorded, with A indicating ambient seawater temperature (no temperature anomaly recorded). *Other abbreviations*: *DR* Depth range, *Temp* Temperature, *Sed* sediment. Substrata are defined in five groups: sediments, hard substratum (rock, bone, wood), bivalves (bathymodiolins, vesicomyids), tubeworms (siboglinids, alvinellids) and crustaceans (bythograeid crabs). A dash (–) indicates missing data or that the species is not recorded from that habitat. A table of all compiled data can be found in Additional file 1. [a]Exact temperature maximum of *A. fauchaldi* is not available, but it is closely associated with *Riftia pachyptila* in Guaymas Basin, which is found in temperatures between 14 and 30 °C [6]

Ampharetids are recorded from CBEs in all world oceans (Fig. 1), but the highest diversity is described from the Pacific Ocean, with eight species in the East-Pacific and six species in the West-Pacific (Table 1). The Atlantic Ocean has six described species, two species are known from the Arctic and the Southern and Indian Oceans has one species each. Most seep-dwelling ampharetids are recorded from the Pacific, while ampharetids from organic falls are hitherto only described from the North Atlantic. There is often more than one species of ampharetids

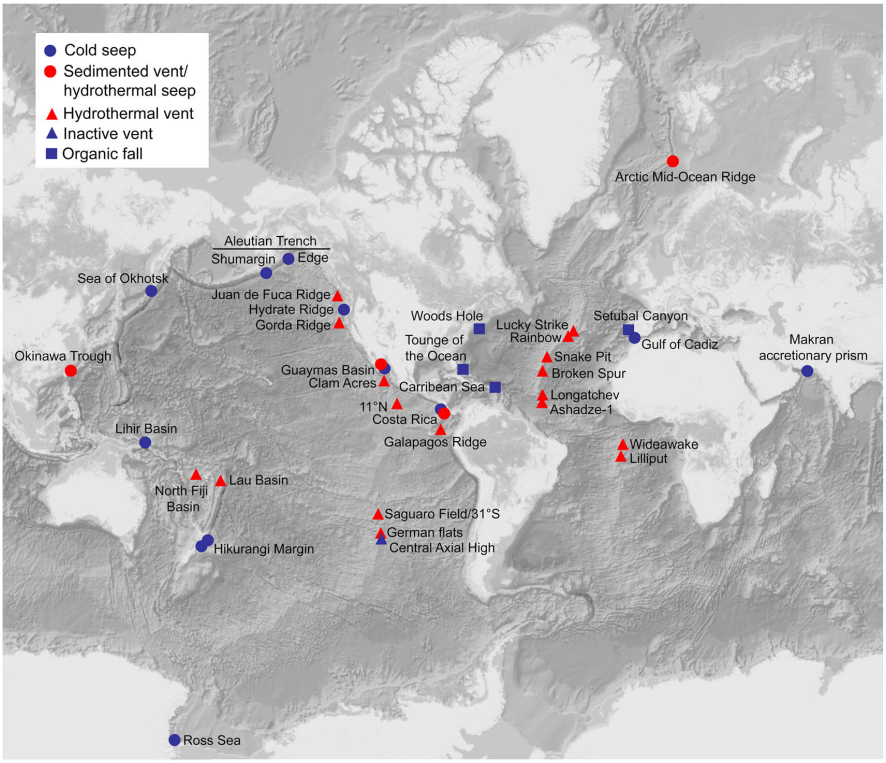

Fig. 1 Map of all sampling localities of the ampharetids included in the review. Habitats are coded as follows: Blue circle = cold seep, red circle = sedimented vent/hydrothermal seep, red triangle = hydrothermal vent, blue triangle = inactive vent, blue square = organic fall. Very closely spaced localities were dislocated slightly for clarity

recorded from the same locality, and the area with the highest number of co-occurring ampharetids is the seeps on Hydrate Ridge (Cascadia Margin, NE Pacific), where four species are recorded (Table 1).

Nine species are known from hydrothermal vents only (six from bare-rock vents and three from sedimented vents), seven species from cold seeps only, three species from organic falls (one from decaying bones and two from decaying wood) and four species from mixed habitats (Table 1). The four species recorded from mixed habitats are: *Amphisamytha fauchaldi*, *Amphisamytha vanuatuensis*, *Anobothrus apaleatus* and *Grassleia hydrothermalis*. *Amphisamytha fauchaldi* has been recorded from cold seeps, a hydrothermal seep and sedimented hydrothermal vents, and is thus exclusively found in sedimented habitats [25]. *Grassleia hydrothermalis* was originally described from Escanaba Trough, which has hydrothermal venting both in hard-surface and sedimented settings [71]. It is, however, unclear which habitat *G. hydrothermalis* was collected from, because the original description states that it was collected from sediments "where hydrothermal fluid percolates to the surface" [72], but in another paper describing the same sampling cruise it is recorded as collected from vestimentifera washings from a hard-surface habitat [71]. For the purpose of this paper we will follow the original description and consider the type locality to be sedimented vents. *Grassleia hydrothermalis* has also been recorded from cold seeps on Hydrate Ridge [73]. *Amphisamytha vanuatuensis* was described from a cold seep on Edison Seamount in the West-Pacific, and at nearby hydrothermal vents [26]. High levels of H_2S have been detected on Edison Seamount, but no temperature anomaly, and it is therefore classified as a cold seep [74, 75]. *Anobothrus apaleatus* was described from cold seeps on Hydrate Ridge, but also from an inactive vent on the Southern East Pacific Rise [26].

Six species (*Grassleia hydrothermalis*, *Amphisamytha lutzi*, *Amphisamytha fauchaldi*, *Anobothrus apaleatus*, *Decemunciger apalea* and *Amphisamytha vanuatuensis*) occupy depth ranges of over 1500 m, but the remaining species have a very

limited recorded depth-distribution (< 500 m). There is a clear connection between depth range and habitat specificity, with the four species recorded from mixed habitats being among the six species with the widest depth ranges (Table 1). *Amphisamytha lutzi*, however, is an outlier among the vent specific species with a very wide depth range (around 2500 m; Table 1). Vent-specific species are generally found at deeper depths than seep-specific species, but the seep-dwelling *Glyphanostomum holthei* from the Aleutian Trench has a deepest recorded depth of nearly 5000 m. The species from organic falls have very variable depth distributions; *Decemunciger apalea* is distributed from 1830 to 3506 m, while *Endecamera palea* and *Paramytha ossicola* have only been recorded from 3995 m and 1000 m, respectively.

Although exact temperature data were not available for most species, the data reviewed show that ampharetids at hydrothermal vents usually occupy areas with low to medium temperatures (from ambient up to ~20 °C), and most species for which temperature data were available are found in a wide range of temperatures (Table 1). *Amphisamytha vanuatuensis* and *Amphisamytha fauchaldi*, which inhabit both vents and seeps, have a similar temperature range as the vent-specialist species (Table 1). The only species found at high temperatures is *Amphisamytha carldarei*, which is found together with *Paralvinella sulfincola* near high temperature venting (as *Amphisamytha galapagensis* [31]). *Paralvinella sulfincola* is always found in the warmest areas around the vent, and is known to tolerate temperatures well over 40 °C [76]. *Amphisamytha carldarei* is, however, most common in cooler areas occupied by *Riftia pachyptila*, and even quite abundant at old chimneys with reduced flow and dead tubeworms [31]. The ability to live in very low flow conditions is also demonstrated by *Anobothrus apaleatus*, which is described from an inactive vent on the Southern East-Pacific Rise [26].

Ampharetids in CBEs are found on a wide range of substrata, but for simplicity they were grouped into the five categories shown in Table 1. The most common substratum among all species is sediments (17 species), while 8 species are recorded on/among other animals (bivalves, tubeworms, crabs) and 6 species are recorded from hard substrata. Many species are recorded from multiple types of substrata, but this is most common with vent-specific species and species from mixed habitats. Species that are recorded as sitting on other animals do not appear to have a very close association to the "substratum species", most of these are found on several different animals, and often on sediment and hard substrata as well. Most of the seep-specific species are only known from sediments (*Pavelius* spp., *Grassleia* sp. A and *Anobothrus* sp. B), but *Glyphanostomum holthei* is an exception, this species is also associated with clam beds (Vesicomyidae). Species from organic falls are either dwelling in the enriched sediments around the fall (*Decemunciger apalea* and *Endecamera palea*) or sitting on the fall itself (*Paramytha ossicola*).

Phylogenetic analyses

In total 321 sequences (from 51 putative species) were included in the phylogenetic analyses, of which 227 were newly generated for this study (Additional file 3).

Analyses of the concatenated complete dataset recovered Alvinellidae within the subfamily Ampharetinae, making this subfamily paraphyletic (Fig. 2). The positions of *Samythella neglecta* and Alvinellidae varied between the gene trees (Additional files 4, 5, 6, 7), and the position of Alvinellidae within Ampharetinae was unresolved in the resulting tree from the concatenated analysis. *Samythella neglecta* was recovered as sister to the rest of Ampharetinae + Alvinellidae in the tree from the concatenated analysis with high support (PP = 1, BS = 84, see Fig. 2). Apart from *Samythella neglecta*, the remaining species of Ampharetinae sensu stricto (excluding Alvinellidae) were recovered in three well-supported clades, which were also recovered in all gene-trees (Additional files 4, 5, 6, 7). A sister relationship between clade A and B received maximum support in the Bayesian analysis (PP = 1), but bootstrap support was low (BS = 69).

Two of the ampharetin clades, clade A and C, contained species from CBEs (Fig. 2). The topology within clades A and C varied between the gene trees, and some nodes received poor support in the concatenated analysis. These clades were realigned separately with *Melinna cristata* as outgroup. The new alignments contained fewer gaps, and a smaller proportion of the alignments was removed by Gblocks, allowing a higher total number of positions to be included in the analyses (see Additional file 8 for alignment statistics).

Several of the morphologically delimited species in clade A and C were not supported as a single cluster by the species delimitation in STACEY when applying a threshold of 95% posterior probability (Additional files 9 and 10). However, with a lower threshold (80%) most of the morphological species were supported as single clusters, with two exceptions: *Sosane wireni* and *Sosane* sp. A were originally identified as the same species (*Sosane wireni*), but this was not supported by the analyses (PP = 0.11), and the same was the case for *Ampharete* sp. A and B (PP = 0.16). The specimens in these clusters with PP < 0.8 were then assigned as separate putative species and given distinct names (e.g. *Ampharete* sp. A and sp. B) in all figures.

The topologies recovered from the species tree analyses of clades A and C were largely the same as from the concatenated analyses, but with higher support (Figs. 3 and 4). In clade A the species from CBEs were recovered in three sub-clades; one clade consisting of two species in *Anobothrus* (Clade A1), one clade consisting of *Pavelius* and *Grassleia* (Clade A2, five species)

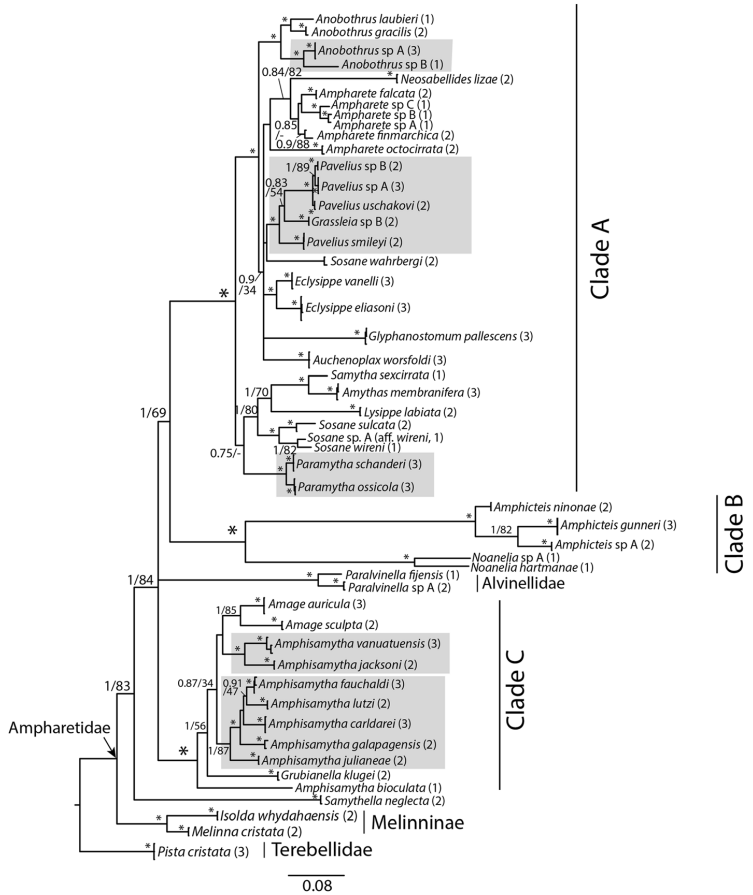

Fig. 2 Consensus tree from the MrBayes analysis of the concatenated, complete dataset. Clades from CBEs are indicated with a grey box. Branch labels are showing posterior probabilities and bootstrap values (PP/BS). Support values lower than 0.75/50 are not shown. An asterisk (*) indicates PP = 1 and BS = 95–100, and a dash (–) indicates the node was not recovered in the best maximum likelihood tree. Tips are labelled following the morphological species delimitation, but specimens that were not clustered together with a posterior probability above 0.8 in the Stacey analysis were given distinct names (e.g. *Ampharete* sp. A and sp. B). Numbers in brackets indicate the number of specimens per species

and one clade corresponding to *Paramytha* (Clade A3, two species). It should also be noted that *Ampharete* and *Sosane* were recovered as polyphyletic, with the species *Ampharete octocirrata* and *Sosane wahrbergi* failing to form clades with their respective congeners (Fig. 3). In clade C, *Amphisamytha* was polyphyletic (Fig. 4). The deep-sea *Amphisamytha* species from CBEs (Clade C1 and C2) formed a well-supported clade with *Amage* spp. The shallow-water *Amphisamytha bioculata* was recovered outside the clade consisting of the remaining *Amphisamytha* species + *Amage*, but its exact position relative to that clade was unresolved (Fig. 4).

Ampharetids from CBEs fell into five clades, with multiple types of CBEs represented in each clade. There was a predominance of vent-specific species in clade C2 (four of five species) and of seep-specific species in clade A2 (four of five species). Ancestral state reconstruction in Clade A gave ambiguous results for the ancestor of Clade A1 and A2, but for Clade A2 the ancestor was recovered as seep-dwelling, with one transition to sedimented vents in *Pavelius smileyi* (Fig. 5). In Clade C it is unresolved whether the ancestor of the clade of deep-sea *Amphisamytha* + *Amage* was from vents or non-CBEs, and thus it is unclear if the transition to CBEs happened once (with a

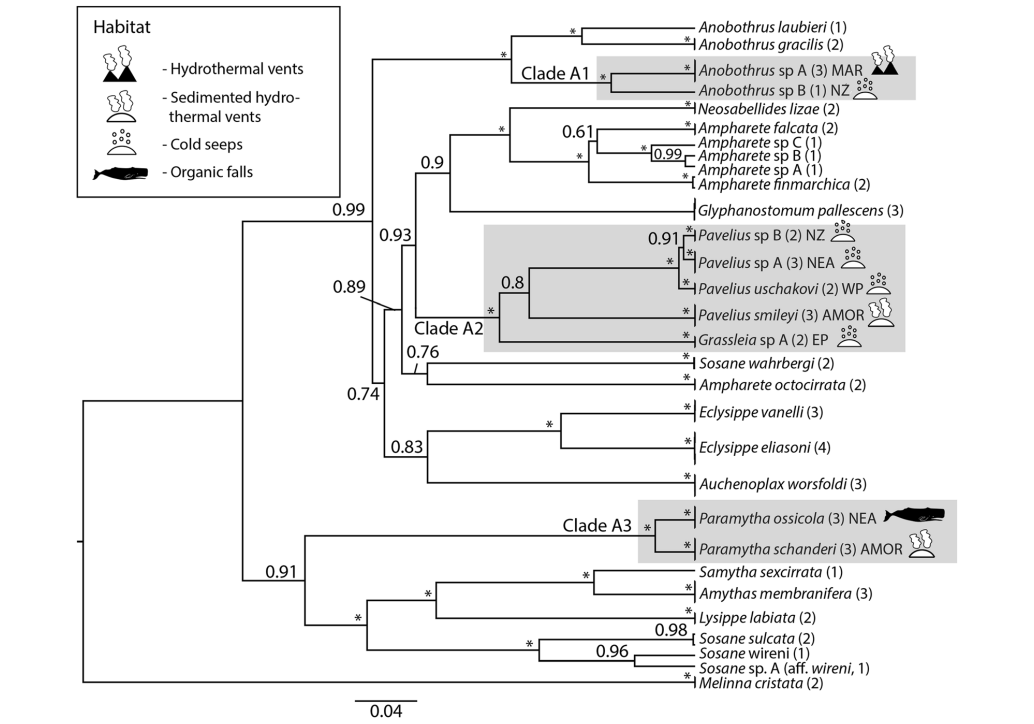

Fig. 3 Species tree of Clade A, including *Melinna cristata* as outgroup. Tips were labelled following the species delimitation by Stacey, and specimens that were not clustered together with a posterior probability above 0.8 were given distinct names. Branch labels are showing posterior probabilities, and an asterisk (*) indicates PP = 1. Clades from CBEs are indicated with a grey box, and the habitats of each species from CBEs are shown with symbols. Numbers in brackets indicate the number of specimens per species

back-transition in *Amage*) or twice independently in this clade. The ancestor of clades C1 and C2 were recovered as vent dwelling, with a transition to vent and seep in *Amphisamytha vanuatuensis* and to sedimented vent, hydrothermal seep and cold seep in *Amphisamytha fauchaldi* (Fig. 5).

Discussion

Ampharetids are among the most commonly encountered taxa in CBEs, but their ecology and evolutionary history is poorly known. The present study provides a thorough review of their habitat-use and a phylogenetic reconstruction with the by far most comprehensive taxon sampling of the family to date. The review shows that ampharetid species can inhabit a wide range of environmental conditions, and no apparent differences in substratum use or temperature tolerance were identified that could explain their habitat specificity. The phylogeny demonstrates the need for a taxonomic revision of the family, both on the generic, subfamily and family level. Ancestral state reconstruction of habitats in two clades of Ampharetidae shows that CBEs have been colonized multiple times independently, confirming previous findings [23]. Transitions between habitats is common within Ampharetidae, and the phylogeny indicates a potential role of intermediate habitats such as sedimented vents in the transition between different CBEs.

Distributions, environment and habitat specificity of ampharetids in CBEs

The ability of ampharetids to occupy a wide variety of habitats was remarked upon by McHugh and Tunnicliffe [31] with reference to *Amphisamytha galapagensis*. Molecular phylogenetics has since showed that *A. galapagensis* was a cryptic species complex, and some of the widespread records of this species have been assigned to other species [25]. However, the present study shows that the impression of ampharetid species as being very adaptable still holds true. Despite this apparent lack of specialization, most ampharetid species are restricted to one type of CBE, which may indicate that they are

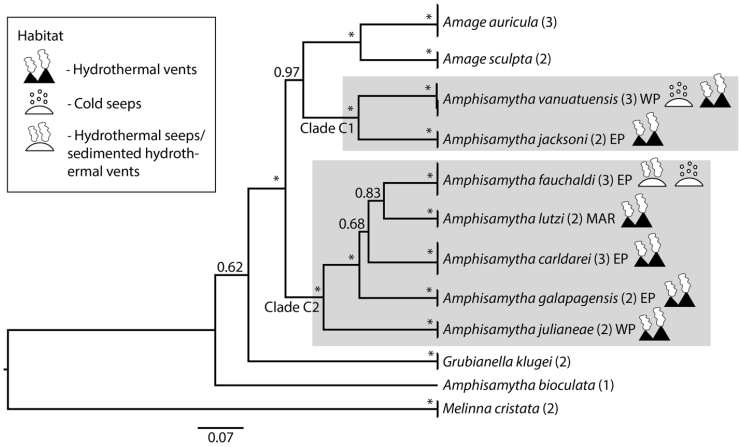

Fig. 4 Species tree of Clade C, including *Melinna cristata* as outgroup. Tips were labelled following the species delimitation by Stacey, and specimens that were not clustered together with a posterior probability above 0.8 were given distinct names. Branch labels are showing posterior probabilities, and an asterisk (*) indicates PP = 1. Clades from CBEs are indicated with a grey box, and the habitats of each species from CBEs are shown with symbols. Numbers in brackets indicate the number of specimens per species

limited by environmental factors other than temperature or substratum.

The community of free-living microbes that ampharetids feed on varies both within and between CBEs [77, 78], and therefore trophic specialization may affect the habitat specificity of ampharetid species. Trophic studies of grazing gastropods at hydrothermal vents have revealed that some species are specialized on a particular microbial food-source, while others are more generalistic [79]. At present the trophic ecology of ampharetids is poorly known, hindering inferences about the influence of trophic specialization on habitat selectivity. However, *Amphisamytha* aff. *Fauchaldi,* which inhabits both sedimented hydrothermal vents and cold seeps in the Guaymas Basin, has been shown to have

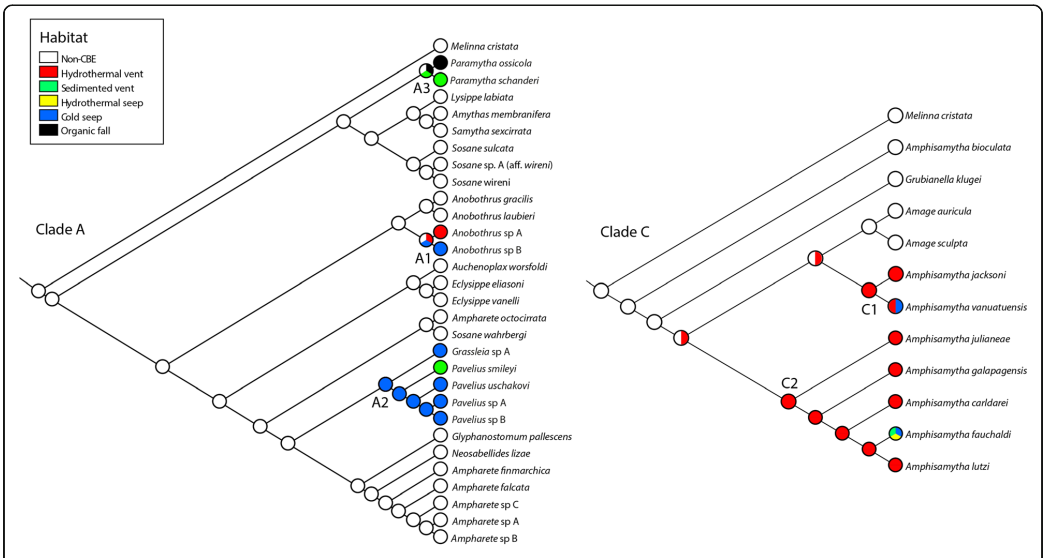

Fig. 5 Ancestral states reconstruction of clade A and clade C performed by parsimony analysis in Mesquite

clear shifts in isotopic values between habitats, indicating a flexible diet [77]. It is possible that this flexibility is one factor that allows *A. fauchaldi* to inhabit different CBEs.

Interactions with other species is another factor that may be important in shaping the geographic ranges and habitat specificity of ampharetids in CBEs. There are several cases of multiple species of ampharetids inhabiting the same localities, e.g. up to four species are found at Hydrate Ridge (Table 1). This means that ampharetids are probably affected by competition from confamilial species, which may lead to niche partitioning and trophic specialization [79, 80]. If several species of ampharetids are present in a given CBE it might be difficult for new species to establish, and this effect could be reinforced if the colonizing species is mainly adapted to a different habitat.

The fact that all the species inhabiting multiple habitats have wide depth-ranges,whereas species exclusive to a single CBE mostly have narrow depth-ranges indicates that depth limitation might be a relevant factor for habitat specificity. This also follows logically, since vents are usually located at deeper depths than seeps and falls. A putative example of depth limitation can be found in *Amphisamytha carldarei*, which is found on the vents on the Juan de Fuca Ridge (2200–2500 m). This species might be unable to colonize the much shallower seeps on Hydrate Ridge (500–800 m), even though these are located in close geographic proximity. Another example is found in the Nordic Seas, where the ampharetids *Pavelius smileyi* and *Paramytha schanderi* are found at the Lokis Castle sedimented vents (ca. 2350 m [23]), but not at the nearby Håkon Mosby mud volcano (ca. 1250 m [29]). Again, it is possible that depth difference is limiting colonization of the seep. However, while depth differences might be a barrier for some species, this explanation probably does not apply to all ampharetids. For example, it is unlikely that differences in depth is preventing *A. galapagensis* (depth range 2335–2725 m) from colonizing the hydrothermal seep at Jaco Scar off Costa Rica (ca. 1800 m) or the seeps and sedimented vents in the Guaymas Basin (ca. 1500–2000 m).

Habitat-use is likely the result of a complex interplay between biotic, abiotic and evolutionary factors/processes; depth might be a limiting factor for some species, while for others it might be trophic specialization, competition or an interaction between the two. Given the limitations of the available data, it is also likely that more ampharetid species will be found to occupy multiple habitats as CBEs are explored further. CBEs are poorly sampled in some geographical regions such as the Indian, Southern and Arctic Oceans (see Fig. 1). In addition, cold seeps and organic falls are still under sampled compared to hydrothermal vents, and there is a significant lag between the discovery of CBEs and publications of taxonomically assured species records and species descriptions, which further limits the available data. Ampharetids are also small and easily overlooked, and the absence of ampharetids on species lists from CBEs might be due to insufficient sampling. Continued taxonomic effort, including the use of molecular data, is needed to test the validity of species with wide geographic distributions and ecological niches.

Taxonomic implications of the phylogeny

The present phylogeny recovered Alvinellidae (represented by two species of *Paralvinella*) within Ampharetidae, supporting previous findings by Stiller et al. [25]. *Alvinella* and *Paralvinella* were originally described as belonging to a subfamily of Ampharetidae, Alvinellinae [81, 82], but they were subsequently erected as a separate family, Alvinellidae [83]. Our results suggest that Alvinellidae should be placed within Ampharetidae. However, in the present study Ampharetinae was recovered as paraphyletic with respect to Alvinellidae, and the position of Alvinellidae relative to clades A, B and C was unresolved (Fig. 2). More data and even denser taxon sampling is needed to revise the subfamilies of Ampharetidae.

The taxonomy of Ampharetidae is complex, with a high number of genera, of which many only include one or a few species [84]. Efforts have been made previously to reduce the number of genera, but there is disagreement on which morphological characters should be emphasized [84–86]. Our results show that *Ampharete octocirrata* (formerly *Sabellides octocirrata* [86]) does not form a clade with the remaining species of *Ampharete*, and *Sosane wahrbergi* (previously *Mugga wahrbergi* [86]) was not recovered together with the remaining species of *Sosane*. The two putative new species from cold seeps on the Hikurangi Margin (*Anobothrus* sp. B and *Pavelius* sp. B) were previously suggested to constitute two new genera [32], but the current phylogeny places them with *Anobothrus* and *Pavelius* respectively. These incongruences between morphology-based taxonomy and molecular phylogenetics illustrate the importance of including molecular data in the much-needed taxonomic revision of Ampharetidae.

Amphisamytha was also found to be non-monophyletic. *Amphisamytha* spp. from CBEs are more closely related to *Amage* (here represented by *Amage auricula* and *Amage sculpta*) than to the shallow-water species *Amphisamytha bioculata*. *Amage auricula* is the type species of *Amage*, which is a large genus with 24 recognized species [87]. Further study including a larger taxon-sampling of *Amage* is needed to resolve the relationship between this genus and *Amphisamytha*. Molecular data from the type species of *Amphisamytha*, *A. japonica*, will be critical to revise the genus, but this is unfortunately not available at present. However, it seems likely that the *Amphisamytha* species from CBEs should be placed in another genus.

The species delimitation results in this study showed more 'splitting' relative to morphological species delimitation when applying a 95% threshold for posterior probabilities. However, when lowered to an to an 80% threshold, all morphological species were supported except two, which had much lower support values. The low levels of support for many species could be due to population structure, which may be misinterpreted under the MSC as distinct species [88], or an effect of missing data. However, the two morphologically identified species (*Sosane wireni* and *Ampharete* sp. A + B) that were recovered with much lower levels of support (PP < 0.2), warrants further study to reveal potential cryptic diversity.

Evolutionary history of Ampharetidae in CBEs

The reconstruction of ancestral habitats indicates that adaptation into CBEs has happened at least four times independently within Ampharetidae. However, eight described species of ampharetids from CBEs were not included in the present phylogeny (Table 1). Based on morphological characteristics, three of these (*Anobothrus apaleatus, Grassleia hydrothermalis* and *Pavelius makranensis*) probably fall within the clades named here as Clades A1 and A2, and *Amage benhami* is probably related to clade C1 or C2. *Glypanostomum bilabiatum* and *Glyphanostomum holthei* are the only two species in the genus *Glyphanostomum* (which has six described species) adapted to CBEs [24, 26], and the position of the type species, *G. pallescens*, in the phylogenetic analysis presented here indicates that these species represent an additional clade adapted to CBEs. *Decemunciger apalea* and *Endecamera palea* are both the type species of a monotypic genus [28]. Kongsrud et al. [23] suggested that *Decemunciger* might be related to *Paramytha*, and a comparison of our data with COI sequences of *Decemunciger* sp. from GenBank (accession nos. KY972414–16) supports this suggestion. *Endecamera* has no clear morphological similarities to other ampharetid genera [84]. Although the phylogenetic position of these species cannot be resolved without more data, the inference that ampharetids have adapted into CBEs four times independently must be a minimum estimate.

To our knowledge, multiple independent adaptations into CBEs within one major clade has, to date, only been shown for Dorvilleidae [89]. Since most of the phylogenetic studies on fauna from CBEs have focused on symbiotrophic taxa (e.g. [12, 13, 17]), it is possible that this pattern is more common in heterotrophic animals, such as Ampharetidae and Dorvilleidae. Although the adaptation to CBEs has happened several times in Ampharetidae, there are multiple species in each of the specialized clades, which shows that the colonization of CBEs leads to a subsequent diversification. This implies that the ancestor of these clades has acquired a novel adaptation enabling the worms to diversify within CBEs, possibly related to tolerance of the chemical environment in CBEs or to a bacterivore diet.

There are several habitats represented in each of the specialized clades, which shows that evolutionary shifts between CBEs are common within Ampharetidae. The low number of species in some clade makes the inference of ancestral habitats ambiguous, but three habitat transitions are recovered: two from vent to vent and seep, and one from seep to sedimented vent (Fig. 5). The direction of colonization from vent to seep appears to be rare as most phylogenetic studies of taxa with representatives from different CBEs show that vent taxa evolved from fall or seep-dwelling ancestors [14, 15, 18, 21, 22]. In both clades A2 and C2, the shift between vent and seep habitats is associated with sedimented vents, which indicates a potential role of sedimented vents in transitions between different CBEs in Ampharetidae. Clade A3 also shows a link between sedimented vents and organic falls. However, three of the four species recorded from sedimented vents do not use the sediments as substratum, but are associated with structure-forming animals (Table 1). This indicates that the link between these two habitats might not lie in the sediment *as substratum*, but rather with the interaction between the sediments and vent fluids, which makes them more similar to seep fluids [90, 91]. This could again be related to the trophic ecology of the ampharetids, since fluid composition shapes the microbial community that the worms feed on [78].

Conclusions

The review of habitat use of ampharetids in CBEs did not reveal any apparent differences in substratum use or temperature tolerance which could explain their habitat specificity, but differences in depth may limit some species to a certain habitat. Trophic specialization or competition were also identified as potential factors influencing habitat-specificity. However, data on the ecology of Ampharetidae is still limited, and future studies on trophic ecology and biological interactions of ampharetids in CBEs are needed to fully understand which factors are shaping their distributions and habitat use.

The phylogeny presented here shows that adaptation into CBEs has happened at least four times within Ampharetidae, with subsequent diversification within CBEs. Multiple colonizations of CBEs within a family is unusual, but we hypothesize that this might be more common among heterotrophic taxa. Habitat shifts between CBEs are common in Ampharetidae, and the phylogeny indicates a potential role of sedimented vents in the transition between vent and seep habitats. The high number of ampharetid species described from CBEs recently, and the putative new species

included in this phylogeny, indicate that there is a lot of diversity still to be discovered. This study provides a molecular framework for future studies to build upon and identifies some ecological and evolutionary hypotheses to be tested as new data becomes available.

Additional files

Additional file 1: Review table of habitat of Ampharetidae in CBEs including references of the literature included in the review and taxonomic authorities for all species (XLSX 22 kb)

Additional file 2: List of specimens included in phylogenetic analysis with sampling data and GenBank accession numbers. Sequences that were produced for this study are highlighted in bold. Abbreviations: AuM, Australian Museum; AUM, Auburn University Museum, USA; DBUA, Biological Research Collection of Marine Invertebrates of Universidade de Aveiro, Portugal; ; NTNU-VM, Department of Natural History, NTNU University Museum, Trondheim, Norway; NZ, NIWA, New Zealand; SIO-BIC, Scripps Institution of Oceanography, Benthic Invertebrate Collection, USA; SMF, Senckenberg Museum Frankfurt, Germany; ZMBN, Department of Natural History, University Museum of Bergen, Norway (XLSX 109 kb)

Additional file 3: Best fit models for each partition as suggested by PartitionFinder. Shown for the complete dataset and the datasets of Clade A and Clade C. COI 1, 2 and 3 refers to first, second and third codon position of COI, but third codon position was not included in analyses due to saturation (XLSX 36 kb)

Additional file 4: COI gene tree of the complete dataset. The tree shown was inferred in MrBayes, branch labels are showing posterior probabilities and bootstrap values (PP/BS). Support values lower than 0.75/50 are not shown. An asterix (*) indicates PP = 1 and BS = 95–100, – indicates the node was not recovered in the best maximum likelihood tree. Identical sequences were removed prior to analyses (TIFF 20491 kb)

Additional file 5: 16S gene tree of the complete dataset. The tree shown was inferred in MrBayes, branch labels are showing posterior probabilities and bootstrap values (PP/BS). Support values lower than 0.75/50 are not shown. An asterix (*) indicates PP = 1 and BS = 95–100, – indicates the node was not recovered in the best maximum likelihood tree. Identical sequences were removed prior to analyses. (TIFF 21529 kb)

Additional file 6: 18S gene tree of the complete dataset. The tree shown was inferred in MrBayes, branch labels are showing posterior probabilities and bootstrap values (PP/BS). Support values lower than 0.75/50 are not shown. An asterix (*) indicates PP = 1 and BS = 95–100, – indicates the node was not recovered in the best maximum likelihood tree. Identical sequences were removed prior to analyses. (TIFF 18611 kb)

Additional file 7: 28S gene tree of the complete dataset. The tree shown was inferred in MrBayes, branch labels are showing posterior probabilities and bootstrap values (PP/BS). Support values lower than 0.75/50 are not shown. An asterix (*) indicates PP = 1 and BS = 95–1, – indicates the node was not recovered in the best maximum likelihood tree. Identical sequences were removed prior to analyses. (TIFF 18438 kb)

Additional file 8: Alignment statistics for the three datasets (complete, Clade A and Clade C) (XLSX 39 kb)

Additional file 9: Heatmap based on the output from Stacey showing the posterior probability of two specimens belonging to the same species. The probability matrix was calculated from the output of the Stacey analysis (see Methods – Phylogenetic analyses). Colors represent posterior probability values: 0–0.8 – blue, 0.8–0.9 – yellow, 0.9–0.95 – orange, 0.95–1 – red. Species names are abbreviated by the tree first letters of the genus and species epithet (PDF 315 kb)

Additional file 10: Heatmap based on the output from Stacey showing the posterior probability of two specimens belonging to the same species. The probability matrix was calculated from the output of the Stacey analysis (see Methods – Phylogenetic analyses). Colors represents posterior probability values: 0–0.8 – blue, 0.8–0.9 – yellow, 0.9–0.95 – orange, 0.95–1 – red. Species names are abbreviated by the tree first letters of the genus and species epithet (PDF 12 kb)

Abbreviations

16S: mitochondrial 16S ribosomal DNA; 18S: nuclear 18S ribosomal DNA; 28S: nuclear 28S ribosomal DNA; CBE: Chemosynthesis based ecosystem; COI: mitochondrial cytochrome oxidase subunit I; SIO-BIC: Scripps Oceanography Benthic Invertebrate Collection; ZMBN: Department of Natural History, University Museum of Bergen

Acknowledgements

We would like to thank Ken Halanych and Viktoria Bogantes for material from the Antarctic, Marina Cunha, Ascensão Ravara and Ana Hilário for material from the Gulf of Cadiz and Setùbal Canyon, Lenaick Menot for material from the Snake Pit vent field, Andrew Thurber for material from the Hikurangi Margin seeps, Igor Jirkov for the material of *Pavelius uschakovi*, the MAREANO project for material from Norwegian waters, the German Centre for Marine Biodiversity Research (DZMB) and Karin Meißner for material from Icelandic waters and the North Sea, the EAF-Nansen Programme, the Gulf of Guinea LME (GCLME) and the Canary Current LME (CCLME) for material collected in NW African waters. We also thank Bob Vrijenhoek for inviting GWR on cruises and the captain and crew of the R/V *Western Flyer* and pilots of the ROVs *Tiburon* and *Doc Ricketts* (Monterey Bay Aquarium and Research Institute) who enabled the collection of ampharetids from the East Pacific. Thanks also to Nataliya Budaeva, Solveig Thorkildsen, Morten Stokkan and Louise Lindblom for their help with the labwork, Endre Willasen for advice on the phylogenetic analyses, Graham Jones for his help with the Stacey analyses, Katrine Kongshavn for her help with production of the locality-map, and to Joana B. Xavier and Caroline Armitage for valuable discussions and input on the manuscript. We also want to thank two anonymous reviewers for their constructive comments on an earlier version of this paper.

Availability of data and material

Sequence data produced for this study have been deposited in GenBank, see Additional file 2 for accession numbers. Geographic coordinates of records of Ampharetids in chemosynthesis-based ecosystems and DNA sequence alignments are available in a Figshare repository (http://dx.doi.org/10.6084/m9.figshare.5519044).

Funding

This work has been supported by the NFR through Centre for Geobiology (project number 179560), the Norwegian Academy of Science and Letters and The Norwegian Deep Sea Program (the taxonomy fund), the Norwegian Taxonomy Initiative (project 'Polychaete diversity in the Norwegian Sea - from coast to the deep sea' – PolyNor: project number 70184227) through the Norwegian Biodiversity Information Centre, and the JRS Biodiversity Foundation. DNA-barcode data generated in this project is part of the Norwegian Barcode of Life (NorBOL) project funded by the Research Council of Norway and the Norwegian Biodiversity Information Centre. The project was also funded in part by a student grant from the Meltzer Foundation awarded to the first author.

Authors' contributions

MHE contributed to study design, performed most of the DNA sequencing, phylogenetic analyses, and wrote the manuscript. JAK contributed to study design, identified specimens, subsampled for DNA work and helped with taxonomic aspects of the manuscript. TA identified specimens and subsampled for DNA work. JS performed DNA sequencing of 28S from *Amphisamytha* spp. and identified material from the East Pacific. GR contributed with material from the East Pacific and details on the habitat of *Amphisamytha* spp. HTR contributed to the study design, coordinated the study, and helped to draft the manuscript. All authors read and approved the final manuscript.

Ethics approval and consent to participate

Ethics approval is not required for the collection and investigation of the morphology and DNA of annelid worms.

Consent for publication

NA

Competing interests
The authors declare that they have no competing interests.

Publisher's Note

Author details
[1]Department of Biology, University of Bergen, Bergen, Norway. [2]K.G. Jebsen Centre for Deep-Sea Research, University of Bergen, Bergen, Norway. [3]Department of Natural History, University Museum of Bergen, Bergen, Norway. [4]Scripps Institution of Oceanography, University of California San Diego, California, USA. [5]Uni Research, Uni Environment, Bergen, Norway.

Received: 1 June 2017 Accepted: 15 October 2017
Published online: 31 October 2017

References

1. Childress JJ, Fisher CR. The biology of hydrotermal vent animals: physiology, biochemistry and autotrophic symbioses. Oceanogr Mar Biol. 1992;30:337–441.
2. Thurber AR, Levin LA, Rowden AA, Sommer S, Linke P, Kröger K. Microbes, macrofauna, and methane: a novel seep community fueled by aerobic methanotrophy. Limnol Oceanogr. 2013;58:1640–56.
3. Tunnicliffe V, Juniper SK, Sibuet M. Reducing environments of the deep-sea floor. In: Tyler PA, editor. Ecosystems of the deep oceans. Amsterdam: Elsevier Science; 2003. p. 81–110.
4. Bernardino AF, Levin LA, Thurber AR, Smith CR. Comparative composition, diversity and trophic ecology of sediment macrofauna at vents, Seeps and Organic Falls. PLoS ONE. 2012;7:e33515.
5. Levin LA, Orphan VJ, Rouse GW, Rathburn AE, Ussler W, Cook GS, Goffredi SK, Perez EM, Waren A, Grupe BM, et al. A hydrothermal seep on the Costa Rica margin: middle ground in a continuum of reducing ecosystems. Proc R Soc B. 2012;279:2580–8.
6. Portail M, Olu K, Escobar-Briones E, Caprais JC, Menot L, Waeles M, Cruaud P, Sarradin PM, Godfroy A, Sarrazin J. Comparative study of vent and seep macrofaunal communities in the Guaymas Basin. Biogeosciences. 2015;12:5455–79.
7. Kiel S. A biogeographic network reveals evolutionary links between deep-sea hydrothermal vent and methane seep faunas. Proc R Soc B. 2016;283: 20162337.
8. Van Dover CL, German CR, Speer KG, Parson LM, Vrijenhoek RC: Evolution and biogeography of deep-sea vent and seep invertebrates. Science 2002; 295:1253–1257.
9. Wolff T: Composition and endemism of the deep-sea hydrothermal vent fauna. Cah Biol Mar. 2005;46:97–104.
10. Watanabe H, Fujikura K, Kojima S, Miyazaki J-I, Fujiwara Y. Japan: vents and seeps in close proximity. In: Kiel S, editor. The vent and seep biota. Netherlands: Springer; 2010. p. 379–401.
11. Olu K, Cordes EE, Fisher CR, Brooks JM, Sibuet M, Desbruyères D. Biogeography and potential exchanges among the Atlantic equatorial belt cold-seep faunas. PLoS One. 2010;5:e11967.
12. Thubaut J, Puillandre N, Faure B, Cruaud C, Samadi S. The contrasted evolutionary fates of deep-sea chemosynthetic mussels (Bivalvia, Bathymodiolinae). Ecol Evol. 2013;3:4748–66.
13. Johnson SB, Krylova EM, Audzijonyte A, Sahling H, Vrijenhoek RC. Phylogeny and origins of chemosynthetic vesicomyid clams. Syst Biodivers. 2016:1–15.
14. Decker C, Olu K, Cunha RL, Arnaud-Haond S. Phylogeny and diversification patterns among Vesicomyid bivalves. PLoS One. 2012;7:e33359.
15. Jones WJ, Won YJ, Maas PAY, Smith PJ, Lutz RA, Vrijenhoek RC. Evolution of habitat use by deep-sea mussels. Mar Biol. 2006;148:841–51.
16. Lorion J, Kiel S, Faure B, Kawato M, Ho SYW, Marshall B, Tsuchida S, Miyazaki J, Fujiwara Y. Adaptive radiation of chemosymbiotic deep-sea mussels. Proc R Soc B. 2013;280:20131243.
17. Li Y, Kocot KM, Whelan NV, Santos SR, Waits DS, Thornhill DJ, Halanych KM. Phylogenomics of tubeworms (Siboglinidae, Annelida) and comparative performance of different reconstruction methods. Zool Scr. 2016;46:200–13.
18. Schulze A, Halanych KM. Siboglinid evolution shaped by habitat preference and sulfide tolerance. Hydrobiologia. 2003;496:199–205.
19. Vrijenhoek RC, Johnson SB, Rouse GW. A remarkable diversity of bone-eating worms (Osedax; Siboglinidae; Annelida). BMC Biol. 2009;7:74.
20. Distel DL, Baco AR, Chuang E, Morrill W, Cavanaugh C, Smith CR. Marine ecology - do mussels take wooden steps to deep-sea vents? Nature. 2000;403:725–6.
21. Roterman CN, Copley JT, Linse KT, Tyler PA, Rogers AD. The biogeography of the yeti crabs (Kiwaidae) with notes on the phylogeny of the Chirostyloidea (Decapoda: Anomura). Proc R Soc B. 2013;280:20130718.
22. Yang J-S, Lu B, Chen D-F, Yu Y-Q, Yang F, Nagasawa H, Tsuchida S, Fujiwara Y, Yang W-J. When did decapods invade hydrothermal vents? Clues from the western Pacific and Indian oceans. Mol Biol Evol. 2013; 30:305–9.
23. Kongsrud JA, Eilertsen MH, Alvestad T, Kongshavn K, Rapp HT. New species of Ampharetidae (Annelida: Polychaeta) from the Arctic Loki Castle vent field. Deep Sea Res Part II Top Stud Oceanogr. 2017;137:232–45.
24. Reuscher MG, Fiege D. Ampharetidae (Annelida: Polychaeta) from cold seeps off Pakistan and hydrothermal vents off Taiwan, with the description of three new species. Zootaxa. 2016;4139:197–208.
25. Stiller J, Rousset V, Pleijel F, Chevaldonné P, Vrijenhoek RC, Rouse GW. Phylogeny, biogeography and systematics of hydrothermal vent and methane seep *Amphisamytha* (Ampharetidae, Annelida), with descriptions of three new species. Syst Biodivers. 2013;11:35–65.
26. Reuscher M, Fiege D, Wehe T. Four new species of Ampharetidae (Annelida: Polychaeta) from Pacific hot vents and cold seeps, with a key and synoptic table of characters for all genera. Zootaxa. 2009:1–40.
27. Queirós JP, Ravara A, Eilertsen MH, Kongsrud JA, Hilário A. *Paramytha ossicola* sp. nov. (Polychaeta, Ampharetidae) from mammal bones: reproductive biology and population structure. Deep Sea Res Part II Top Stud Oceanogr. 2017;137:349–58.
28. Zottoli RA. Two new genera of deep sea polychaete worms of the family Ampharetidae and the role of one species in deep sea ecosystems. Proc Biol Soc Wash. 1982;95:48–57.
29. Gebruk AV, Krylova EM, Lein AY, Vinogradov GM, Anderson E, Pimenov NV, Cherkashev GA, Crane K. Methane seep community of the Håkon Mosby mud volcano (the Norwegian Sea): composition and trophic aspects. Sarsia. 2003;88:394–403.
30. Zottoli RA. *Amphisamytha galapagensis*, a new species of ampharetid polychaete from the vicinity of abyssal hydrothermal vents in the Galapagos rift, and the role of this species in rift ecosystems. Proc Biol Soc Wash. 1983;96:379–91.
31. McHugh D, Tunnicliffe V. Ecology and reproductive biology of the hydrothermal vent polychaete *Amphisamytha galapagensis* (Ampharetidae). Mar Ecol Prog Ser. 1994;106:111–20.
32. Sommer S, Linke P, Pfannkuche O, Niemann H, Treude T. Benthic respiration in a seep habitat dominated by dense beds of ampharetid polychaetes at the Hikurangi margin (New Zealand). Mar Geol. 2010;272:223–32.
33. Fontanillas E, Galzitskaya OV, Lecompte O, Lobanov MY, Tanguy A, Mary J, Girguis PR, Hourdez S, Jollivet D. Proteome evolution of deep-sea hydrothermal vent alvinellid polychaetes supports the ancestry of thermophily and subsequent adaptation to cold in some lineages. Genome Biol Evol. 2017;9:279–96.
34. PANGAEA. Data Publisher for Earth & Environmental Science. Expeditions. https://http://www.pangaea.de/expeditions/. Accessed 20 March 2017.
35. Read G: Ampharetidae Malmgren, 1866. 2017. In: Read G, Fauchald K, editors. World Polychaeta database. http://www.marinespecies.org/aphia.php?p=taxdetails&id=981. Accessed 30 March 2017.
36. Cunha MR, Rodrigues CF, Génio L, Hilário A, Ravara A, Pfannkuche O. Macrofaunal assemblages from mud volcanoes in the Gulf of Cadiz: abundance, biodiversity and diversity partitioning across spatial scales. Biogeosciences. 2013;10:2553–68.
37. Struck TH, Pursche G, Halanych KM. Phylogeny of Eunicida (Annelida) and exploring data congruence using a partition addition bootstrap alteration (PABA) approach. Syst Biol. 2006;55:1–20.
38. Passamaneck YJ, Schander C, Halanych KM. Investigation of molluscan phylogeny using large-subunit and small-subunit nuclear rRNA sequences. Mol Phylogenet Evol. 2004;32:25–38.
39. Altschul SF, Gish W, Miller W, Myers EW, Lipman DJ. Basic local alignment search tool. J Mol Biol. 1990;215:403–10.
40. Edgar RC. MUSCLE: multiple sequence alignment with high accuracy and high throughput. Nucleic Acids Res. 2004;32:1792–7.
41. MAFFT. Version 7. Online version. http://mafft.cbrc.jp/alignment/server/. Accessed 20 March 2017
42. Katoh K, Standley DM. MAFFT multiple sequence alignment software version 7: improvements in performance and usability. Mol Biol Evol. 2013; 30:772–80.
43. Katoh K, K-i K, Toh H, Miyata T. MAFFT version 5: improvement in accuracy of multiple sequence alignment. Nucleic Acids Res. 2005;33:511–8.

44. Castresana J: Gblocks server. 2002. http://molevol.cmima.csic.es/castresana/Gblocks_server.html. Accessed 20 March 2017.
45. Talavera G, Castresana J. Improvement of phylogenies after removing divergent and ambiguously aligned blocks from protein sequence alignments. Syst Biol. 2007;56:564–77.
46. Kück P, Meusemann K, Dambach J, Thormann B, von Reumont BM, Wägele JW, Misof B. Parametric and non-parametric masking of randomness in sequence alignments can be improved and leads to better resolved trees. Front Zool. 2010;7:10.
47. Xia X. DAMBE5: a comprehensive software package for data analysis in molecular biology and evolution. Mol Biol Evol. 2013;30:1720–8.
48. Xia X, Xie Z, Salemi M, Chen L, Wang Y. An index of substitution saturation and its application. Mol Phylogenet Evol. 2003;26:1–7.
49. Xia X, Lemey P. Assessing substitution saturation with DAMBE. In: Lemey P, Salemi M, Vandamme AM, editors. The phylogenetic handbook. Cambridge: Cambridge University Press; 2009. p. 615–30.
50. Vaidya G, Lohman DJ, Meier R. SequenceMatrix: concatenation software for the fast assembly of multi-gene datasets with character set and codon information. Cladistics. 2011;27:171–80.
51. Guindon S, Dufayard JF, Lefort V, Anisimova M, Hordijk W, Gascuel O. New algorithms and methods to estimate maximum-likelihood phylogenies: assessing the performance of PhyML 3.0. Syst Biol. 2010;59:307–21.
52. Lanfear R, Calcott B, Ho SY, Guindon S. PartitionFinder: combined selection of partitioning schemes and substitution models for phylogenetic analyses. Mol Biol Evol. 2012;29:1695–701.
53. Lanfear R, Frandsen PB, Wright AM, Senfeld T, Calcott B. PartitionFinder 2: new methods for selecting partitioned models of evolution for molecular and morphological phylogenetic analyses. Mol Biol Evol. 2016;34:772–3.
54. Stamatakis A: The RAxML 8.2.X Manual. 2016. https://sco.h-its.org/exelixis/web/software/raxml/. Accessed 20 March 2017.
55. Stamatakis A. RAxML version 8: a tool for phylogenetic analysis and post-analysis of large phylogenies. Bioinformatics. 2014;30:1312–3.
56. Silvestro D, Michalak I. raxmlGUI: a graphical front-end for RAxML. Org Divers Evol. 2012;12:335–7.
57. Ronquist F, Huelsenbeck JP. MrBayes 3: Bayesian phylogenetic inference under mixed models. Bioinformatics. 2003;19:1572–4.
58. Lifeportal. University of Oslo. https://lifeportal.uio.no. Accessed 20 March 2017.
59. Jones G: STACEY package documentation: species delimitation and species tree estimation with BEAST2. 2014. http://www.indriid.com/software.html. Accessed 20 March 2017.
60. Jones G. Algorithmic improvements to species delimitation and phylogeny estimation under the multispecies coalescent. J Math Biol. 2017;74:447–67.
61. Bouckaert R, Heled J, Kühnert D, Vaughan T, C-H W, Xie D, Suchard MA, Rambaut A, Drummond AJ. BEAST 2: a software platform for Bayesian evolutionary analysis. PLoS Comput Biol. 2014;10:e1003537.
62. Miller MA, Pfeiffer W, Schwartz T: Creating the CIPRES Science Gateway for inference of large phylogenetic trees. Proceedings of the Gateway Computing Environments Workshop (GCE). 2010:1–8.
63. Rambaut A, Drummond AJ: Tracer v1.5. 2009. http://beast.community/tracer. Accessed 20 March 2017.
64. Rambaut A: FigTree. Version 1.4.0. 2012. http://tree.bio.ed.ac.uk/software/figtree. Accessed 20 March 2017.
65. Jones G: Software page. 2017. http://www.indriid.com/software.html. Accessed 20 March 2017.
66. Jones G, Aydin Z, Oxelman B. DISSECT: an assignment-free Bayesian discovery method for species delimitation under the multispecies coalescent. Bioinformatics. 2015;31:991–8.
67. Kolde R: pheatmap: Pretty Heatmaps. 2015. https://cran.rproject.org/web/packages/pheatmap/index.html. Accessed 20 March 2017.
68. Maddison WP, Maddison DR: Mesquite: a modular system for evolutionary analysis. 2017. http://mesquiteproject.org. Accessed 20 April 2017.
69. Benham WB. Polychaeta. British Antarctic 'Terra Nova' expedition natural history reports. Zoology. 1927;7(2):47–182.
70. Marshall BA, Tracey D. First evidence for deep-sea hot venting or cold seepage in the Ross Sea (Bivalvia: Vesicomyidae). Nautilus Greenville then Sanibel. 2015;129:140–1.
71. Grassle JF, Petrecca R. Soft-sediment hydrothermal vent communities of Escanaba trough. US Geol Surv Bull. 1994;2022:327–35.
72. Solís-Weiss V. *Grassleia hydrothermalis*, a new genus and species of Ampharetidae (Annelida: Polychaeta) from the hydrothermal vents off the Oregon coast (U.S.A.) at Gorda ridge. Proc Biol Soc Wash. 1993;106(4):661–5.
73. Reuscher M, Fiege D, Wehe T. Terebellomorph polychaetes from hydrothermal vents and cold seeps with the description of two new species of Terebellidae (Annelida: Polychaeta) representing the first records of the family from deep-sea vents. J Mar Biol Assoc U K. 2012;92:997–1012.
74. Herzig PM, Hannington MD, Stoffers P, Becker K-P, Drischel M, Franklin J, Franz L, Gemmell JB, Hoeppner B, Horn C, et al. Petrology, gold mineralization and biological communities at shallow submarine volcanoes of the New Ireland fore-arc (Papua New Guinea): preliminary results of R/V Sonne cruise SO-133. InterRidge News. 1998;7:34–8.
75. Stecher J, Tunnicliffe V, Türkay M. Population characteristics of abundant bivalves (Mollusca, Vesicomyidae) at a sulphide-rich seafloor site near Lihir Island, Papua New Guinea. Can J Zool. 2003;81:1815–24.
76. Lee RW. Thermal tolerances of deep-sea hydrothermal vent animals from the Northeast Pacific. Biol Bull. 2003;205:98–101.
77. Portail M, Olu K, Dubois SF, Escobar-Briones E, Gelinas Y, Menot L, Sarrazin J. Food-web complexity in Guaymas Basin hydrothermal vents and cold seeps. PLoS One. 2016;11:e0162263.
78. Steen IH, Dahle H, Stokke R, Roalkvam I, Daae F-L, Rapp HT, Pedersen RB, Thorseth IH. Novel barite chimneys at the Loki's castle vent field shed light on key factors shaping microbial communities and functions in hydrothermal systems. Front Microbiol. 2015;6
79. Govenar B, Fisher CR, Shank TM. Variation in the diets of hydrothermal vent gastropods. Deep-Sea Res II Top Stud Oceanogr. 2015;121:193–201.
80. Levin LA, Ziebis W, Mendoza GF, Bertics VJ, Washington T, Gonzalez J, Thurber AR, Ebbe B, Lee RW. Ecological release and niche partitioning under stress: lessons from dorvilleid polychaetes in sulfidic sediments at methane seeps. Deep-Sea Res II Top Stud Oceanogr. 2013;92:214–33.
81. Desbruyères D, Laubier L. *Paralvinella grasslei*, new genus, new species of Alvinellinae (Polychaeta: Ampharetidae) from the Galapagos rift geothermal vents. Proc Biol Soc Wash. 1982;95:484–94.
82. Desbruyeres D, Laubier L. *Alvinella pompejana* gen. sp. nov., Ampharetidae aberrant des sources hydrothermales de la ride Est-Pacifique. Oceanol Acta. 1980;3:267–74.
83. Desbruyères D, Laubier L. Les Alvinellidae, une famille nouvelle d'annélides polychètes inféodées aux sources hydrothermales sous-marines: systématique, biologie et écologie. Can J Zool. 1986;64:2227–45.
84. Jirkov IA. Discussion of taxonomic characters and classification of Ampharetidae (Polychaeta). Italian Journal of Zoology. 2011;78:78–94.
85. Salazar-Vallejo SI, Hutchings P. A review of characters useful in delineating ampharetid genera (Polychaeta). Zootaxa. 2012;3402:45–53.
86. Jirkov IA. [Polychaeta of the Arctic Ocean] Polikhety severnogo Ledovitogo Okeana. Moskva: Yanus-K; 2001.
87. Reuscher M, Bellan G: Amage. 2013. In: Read G, Fauchald K, editors. World Polychaeta database. http://marinespecies.org/aphia.php?p=taxdetails&id=129153. Accessed 28 March 2017.
88. Sukumaran J, Knowles LL. Multispecies coalescent delimits structure, not species. Proc Nat Acad Sci. 2017;114:1607–12.
89. Thornhill DJ, Struck TH, Ebbe B, Lee RW, Mendoza GF, Levin LA, Halanych KM. Adaptive radiation in extremophilic Dorvilleidae (Annelida): diversification of a single colonizer or multiple independent lineages? Ecol Evol. 2012;2:1958–70.
90. Von Damm KL, Edmond JM, Measures CI, Grant B. Chemistry of submarine hydrothermal solutions at Guaymas Basin, gulf of California. Geochim Cosmochim Acta. 1985;49:2221–37.
91. Baumberger T, Früh-Green GL, Thorseth IH, Lilley MD, Hamelin C, Bernasconi SM, Okland IE, Pedersen RB. Fluid composition of the sediment-influenced Loki's castle vent field at the ultra-slow spreading Arctic Mid-Ocean ridge. Geochim Cosmochim Acta. 2016;187:156–78.

III

Georgieva et al. BMC Evolutionary Biology (2015) 15:280
DOI 10.1186/s12862-015-0559-y

BMC Evolutionary Biology

RESEARCH ARTICLE Open Access

A chemosynthetic weed: the tubeworm *Sclerolinum contortum* is a bipolar, cosmopolitan species

Magdalena N. Georgieva[1,2*], Helena Wiklund[1], James B. Bell[1,3], Mari H. Eilertsen[4,5], Rachel A. Mills[6], Crispin T. S. Little[2] and Adrian G. Glover[1]

Abstract

Background: *Sclerolinum* (Annelida: Siboglinidae) is a genus of small, wiry deep-sea tubeworms that depend on an endosymbiosis with chemosynthetic bacteria for their nutrition, notable for their ability to colonise a multitude of reducing environments. Since the early 2000s, a *Sclerolinum* population has been known to inhabit sediment-hosted hydrothermal vents within the Bransfield Strait, Southern Ocean, and whilst remaining undescribed, it has been suggested to play an important ecological role in this ecosystem. Here, we show that the Southern Ocean *Sclerolinum* population is not a new species, but more remarkably in fact belongs to the species *S. contortum*, first described from an Arctic mud volcano located nearly 16,000 km away.

Results: Our new data coupled with existing genetic studies extend the range of this species across both polar oceans and the Gulf of Mexico. Our analyses show that the populations of this species are structured on a regional scale, with greater genetic differentiation occurring between rather than within populations. Further details of the external morphology and tube structure of *S. contortum* are revealed through confocal and SEM imaging, and the ecology of this worm is discussed.

Conclusions: These results shed further insight into the plasticity and adaptability of this siboglinid group to a range of reducing conditions, and into the levels of gene flow that occur between populations of the same species over a global extent.

Keywords: Siboglinidae, Polychaeta, Annelida, Antarctica, Gene flow, Deep-sea, Connectivity, Hydrothermal vent, Cold seep, Biogeography

Background

The vastness and inaccessibility of the deep sea has challenged scientists seeking to understand its diversity [1, 2]. A major area of this research concerns improving knowledge on the ranges of deep-sea species, which has become particularly pertinent in light of growing human impacts in this environment [3]. Molecular tools have been applied to this field and have revealed that certain deep-sea species with widespread distributions can exhibit similar morphology but considerable genetic differentiation between regions, and may thereby represent several closely related but geographically restricted species – so called 'cryptic species' [4–8]. Contrastingly, other studies have also revealed that some taxa can indeed be incredibly widespread, displaying distributions that can span both poles, i.e. bipolar. This pattern has been confirmed in bacteria and archaea [9, 10], in benthic foraminifera [11], deep-sea coral [12] and a lineage of the amphipod *Eurythenes gryllus* [8]. While there are problems with the use of molecular data to delimit species, the examination of genetic variation at multiple (both mitochondrial and nuclear) loci within an evolutionary context has become an important addition to our definition of a species alongside morphological, biological and ecological observations [13–15], as well as a critical tool in the investigation of species biogeography. Here we

* Correspondence: eemng@leeds.ac.uk
[1]Life Sciences Department, Natural History Museum, London, UK
[2]School of Earth and Environment, University of Leeds, Leeds, UK
Full list of author information is available at the end of the article

investigate the range and ecological adaptations of a deep-sea siboglinid tubeworm over near 16,000 km spanning from the Arctic to the Antarctic.

The family Siboglinidae is a monophyletic lineage of annelid worms comprised of the vestimentiferans, or giant tubeworms, the bone-eating genus *Osedax*, and two groups of slender tubeworms – *Sclerolinum* and the frenulates [16]. Siboglinidae is exceptional among the annelids due to this family's almost complete reliance on endosymbiotic bacteria for nutrition, and the unusual morphology which its members have adopted for this specialism [17]. The majority of siboglinids (except for *Osedax* and a number of frenulates capable of oxidising methane) harbour sulphur-oxidising symbionts [18] and are characteristically long, often acting like a 'bridge' between a sulphidic substrate where their posterior end is located, and oxygenated seawater into which they extend their anterior end [19].

Although siboglinids are found within all of the world's major oceans, the distribution and genetic structure of certain lineages is poorly constrained. Hydrothermal vent vestimentiferans endemic to the East Pacific Rise (EPR) are perhaps the best studied, where species such as *Riftia pachyptila* and *Tevnia jerichonana* show extensive ranges along the length of this mid ocean ridge system, while the degree of genetic differentiation between populations increases with distance [20, 21]. Vestimentiferans that can colonise seeps, whale and wood falls have the potential to be even more widely distributed. The genus *Escarpia* is found in a variety of reducing environments, and occupies several ocean basins with the three described species *Escarpia laminata*, *E. southwardae*, and *E. spicata* occurring in the Gulf of Mexico (GoM), West Africa, and in the eastern Pacific respectively. However, while there is high genetic similarity between the three species, geographical and hydrological barriers still appear to limit gene flow between them [22].

The genus *Sclerolinum*, which forms the sister clade to the vestimentiferans [23], also exhibits a widespread distribution. The seven formally described species are reported from the northeast Atlantic [24, 25], GoM and Caribbean [26, 27], and southeast Asia [28, 29], however there are also a number of known but not currently described *Sclerolinum* populations from Antarctica, Hawaii [30], the Sea of Okhotsk [31] and off Kushiro, Japan [32, 33], that extend the range of this genus even further. This little studied genus of small, wiry tubeworms have also been found to possesses peculiar organisation that has made it challenging to determine its position in relation to other siboglinids, have been shown to perform important ecological functions within deep-sea sediments, and is capable of colonising a multitude of reducing environments [25–27, 29, 30, 34].

Remarkable substrate choice and geographical range is demonstrated by just one *Sclerolinum* species, *S. contortum*. Initially described from soft sediments at Håkon Mosby Mud Volcano (HMMV) [25], this species was later also found to be residing in the nearby cold seeps of the Storegga Slide, Norwegian Sea [35, 36] as well as in diffuse flow areas of the Arctic vents of Loki's Castle [37, 38]. Colonisation experiments in the northeast Atlantic have shown that in addition to soft sediments, *S. contortum* can inhabit wood, other decaying plant debris, as well as mineral substrates [39]. A population of *Sclerolinum contortum* notably also occurs within the cold seeps of the GoM, a distance of over 7600 km from the nearest northeast Atlantic population [27].

Considerable sampling of the deep waters around Antarctica in recent years has revealed this region to be much more diverse, and not as isolated as traditionally thought [40]. These exploration efforts have also shown that the Southern Ocean possesses a variety of deep-sea chemosynthetic habitats that include areas of high temperature and diffuse venting, cold seeps, and whale falls [41–44]. Hydrothermal activity is currently known to occur within the Bransfield Strait [41, 45], along the East Scotia Ridge [46], Pacific-Antarctic Ridge [47], Australian-Antarctic Ridge [48], and within Kemp Caldera [49], and to support unique vent ecosystems distinct from those of the main mid-ocean ridge systems [43].

Since 2001, *Sclerolinum* has been known to inhabit the sedimented hydrothermal vents of Hook Ridge, Bransfield Strait (Fig. 1) [41]. This population was recently suggested to play an important role in mediating the release of iron and manganese from sediments to the water column [34]. However while aspects of the habitat and function of this population have been investigated [30, 34], the morphology of these worms, their extent within the Southern Ocean, and how this population relates to other known *Sclerolinum* populations remain unknown. This study aims to provide a detailed description of the Antarctic *Sclerolinum* population, place it within a phylogenetic context and thereby establish its relationships to other *Sclerolinum* populations worldwide, and discern its extent and ecology within the Southern Ocean.

Results

Systematics

Phylum Annelida

Family Siboglinidae Caullery, 1914

Genus *Sclerolinum* Southward, 1961

Sclerolinum contortum **Smirnov, 2000**

(Figs. 2, 3 and 4)

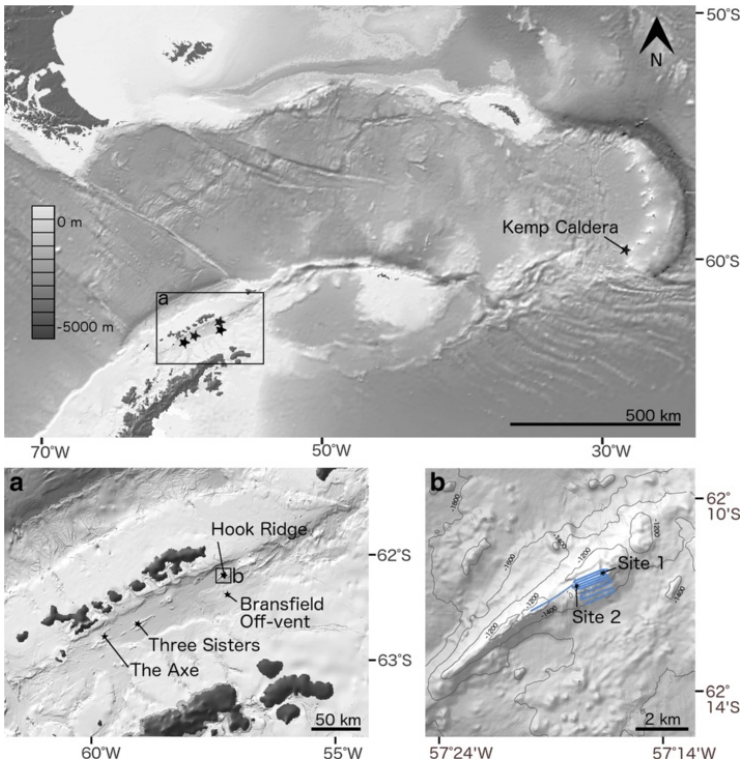

Fig. 1 Southern Ocean sampling sites from which *Sclerolinum* sp. was collected. Box (**a**) shows the locations of JC55 Bransfield Strait sampling locations, and (**b**) shows detail of Hook Ridge sampling sites (Hook Ridge Site 1 and Hook Ridge Site 2), as well as the path traversed by the SHRIMP (in blue). Map created using GeoMapApp (http://www.geomapapp.org) using data from the Global Multi-Resolution Topography (GMRT) Synthesis [92]

Material examined

Southern Ocean, *Hook Ridge Site 1*, 62.1969°S 57.2975° W, 1174 m depth: JC55_19 (RRS *James Cook* operation no.), 15 tube fragments. JC55_19, tubes attached to sampling gear (non-quantitative), 234 tube fragments [NHMUK 2015.1140-1146]. JC55_20, five tube fragments [NHMUK 2015.1153-1155]. JC55_21, 1 worm fragment with forepart, seven tube fragments [NHMUK 2015.1147-1152]. JC55_25, 29 worm fragments with forepart, 302 additional tube fragments [NHMUK 2015.1156-1157, 1188–1189 (subset of examined material)]. *Hook Ridge Site 2*, 62.1924°S 57.2783°W, 1054 m depth: JC55_30, eight tube fragments attached to sampling gear [NHMUK 2015.1158].

Description

Anterior extremity of tubes pale white in colour, thin walled (2 to 7 μm) and flattened. Posteriorly, wall thickness increases (to maximum of 28 μm) and tubes generally exhibit several smooth bends (Fig. 2a). Majority of tube is pale brown/green in colour (Fig. 2a-b), flexible and elastic, often possessing closely but irregularly spaced transverse wrinkles as well as faint longitudinal wrinkles on its outer surface (Fig. 3a), occasional microbial filament and rust patches are also present on outer tube surfaces. Tube walls are multi-layered, comprised of superimposed fibrous sheets in which fibres show an overall disorganised arrangement, inner tube surface shows a similar texture (Fig. 3c-d). Towards posterior extremity, tubes are increasingly thin walled and collapsed, outer tube wall generally smooth but with patches of attached sediment grains (Fig. 3b). Tube diameter ranges from 0.22 to 0.30 mm, longest tube fragment measured 155 mm. Several tubes exhibit branch-like abnormalities (Fig. 2e), a subset of Hook Ridge Site 1 tubes were very dark brown to black in colour (similar to tubes from Kemp Caldera, see later (Fig. 6b)).

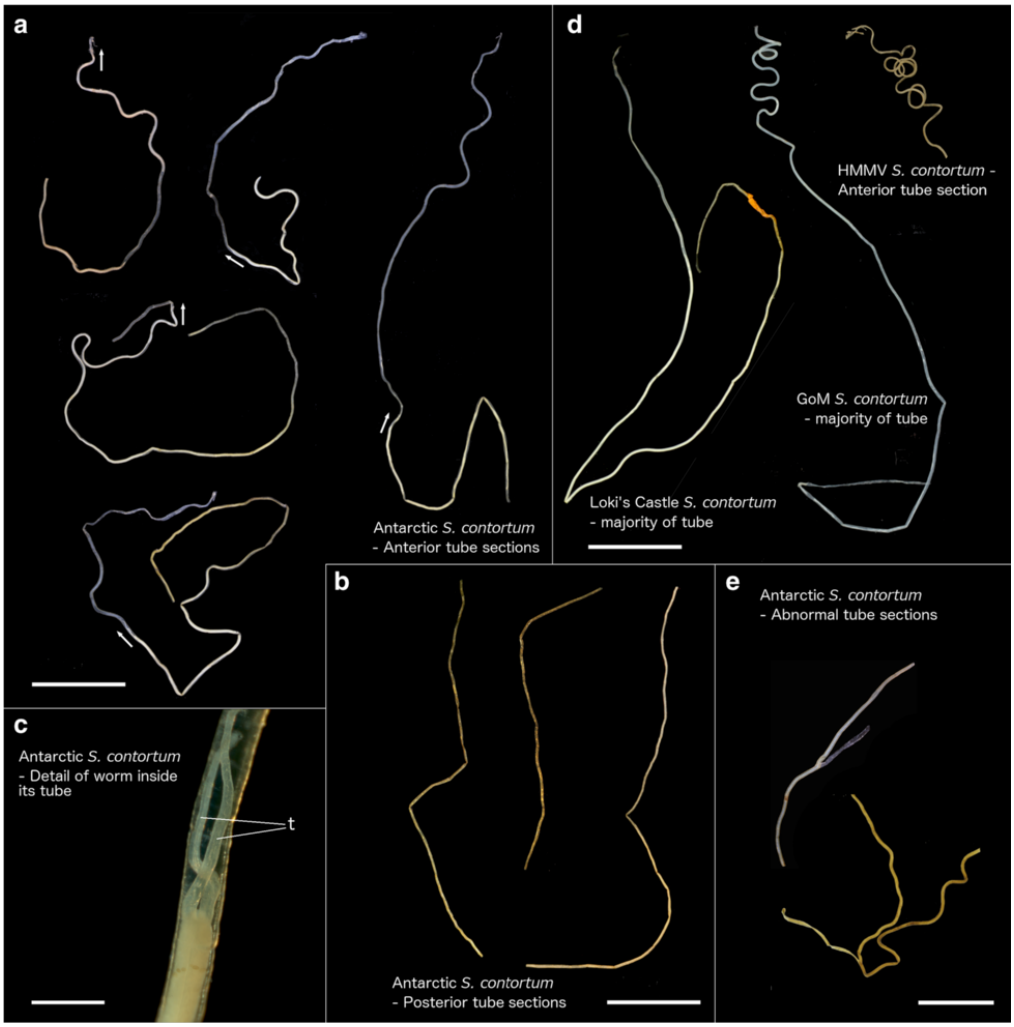

Fig. 2 Broad morphology of *Sclerolinum contortum* tubes. **a** Antarctic *S. contortum* anterior tube sections, arrows indicate position and orientation of the worms' heads. **b** Posterior sections of Antarctic *S. contortum* tubes. **c** Detail of tube with worm inside it, t – tentacles. **d** Tubes of *S. contortum* from Loki's Castle, GoM and HMMV. **e** Antarctic *S. contortum* tube sections showing abnormalities. Scale bars for (**a**-**b**, **d**) are 10 mm, 400 μm for (**c**) and 5 mm for (**e**)

Longest animal measured 52 mm in length (from tip of the cephalic lobe) but all were incomplete with posterior extremity missing, therefore opisthosomal characters could not be elucidated. Animals are bright red when alive, this colouration being most pronounced in trunk tissues (Fig. 3e-f). Two tentacles (Fig. 2c) often slightly different in length in individuals, tentacle lengths overall varied greatly between measured worms, from 0.83 to 3.00 mm. Tentacles smooth or occasionally wrinkled on inner surfaces, longitudinal blood vessels visible within them (Fig. 4a-b). Dense epidermal glands occur around the base of tentacles, which are more scattered distally (Fig. 4a-b). Diameter of forepart ranges between 0.15 to 0.23 mm. Cephalic lobe had a small, rounded triangular tip 55 to 75 μm in length that protrudes from forepart (Figs. 3h and 4b). Dorsal furrow deep and wide, extending from base of tentacles (Figs. 3i and 4a). Frenulum positioned 0.13 to 0.37 μm from tip

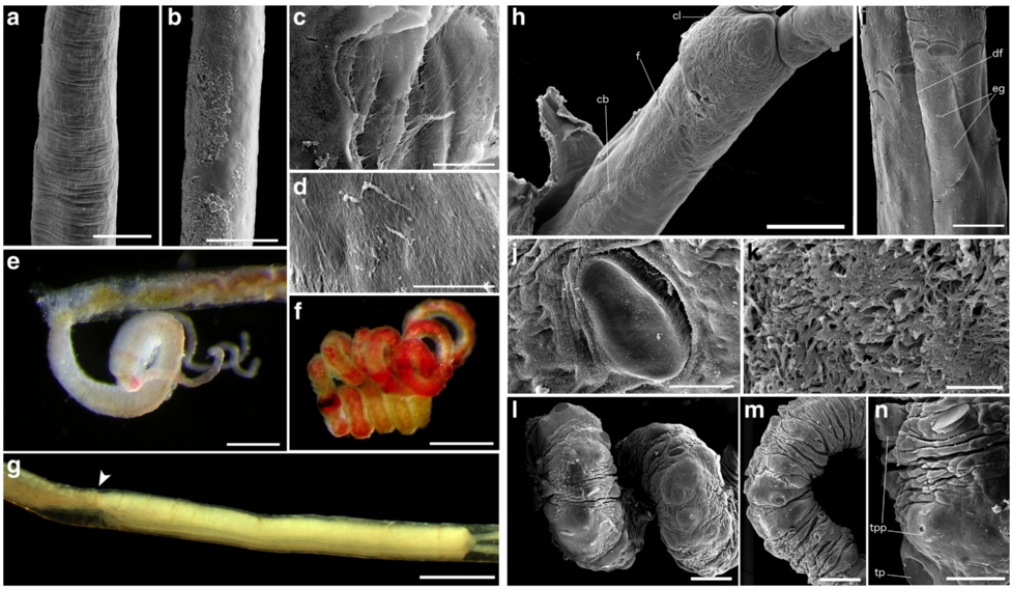

Fig. 3 Details of tubes and tissues of Antarctic *Sclerolinum contortum*. **a** Anterior section of tube showing more pronounced transverse wrinkles and faint longitudinal wrinkles, scale bar is 200 μm. **b** Posterior section of tube showing a smooth tube wall with attached sediment, scale bar is 200 μm. **c** Detail of tube wall showing its multi-layered, fibrous structure, scale bar is 10 μm. **d** Detail of tube wall interior, scale bar is 5 μm. **e** Anterior portion of a live worm, scale bar is 300 μm. **f** Trunk tissue of a live worm, scale bar is 500 μm. **g** Anterior portion of a worm showing the transition between the forepart and trunk (arrow), scale bar is 500 μm. **h** The anterior of a worm in ventral view, scale bar is 100 μm. **i** Detail of the frenulum and surrounding gland openings, dorsal view. Scale bar is 50 μm. **j** Detail of a frenular plaque, scale bar is 10 μm. **k** Detail of the ventral ciliary field, scale bar is 5 μm. **l-n** Trunk tissues of a worm, scale bars in (**l-m**) are 100 μm and 50 μm in (**n**). cb – ciliated band; cl – cephalic lobe; df – dorsal furrow; eg – epidermal glands; f – frenulum; tp – trunk plaque; tpp – trunk papillae

of cephalic lobe. Region surrounding frenulum shows dense covering of glands, present on both dorsal and ventral surfaces. Frenulum comprised of 9–19 oval to elongated plaques measuring 14 to 46 μm in diameter (Fig. 3j), occurring as a slightly sparse or dense row. Frenular plaques occur dorsolaterally and ventrally with middle ventral plaque often missing, plaques in middle ventral and middle dorsal areas often smaller (Figs. 3h-i and 4a-b). Densely ciliated band present posterior to frenulum on ventral side of animal, that widens with increasing distance from frenulum (Figs. 3h, k and 4b). Region posterior to frenulum and around the ciliated band contains scattered glands, visible as slits in SEM images (Fig. 3i).

Transition between ending of dorsal furrow and beginning of a narrower, highly wrinkled and densely papillated trunk region clearly distinguished anterior and posterior zones of Antarctic *S. contortum* animals (Fig. 3g), with this forepart region measuring 1.7 to 4.8 μm in length from the tip of the cephalic lobe to the beginning of the trunk. The trunk (Figs. 3l-n and 4c) comprised much of length of animals and was characterised by the presence of scattered oval plaques positioned on top of papillae (Fig. 3l-n). Large papillae without plaques, possibly openings of pyriform glands, also present in trunk region (Fig. 3n).

Remarks

The conspecificity of Antarctic *Sclerolinum* with HMMV, Loki's Castle and GoM *S. contortum* is strongly supported by genetic data (see later). *S. contortum* (from HMMV) was originally distinguished from all other species in this genus based on its long opisthosoma with few segments, and a strongly twisted anterior tube region [25]. The anterior regions of tubes from the Antarctic however lack the characteristic prominent, knot-like contortions that lend *S. contortum* its name, being instead only faintly wavy. These contortions are also absent in some of the Loki's Castle specimens (Fig. 2d). In addition, the GoM population shows that *S. contortum* opisthosoma can be longer than those of *Sclerolinum magdalenae* [26] and possess a similar number of segments. Hence we do not believe the wavy nature of the tube and the length of the ophisthosome are useful characters to delineate species. *S. magdalenae* also has a similar frenulum to *S. contortum*,

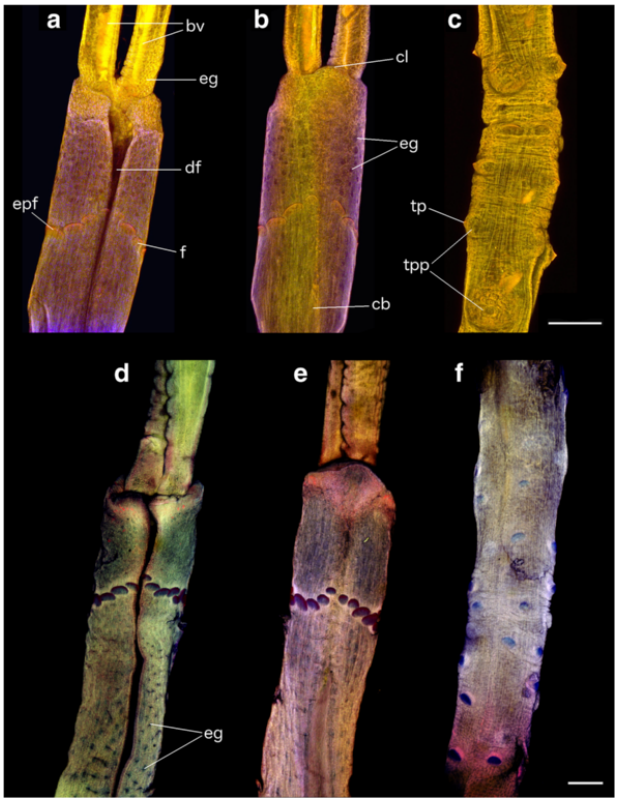

Fig. 4 Confocal laser scanning microscopy images of *Sclerolinum contortum*. **a**-**c** show Antarctic *S. contortum*, and (**d**-**f**) show *S. contortum* from Loki's Castle. **a**, **d** anterior section, dorsal view; (**b**, **e**) anterior section, ventral view; (**c**, **f**) – portion of trunk. All scale bars are 100 μm. bv – blood vessels; cb – ciliated band; cl – cephalic lobe; df – dorsal furrow; eg – epidermal glands; epf – elongated plaque of frenulum; f – frenulum; tp – trunk plaque; tpp – trunk papillae

making these two species difficult to distinguish based on currently used characters. This raises the question of whether *S. magdalenae* may be the same species as *S. contortum* and thereby represent yet a further example of the wide range of this species; molecular analyses on *S. magdalenae* would be needed to clarify this.

Antarctic *S. contortum* most closely resembles the HMMV population in terms of size (diameter of tube and animal, forepart length, frenular plaque size and number; Additional file 1: Table S1). Although animals from the various populations show broad similarity (Fig. 4) [25, 27], this species is known to show pronounced morphological plasticity of its soft tissues [27] and incorporating data from the Antarctic and Loki's Castle extends the ranges of taxonomic characters for this species even further (Additional file 1: Table S1).

Ultrastructurally, tubes do not vary much between the Arctic, GoM and Antarctic populations and all exhibit both transverse and longitudinal wrinkles, while the tube abnormalities pictured in Fig. 2e are similar to those recorded for *Sclerolinum brattstromi*, *Siboglinum ekmani* and *Siboglinum fiordicum* [50].

Ecology

Living animals were most abundant at Hook Ridge Site 1, where *S. contortum* has been reported at high densities (up to 800 individuals m^{-2} [30]), and tube fragments with tissue were also abundant at Hook Ridge Site 2. However, the distribution of *S. contortum* at Hook Ridge appears to be patchy as one of the megacore samples contained only a single specimen with a head, while another contained 71 individuals [51]. Worm specimens

were not visible within the megacore tubes until the samples were processed, suggesting that the majority of the tubes were buried within sediments. The posterior ends of the tubes were recorded as occurring at 15 cm depth by Sahling et al. [30], where temperatures are approximately 20 °C and hydrogen sulphide concentrations reach 150 μm L^{-1}, increasing at greater depths [34]. No temperature anomalies were observed in any sediments during sampling in 2011 [34]. A fully oxic water column, and oxygen penetration to depths of 2–5 cm into the sediment [34] require little of the tubes to project above the sediment. *Sclerolinum* is not reported from parts of the Hook Ridge where temperatures reach 49 °C and siliceous crusts form over the sediments [52]. SHRIMP (Seafloor High Resolution Imaging Platform) images (Fig. 5) in the vicinity of Hook Ridge Site 1 give an indication of the habitat of this species. Diffuse hydrothermal flow in this area is evidenced through the presence of what are inferred to be patchy bacterial mats (white patches in Fig. 5a). These mats also occurred around vent chimneys present at this site (Fig. 5b) the activity of which is unknown but again no temperature anomaly was observed within what appeared to be shimmering water emanating from the chimney structure [45].

***Sclerolinum* sp. Southward, 1961**

(Fig. 6)

Material examined

Kemp Caldera, 59.6948°S 28.35°W, 1432 m depth: JC55_106, lump of sulphurous material attached to sampling gear with embedded tubes. Ninety-one tube fragments removed from lump, and 4 possible tissue fragments removed from tubes and preserved separately [NHMUK 2015.1159-1166].

Description

Tubes clustered and tightly embedded into upper surface of sulphurous material (Fig. 6a), 0.23–0.34 mm in diameter ($n = 10$) and with a tube wall thickness of approximately 30 μm. Wavy to near straight in appearance. Outer tube surfaces exhibit prominent, irregular transverse wrinkles and faint longitudinal wrinkles (Fig. 6b). Tube walls are multi-layered and fibrous, and in some cases have a very rough appearance due to fragmentation of outer tube layers. SEM and EDS (energy dispersive x-ray spectroscopy) of the surface of the sulphurous lump shows large crystalline sulphur grains within a silica matrix (Fig. 6c). When mapped in thin section, sulphur and silica show some zonation but also many sulphur grains incorporated into areas of silica (Fig. 6d). *Sclerolinum* tubes are rooted beneath the surface of the sulphur lump, Fig. 6e shows detail of the sulphurous material with one of the embedded tubes.

Remarks

These tubes show very similar overall and detailed morphology to those made by *Sclerolinum contortum* from Hook Ridge, and it is very likely that they were therefore made by this species, however as no intact animals were found (unidentifiable tissue was present) it was not possible to confirm this. The significant lengths of the tubes (Fig. 6a) suggest that the colony may have reached maturity, however the absence of good quality animal tissue, the inability to DNA sequence tube contents, and the rough appearance of some of the tube walls suggest that the colony had started degrading and that conditions may have become unfavourable for *Sclerolinum*. The sulphur chunk also demonstrates a pathway through which *Sclerolinum* tubes may fossilise, preserved

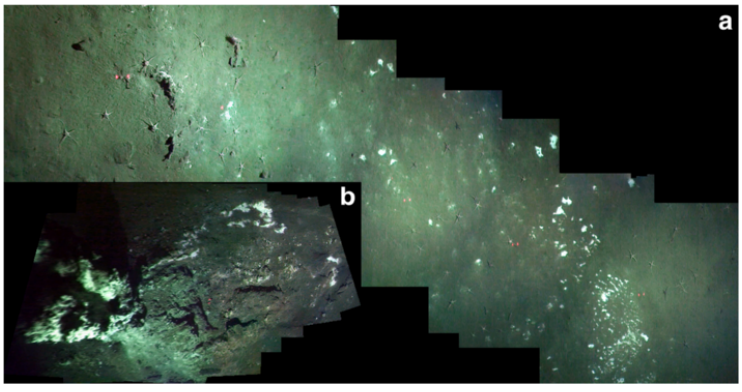

Fig. 5 SHRIMP images of Hook Ridge, Southern Ocean. Images were taken near to where megacore samples containing the highest density of *Sclerolinum contortum* were collected (maximum of 20 m distance). **a** Soft sediment with bacterial mats, (**b**) vent chimney of unknown activity with associated bacterial mats

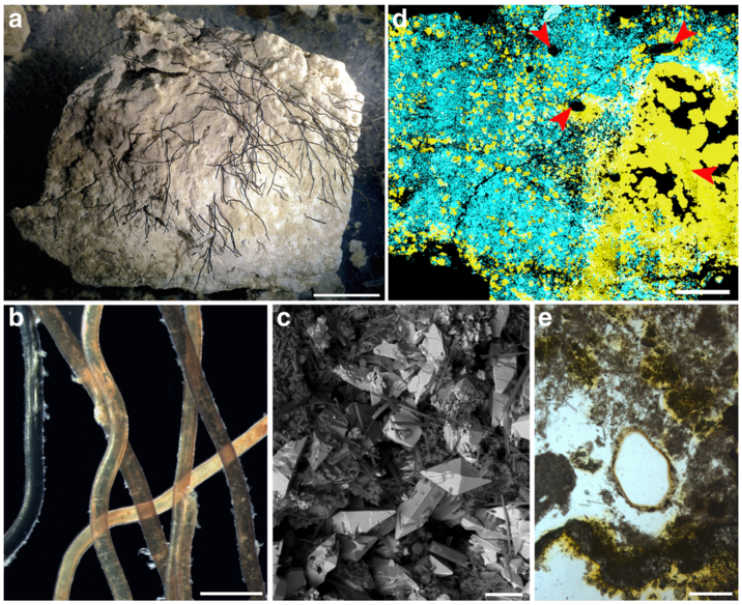

Fig. 6 Sulphurous lump with embedded *Sclerolinum* tubes collected from Kemp Caldera. **a** Sulphurous lump with embedded *Sclerolinum* tubes collected from Kemp Caldera, scale bar is 30 mm. **b** Detail of the tubes embedded in the sulphurous lump pictured in (**a**), scale bar is 1 mm. **c** SEM image of the surface of subsample of the sulphurous lump, scale bar is 50 μm. The bright crystals in this image showed a large sulphur peak when examined using energy dispersive x-ray spectroscopy (EDS). **d** EDS elemental map of sulphur lump subsample, yellow colours highlight the distribution of sulphur, blue of silicon. Red arrows show *Sclerolinum* tubes in section, scale bar is 2 mm. **e** Detail of *Sclerolinum* tube section that is embedded within the sulphurous lump, scale bar is 200 μm

as *Sclerolinum* tube-shaped voids within its matrix (Fig. 6d).

Ecology

Areas of diffuse venting within Kemp Caldera would be favourable habitats for *Sclerolinum*, however the occurrence of these animals within such a highly acidic environment, within a substrate composed largely of sulphur has not previously been observed.

Phylogeny and genetic diversity of *S. contortum*

The three combined molecular analysis runs for the family Siboglinidae converged on the same tree topology and near identical posterior probability values (maximum variation of 4 %). The 50 % majority rule consensus tree (Fig. 7) indicated overall strong branch support for the monophyly of the major clades of Vestimentifera, *Sclerolinum*, *Osedax* and Frenulata. Antarctic *Sclerolinum* falls within a clade comprised of *S. contortum* from GoM and the Arctic, where GoM worms form a sister group to *S. contortum* from the Arctic and Antarctic *Sclerolinum*, with strong branch support. However, support for the sister relationship between Antarctic *Sclerolinum* and Arctic *S. contortum* is weaker. 18S was identical between *Sclerolinum brattstromi*, HMMV *S. contortum*, and Antarctic *Sclerolinum*, whereas for 16S, one change (a transversion) was detected between Antarctic *Sclerolinum*, and *S. contortum* from GoM, Loki's Castle and HMMV (*S. brattstromi* 16S was very different). COI K2P (Kimura 2 Parameter) and '*p*' distances within the *Sclerolinum* clade varied from 0 % between *S. contortum* populations, to 1.4 % between *S. contortum* and Antarctic *Sclerolinum*, and were almost an order of magnitude greater between these taxa and *S. brattstromi* where the minimum distance detected was 8.8 % (Additional file 2: Table S2). Within the *S. contortum* clade, the lowest genetic distances occurred between Loki's Castle and HMMV populations, and the greatest between the Arctic and Antarctic populations (Additional file 2: Table S2).

The phylogenetic and haplotype analyses based on 65 *S. contortum* COI sequences showed 14 distinct haplotypes (Fig. 8; Table 1; maximum variation of 3 % for posterior probability values within the phylogenetic analysis). The number of haplotypes within the Arctic and GoM populations were greater than within the Antarctic population, in which all 27 individuals form a single haplotype

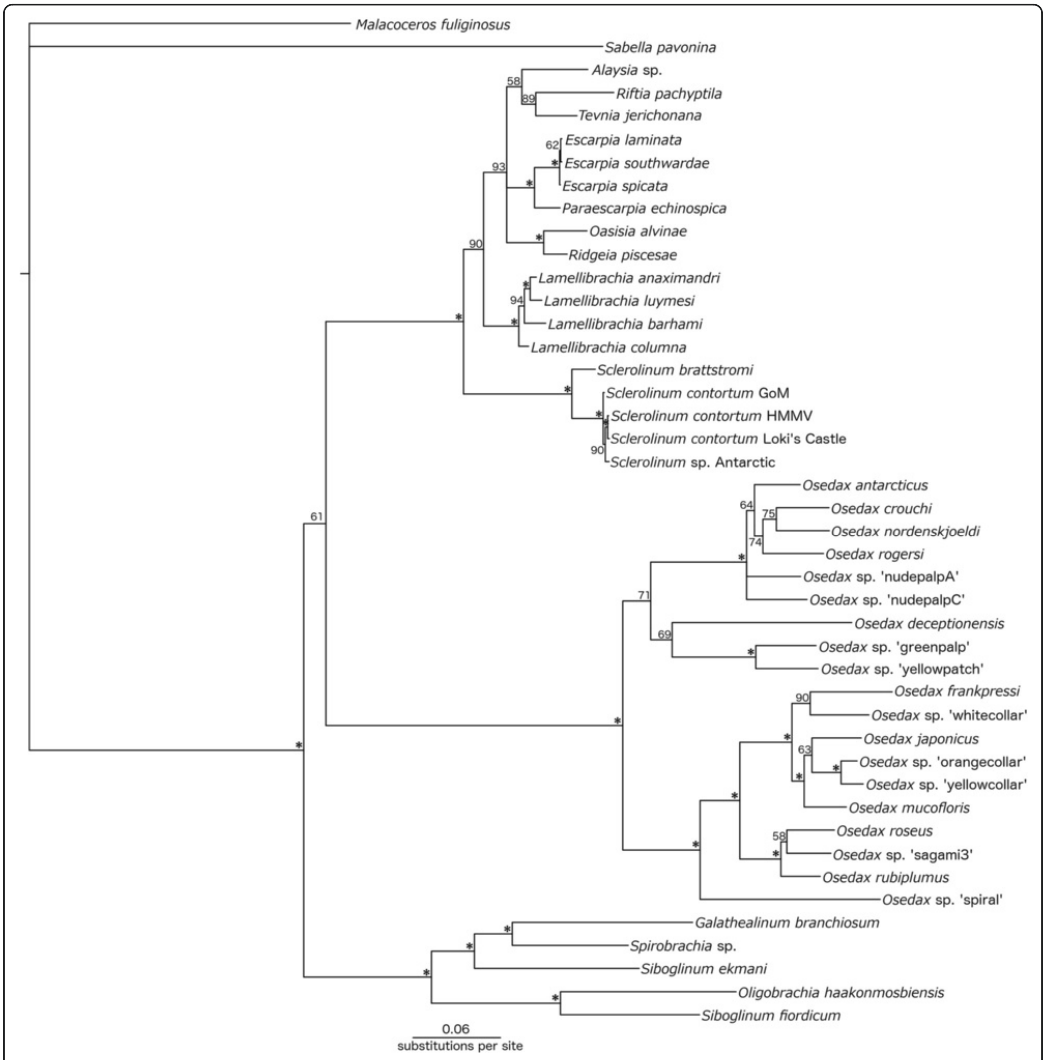

Fig. 7 Phylogeny of the annelid family Siboglinidae. This analysis was performed using a Bayesian approach and a combined dataset of the three genes COI, 16S and 18S. The phylogeny is a 50 % consensus tree, in which numbers represent posterior probability values out of 100, and branches marked with an asterisk (*) indicate posterior probabilities equal to or greater than 95

despite having the largest sample size. An HMMV individual fell within the same haplotype as Loki's Castle worms, and as genetic distances were lowest between these two populations (Additional file 2: Table S2), HMMV and Loki's Castle sequences were henceforth pooled into a single Arctic population. Nucleotide diversity (π) and mean K2P distances within populations were on the whole low, and a non-synonymous substitution was found within the Arctic population (Table 1). The results of the analysis of molecular variance (AMOVA) (Table 2) show that the largest percentage of variation occurs between the three regional populations, which also resulted in a large F_{ST} value, whereas within population variation is considerably lower. Pairwise F_{ST} values are high, significant, and increase with distance between populations, being greatest between the Antarctic and Arctic populations and lowest between the Arctic and GoM populations.

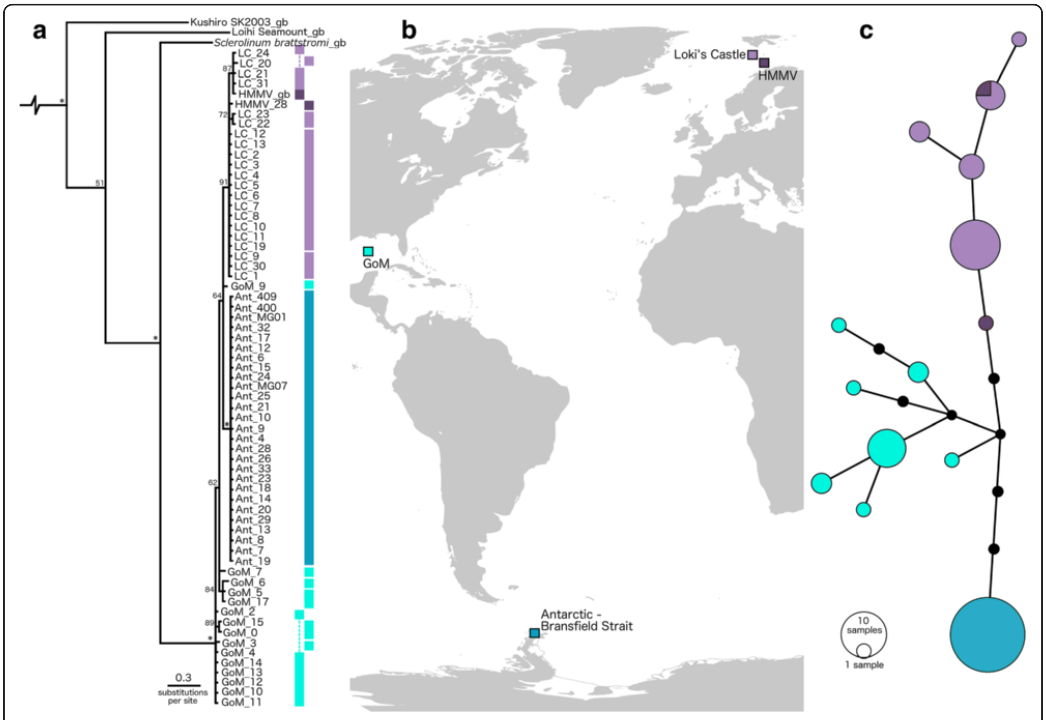

Fig. 8 Results of phylogenetic and haplotype network analyses for *Sclerolinum contortum*. **a** Phylogeny of *S. contortum* individuals using the COI gene with vertical bars representing haplotype groups, coloured according to population location; HMMV -dark purple, Loki's Castle (prefix LC) – light purple, GoM – light blue, and the Antarctic (prefix Ant) – dark blue. The siboglinids *Riftia pachyptila* and *Siboglinum ekmani* were used as outgroups (not shown), and sequences obtained from NCBI GenBank have the suffix '_gb' (see Additional file 5: Table S4 for accession numbers). **b** Map of the Atlantic and part of the Southern Ocean showing the locations of the four *S. contortum* populations used in this study, world map source: Wikipedia. (https://en.wikipedia.org/wiki/Contemporary_history#/media/File:WorldMap.svg). **c** Haplotype network constructed using the gene COI, sequenced from animals from four different *S. contortum* populations. Gaps were treated as missing data, and the connection limit was set to 95 %. Each line represents one change, and black dots represent missing haplotypes. Haplotype network was drawn using PopART (http://popart.otago.ac.nz)

Discussion

First record of a bipolar siboglinid: geographic and genetic patterns

Our data strongly supports the notion that *Sclerolinum contortum* is a bipolar species, with records that span almost 16,000 km from the Arctic to the Antarctic and making it the only siboglinid for which such a range has been observed. Our combined phylogenetic analysis using extended molecular data for the *Sclerolinum* genus demonstrates high levels of similarity of three barcoding genes COI, 16S and 18S between Antarctic *Sclerolinum* and *S. contortum* from the Arctic and GoM, and clearly distinguishes another *Sclerolinum* species (*Sclerolinum brattstromi*) from this group (Fig. 7). In addition, the

Table 1 Measures of COI sequence variation within *S. contortum* populations

Locality	*N*	No. of haplo-types	Haplotype diversity (h)	Nucleotide diversity (π)	No. of polymorphic sites (S)	No. of synonymous/ non-synonymous substitutions	Mean K2P distance (%)
Arctic	23	6	0.700 ± 0.088	0.002 ± 0.0004	5	4/1	0.2
GoM	15	7	0.781 ± 0.102	0.004 ± 0.0008	10	10/0	0.4
Antarctic	27	1	0	0	0	0	0
Total	65	14					

N - sample size, standard deviations are given for h and π

Table 2 Results of the AMOVA for the various *S. contortum* populations

Source of variation	Degrees of freedom	Sum of Squares	Variance components	Percentage of variation
Among populations	2	102.573	2.41055 Va	84.5
Within populations	62	27.424	0.44232 Vb	15.5
Total	64	129.997	2.85287	
Fixation index (F_{ST})	0.84496			
Pairwise F_{ST} values				
	Arctic	GoM		
GoM	**0.7211**			
Antarctic	**0.9095**	**0.8621**		

F_{ST} values in bold are significant ($p < 0.05$)

mitochondrial marker COI also differentiates an additional two *Sclerolinum* species from the *S. contortum* clade (Kushiro SK2003 and Loihi Seamount; Fig. 8). COI genetic distances are more than 6 times greater between *S. contortum* (including the Antarctic population) and *S. brattstromi* compared to within the former clade (Additional file 2: Table S2), in which divergence is well below 3 %, the generally accepted threshold for delimiting species [53, 54]. The morphology of Antarctic *Sclerolinum* also generally fits within the variation observed for *S. contortum* from other areas, most closely resembling the soft tissue morphology of the most distant population, from HMMV (Additional file 1: Table S1). Classifying Antarctic *Sclerolinum* as *S. contortum* despite the great distances between populations highlights the important taxonomic observation that annelids with very similar morphology and DNA can be spread over vast geographical areas, with their distributions controlled by habitat availability and local ecology.

Bipolarity has so far been observed in only a handful of deep-sea organisms, but demonstrates that steep temperature gradients and limited water exchange between the Southern and surrounding oceans have not completely restricted the spread of deep-sea fauna across these barriers [40]. Southern Ocean vent sites such as the East Scotia Ridge differ from sites on Mid-Atlantic Ridge and East Pacific Rise in that fauna such as vestimentiferan and alvinellid polychaetes, vesicomyid clams, bathymodiolid mussels, and alvinocaridid shrimp are absent [43]. However the ability of *S. contortum* to have migrated across Southern Ocean dispersal barriers suggests that the absence of vestimentiferans at Antarctic vent sites may not be the result of historical dispersal limitation (vicariance). The extensive, bipolar nature of this deep-sea chemosynthetic tubeworm also accentuates that being widespread in the deep-sea is a real and common pattern, with examples supported by molecular data emerging from a variety of additional taxa in recent years [8, 55–58].

Although our data support *S. contortum* conspecificity across the Arctic, GoM and Antarctic, at a population level there is evidence that distance is a barrier to gene flow. While mixing appears to occur between the HMMV and Loki's Castle populations that are separated by approximately 270 km (Fig. 8), this does not seem to be the case between the Arctic, GoM and Antarctic. Though these three regional populations show very high genetic similarity, the structure presented by the COI haplotype network (Fig. 8), and the F_{ST} values obtained for population pairs (Table 2), suggest that geographic distance does present a barrier to gene flow for this species. This is largely consistent with research into the connectivity of hydrothermal vent vestimentiferans on the EPR, where for both *Riftia pachyptila* and *Tevnia jerichonana* there appears to be little gene flow between the most distant populations of these species [20, 21]. Pairwise F_{ST} values between the most distant populations of these two species are similar to those reported for *S. contortum* in this study, however it is obvious that many populations of *S. contortum* are likely to exist between those sampled in this study, and sampling gaps have been found to inflate F_{ST} [59].

High genetic correspondence with lack of gene flow over large distances is also characteristic of *Escarpia* spp., species of which show high levels of similarity in the mitochondrial genes 16S, COI and cytochrome *b*, but can be differentiated on their morphology, as well as by using a nuclear gene (haemoglobin subunit B2 intron) and microsatellite markers [22]. Our interpretation of geographically distant *Sclerolinum* populations belonging to one species contrasts with the division of *Escarpia* into three separate species despite their genetic similarity, however we believe our classification to be justified based on the reasons outlined above, and recommend greater caution in describing genetically-similar but geographically distant populations of siboglinids as new species based on morphology.

Despite the evidence for low gene flow at regional scales, *Sclerolinum contortum* has managed to spread to both poles as well as subtropical latitudes, and the question remains as to how this was achieved. Nothing is presently known of the larvae of *Sclerolinum*, but when the larvae of the vestimentiferan *Riftia pachyptila* are considered, which can disperse 100 km along the EPR ridge axis [60], it is unlikely that *S. contortum* larvae

travelled the ~10,000 km between the GoM and Hook Ridge in a single journey. As *S. contortum* appears to be capable of colonising a large range of substrates, dispersal over wide areas through the use of a variety of chemosynthetic habitats as 'stepping stones' [61, 62] might be the most plausible explanation for this species. Such a hypothesis may be supported by our results which show that there is greater genetic similarity between the spatially closer Arctic and GoM populations, and GoM and Antarctic populations, than there is between the two polar populations (Arctic and Antarctic; Table 2). However, the presently known number of *S. contortum* populations is too low to conduct a test for the above scenario, therefore whether this is the best model cannot be resolved at present. Stepping-stone dispersal would suggest that *S. contortum* is more widespread than currently supposed, which does appear to be the case in the Antarctic. The large mass of tubes recovered from Kemp Caldera suggests that *S. contortum* populations come and go, taking advantage of reducing conditions where they are encountered and dying out when these temporary oases dry up.

Such a lifestyle may also explain the low COI haplotype diversity observed within the Antarctic population in comparison to the Arctic and GoM worms used for this study. The Antarctic population may be demonstrating the effects either of a founder event or bottleneck [63], where a founder effect may arise as a result of a number of opportunistic *S. contortum* individuals finding suitable conditions and settling at Hook Ridge, and persisting in the sustained diffuse hydrothermal flow at this site. However, the ephemeral nature of hydrothermal circulation within the Bransfield Strait [45], and repeated glacial-interglacial events affecting the Southern Ocean mean that it may also be plausible for the Antarctic *S. contortum* population to have undergone a bottleneck (loss of genetic diversity following a population crash) [64]. Evidence of a genetic bottleneck linked to glacial cycles has been detected for a number of Antarctic species (see [65] for a review), and ultimately more samples from a wider area of the Southern Ocean would be required to test this in *S. contortum*. *Sclerolinum* has also been shown to be capable of asexual reproduction via breaking and regenerating missing ends [66, 67], which may also account for the low genetic diversity of the Antarctic population.

There is currently no fossil record for *Sclerolinum*. As well as demonstrating a pathway through which *Sclerolinum* tubes may become preserved in the fossil record, this study shows that any future reports of *Sclerolinum* fossil discovery should be mindful of the following: fossils found in a range of ancient chemosynthetic environments, from very distant parts of the world, and exhibiting varying degrees of tube contortion may belong to the same species. Recent reports of Cretaceous *Osedax* fossils [68] imply that Siboglinidae has more ancient origins than indicated by molecular clock estimates [69–71], suggesting that the widespread distribution, morphological and habitat plasticity exhibited by *Sclerolinum* may have contributed to the survival of this genus over long evolutionary timescales too [72].

Natural history of *S. contortum* in the Southern Ocean

We have shown that *S. contortum* can exhibit even greater morphological plasticity than was previously noted for this species by Eichinger et al. [27]. Much of this plasticity is in the tubes constructed by this worm after which the species is named. Tube morphology may be a condition that is dictated by environmental factors, as has previously been shown for the highly plastic tubes built by the vent dwelling vestimentiferan *Ridgeia piscesae* [73]. Environmental factors can also influence the physiology of these worms, thereby affecting their genetic diversity [74]. While environmental parameters were not measured by the present study, we speculate that contortion of the anterior of *S. contortum* tubes increases their surface area to volume ratio, thus improving the efficiency of oxygen uptake and may therefore result from settlement in lower oxygen conditions.

The obvious morphological plasticity of *Sclerolinum contortum* is matched by its remarkable ecological and habitat plasticity. With our new data from the Antarctic we can now show that it is able to colonise a vast range of chemosynthetic habitats including high-temperature acidic white smoker vent fields, low-temperature sedimented diffuse vent fields, hydrocarbon cold seeps and mud volcanoes. Chemosynthetic invertebrates have been likened to terrestrial weeds [75] in virtue of their ability to colonise ephemeral/disturbed environments, as well as their effective dispersal, rapid growth rates, and early reproduction [76, 77], and in this sense, we can also think of *S. contortum* as a 'chemosynthetic weed' due to its ability to quickly populate a wide range of sulphur-rich habitats and spread over great distances.

Weedy species can have a dramatic influence on the environments they colonise. Their impacts are well-documented particularly in reference to terrestrial non-native species, and have demonstrated the ability of weedy species to have pronounced ecosystem, community and population-level effects [78, 79]. Supporting the concept of the *Sclerolinum* weed is the observation that the species can have a considerable influence on the biogeochemistry of the sediment at the sediment-hosted Bransfield hydrothermal vents [34]. Along with the maldanid *Nicomache lokii*, *S. contortum* forms a complex three-dimensional habitat for free-living invertebrates at Loki's Castle [38], as well as in the Nyegga seep area of the Storegga Slide where filamentous bacteria cover *S.*

contortum tube surfaces, thereby also providing substrate and food for associated organisms [35]. *S. contortum* therefore represents an important keystone species within the range of reducing environments it inhabits.

Conclusions

Since their initial discovery alongside hydrothermal vent chimneys in the late 1970s, siboglinid worms have continued to surprise and amaze with their unusual adaptations to a mode of life in the deep sea dependant solely on endosymbionts. By investigating in detail the DNA, morphology and a novel inhabiting substrate of the very poorly studied *Sclerolinum* genus, the present study has found that they too conform to this pattern, by possessing extraordinary morphological and ecological plasticity that has allowed them to occupy a remarkable range that spans across all of the world's oceans. However, fundamental knowledge of the biology of these worms is still lacking - there is presently no information on *Sclerolinum* reproduction, larvae and their dispersal, and symbionts from the range of chemosynthetic environments which this genus occupies. We therefore suggest these areas as potential directions for future research into this group.

Methods

Sample collection

Antarctic sample collection was conducted on board RRS *James Cook* expedition JC55 during January-February 2011 (Table 3), during which *Sclerolinum* was collected from two locations: Hook Ridge, Bransfield Strait, and Kemp Caldera. At Hook Ridge, venting occurs through sediment as low temperature discharge of phase-separated fluids that are highly diluted by seawater [45]. At Kemp Caldera, both hot and diffuse venting has been found that is characterised by unusual, highly acidic and sulphidic fluid composition. At a site named 'Winter Palace', crumbly chimneys release white smoker-type hydrothermal fluids up to 212 °C, while at 'Great Wall' a seafloor fissure releases low temperature diffuse fluids from which sulphur-rich minerals precipitate [80] [Copley et al. *in prep*.].

Samples were obtained using a Bowers & Connelly megacorer fitted with multiple 10 cm-diameter polycarbonate core tubes. *Sclerolinum* sp. tubes containing animal tissues and empty *Sclerolinum* sp. tubes were collected from two Hook Ridge sites, Hook Ridge Site 1 and Hook Ridge Site 2 (Fig. 1; Table 3). *Sclerolinum* sp. tubes from Kemp Caldera were acquired using a gravity corer, to which a sulphurous lump containing embedded tubes had become attached. Possible Siboglinidae tube fragments were collected from The Axe and Bransfield Off-vent, the latter comprising a non-active site located approximately 21 km south of the Hook Ridge sites. Samples were preserved in 80 % ethanol or 6 % formalin on board the ship. SHRIMP was used to visualise the seabed within a 20 m radius of Hook Ridge Site 1. *S. contortum* specimens from Loki's Castle and HMMV, Arctic Ocean, and the GoM (Additional file 3: Methods supplement) were used for morphological and genetic comparisons with Antarctic *Sclerolinum* sp. (Table 3).

Morphological and compositional analyses

Taxonomic characters were measured in 10 Antarctic and 10 Loki's Castle worms. Unfortunately no complete animals were found, therefore only characters of the anterior and trunk regions of the worms were recorded. Tubes were either cut around sections of the worms, or they were visualised through their tubes using a ZEISS Discovery V.20 stereomicroscope. Measurements were performed using ZEISS AxioVision digital processing software as well as ImageJ (version 1.46r). To visualise taxonomic characters more clearly, sections of Antarctic and Loki's Castle worms were cut out of their tubes, and imaged using laser-induced autofluorescence within a Nikon A1-Si Confocal microscope at the Natural History Museum, UK (NHM), operated in spectral imaging mode. In addition, the forepart and trunk regions of a *Sclerolinum* sp. worm fragment from the Antarctic were critical-point dried, coated in gold-paladium, and imaged

Table 3 Collection details of Siboglinidae specimens examined within this study

Locality	Taxon	Site	Latitude	Longitude	Depth (m)	No. of tube fragments*
Antarctic	*Sclerolinum* sp.	Hook Ridge Site 1	−62.1969	−57.2975	1174	686*
		Hook Ridge Site 2	−62.1924	−57.2783	1054	87*
		Kemp Caldera	−59.6948	−28.35	1432	95*
Arctic	*S. contortum*	Loki's Castle CG2009	73.5662	8.1585	2357	33*
		Loki's Castle CG2008	73.5662–73.5683	8.1585–8.1563	-	8*
		HMMV CG2010	71.9975–71.9999	14.7329–14.7316	1262	1*
		HMMV VICKING 2006	72.0013	14.7225	1270	50+
GoM	*S. contortum*	Walker Ridge WR269	26.6833	−91.65	1954	21*

Asterisk (*) denotes samples within which a subset of the tube fragments contained animal tissues

using a secondary electron detector within a FEI Quanta 650 FEG-ESEM (NHM).

A subsection of the sulphurous lump with embedded *Sclerolinum* sp. tubes (recovered from Kemp Caldera, Southern Ocean) was viewed within a LEO 1455VP SEM (at the NHM), and point EDS spectra were obtained from its surface within the same SEM. The subsection was then prepared into a polished thin section and its elemental composition was mapped using EDS within a Carl Zeiss Ultra Plus Field Emission SEM, also at the NHM.

Phylogenetic sequencing and analyses

Total genomic DNA was extracted from 64 *Sclerolinum* worm fragments: 27 Antarctic *Sclerolinum* sp., 15 *S. contortum* from the GoM, 21 *S. contortum* from Loki's Castle, and one *S. contortum* individual from HMMV. Worm fragments with tentacles and forepart, and long worm fragments were selected for extractions to increase the likelihood of sampling from different individuals. DNA extractions of Antarctic and GoM specimens were performed using a Hamilton Microlab STAR Robotic Workstation combined with a DNeasy kit (Qiagen, Valencia, CA). Approximately 400 bp of the mitochondrial gene 16S, 600 bp of the mitochondrial gene COI, and 840–1370 bp of the nuclear 18S gene were amplified (all primers used for PCRs and sequencing are listed in Additional file 4: Table S3). PCR mixtures for Antarctic and GoM specimens contained 1 μl of each primer (10 μM), 2 μl of DNA template, and 21 μl of *Taq* PCR Master Mix (Qiagen). The PCR profile was as follows: 94 °C/300 s, (94 °C/60s, 50 °C/60s, 72 °C/120 s)*35 cycles, 72 °C/300 s. PCR products were visualised on 1.5 % agarose gels following electrophoresis, and sequenced using an Applied Biosystems 3730XL DNA Analyser at the NHM. DNA extraction and PCR of Arctic specimens (Loki's Castle and HMMV) were carried out at the Biodiversity Laboratories, University of Bergen (BDL, DNA-lab section, Department of Biology) where an Applied Biosystems 3730XL DNA Analyser was used for sequencing. The PCR mixtures for amplification of 16S and COI contained 1 μl of each primer (10 μM), 1 μl of DNA template, 2.5 μl Qiagen CoralLoad buffer (10x), 1 μl Qiagen MgCl (25 μM), 2 μl dNTPs (TaKaRa; 2.5 μM of each dNTP), 0.15 μl TaKaRa HS taq, and 16.35 μl PCR water. The PCR profile for 16S was as follows: 95 °C/300 s, (95 °C/30s, 50 °C/30s, 72 °C/90s)*35 cycles, 72 °C/600 s, while the following profile was used for COI: 95 °C/300 s, (95 °C/45 s, 45 °C/45 s, 72 °C/60s)*5 cycles, (95 °C/45 s, 51 °C/45 s, 72 °C/60s)*35 cycles, 72 °C/600 s. In total, 16S was sequenced for 28 worm fragments, COI for 64, and 18S for two worm fragments.

Molecular phylogenetic analyses were performed using a combined dataset of 16S, COI and 18S sequences for members of the family Siboglinidae. A total of 44 terminal taxa were included in the analyses, of which five were *Sclerolinum*, and 39 were from other Siboglinidae genera. For the above analyses 111 sequences were obtained from NCBI Genbank, accession numbers for which are listed in Additional file 5: Table S4. The sabellid *Sabella pavonina* and spionid *Malacoceros fuliginosus* were used as outgroup taxa, of which *M. fuliginosus* was used to root the tree. Outgroup choice was based on the analyses of Rousset et al. [81] and Weigert et al. [82]. Overlapping sequence fragments were concatenated into consensus sequences using Geneious [83], and aligned using the following programs (provided as plug-ins in Geneious): MUSCLE for COI [84], and MAFFT for 18S and 16S [85]. The evolutionary models used for each gene were selected using jModelTest [86]. Based on the Akaike Information Criterion (AIC), the best fitting models of nucleotide substitution were TIM1 + I + G for COI and 18S, and TIM2 + G for 16S. As the model GTR + I + G is the closest approximation of the TIM models available in MrBayes, the GTR + I + G model was used for all three genes in the combined analysis. A Bayesian molecular phylogenetic analysis was conducted using MrBayes 3.1.2 [87]. Analyses of the combined dataset were run three times for 10,000,000 generations, with 2,500,000 generations discarded as burn-in. Genetic distances for the COI gene within the genus *Sclerolinum* were calculated using the K2P model, and *p*-distances were determined in MEGA 5.1 [88].

Genetic diversity

A close relationship between Antarctic *Sclerolinum* sp. and *S. contortum* was detected from the above investigations, therefore an additional alignment was used for a phylogenetic analysis using a total of 68 COI *Sclerolinum* sp. sequences (*Sclerolinum brattstromi*, Kushiro-SK-2003 *Sclerolinum* sp., Loihi Seamount *Sclerolinum* sp., 27 Antarctic *Sclerolinum* sp., 15 GoM, 21 Loki's Castle, and 2 HMMV *S. contortum*) for which two additional siboglinid COI sequences (*Riftia pachyptila* and *Siboglinum ekmani*) were used as outgroups. The alignment was trimmed to standardise sequence lengths, and the analysis was performed in the same way as the combined analysis outlined above. In addition, a haplotype distribution was created using only Antarctic *Sclerolinum* sp. and *S. contortum* sequences in TCS 1.21 [89] and drawn in PopART (http://popart.otago.ac.nz). Gaps were treated as missing data, and the connection limit was set to 95 %. There appeared to be little genetic differentiation between HMMV and Loki's Castle *S. contortum* therefore sequences from these localities were subsequently pooled into one Arctic population, while GoM *S. contortum* and Antarctic *Sclerolinum* sp. were treated as two additional populations. Haplotype diversity, nucleotide diversity, and number of

polymorphic sites were calculated within each population (Arctic, GoM and Antarctic) using DnaSP 5.10.1 [90]. Average genetic distances (K2P) within each population were calculated using MEGA 5.1 [88]. Pairwise F_{ST} values and an AMOVA were computed using Arlequin 3.5.1.3 [91]. The AMOVA was performed using K2P distances and 1000 permutations.

Ethics statement

Ethics approval is not required for the collection and investigation of the morphology and DNA of annelid worms. Antarctic specimens were collected under the Foreign and Commonwealth Office Antarctic permit number S5-4/2010 issued to National Marine Facilities for the JC55 research expedition. Permits were not required by the collectors of Arctic and Gulf of Mexico material.

Availability of supporting data

Morphological data supporting the results of this article are included within Additional file 1: Table S1. Occurrence data on specimens used in this study (in DarwinCore Archive format) and additional data sets (DNA sequence alignments) are available in the figshare repository (http://dx.doi.org/10.6084/m9.figshare.1613855). DNA sequences are available in GenBank (http://www.ncbi.nlm.nih.gov/genbank/), with NCBI accession numbers detailed in Additional file 5: Table S4 (a sequence for each detected *Sclerolinum contortum* COI haplotype is available).

Additional files

Additional file 1: Table S1. Comparison of morphological characters between Antarctic *Sclerolinum* and three populations of *S. contortum*. (DOCX 100 kb)

Additional file 2: Table S2. P-distance (above diagonal) and K2P (below diagonal) genetic distances (in %) among the genus, as well as putative, *Sclerolinum*. (DOCX 49 kb)

Additional file 3: Methods supplement. Details on the collection of additional *Sclerolinum contortum* specimens for comparison with Antarctic material. (DOCX 73 kb)

Additional file 4: Table S3. Primers used for PCR and sequencing. (DOCX 118 kb)

Additional file 5: Table S4. Taxa used in Bayesian molecular analyses and GenBank accession numbers. (DOCX 118 kb)

Abbreviations

16S: Mitochondrial large subunit ribosomal RNA; 18S: Nuclear small subunit subunit ribosomal RNA; AIC: Akaike information criterion; AMOVA: Analysis of molecular variance; COI: Cytochrome oxidase subunit I; EDS: Energy dispersive x-ray spectroscopy; EPR: East Pacific Rise; GoM: Gulf of Mexico; HMMV: Håkon Mosby Mud Volcano; K2P: Kimura 2 Parameter; MAFFT: Multiple Alignment using Fast Fourier Transform; MUSCLE: Multiple Sequence Comparison by Log-Expectation; NHM, NHMUK: Natural History Museum, United Kingdom; SHRIMP: Seafloor High Resolution Imaging Platform.

Competing interests

The authors declare that they have no competing interests.

Authors' contributions

MG contributed to study design, performed measurements, imaging and genetic analyses and wrote the manuscript. HW helped to design the study and with all aspects of the molecular work. JB processed JC55 cruise samples and provided SHRIMP imagery. ME performed DNA sequencing of Loki's Castle material. RM provided sulphurous chunk with embedded *Sclerolinum* tubes and biogeochemical components of the manuscript. CL helped with taphonomical observations. AG collected Antarctic *S. contortum* material, imaged specimens live at sea, designed the study, participated in its coordination, and helped to draft the manuscript. All authors read and approved the final manuscript.

Acknowledgements

We would like to thank the masters and crews of the NERC 'Chemosynthetically-driven ecosystems in the Southern Ocean' (ChEsSo) research cruise on RRS *James Cook* JC055 (Professor Paul Tyler PI), the National Oceanography Centre technicians who operated the SHRIMP and ROV *Isis* platforms, the University of Bergen Centre for Geobiology expeditions on RV G. O. Sars during 2008–2010, the NOAA *Ronald H. Brown* expedition no. RB-07-04, and the 2006 VICKING cruise on board R/V *Pourquoi pas?* for their help in collecting specimens used in this study. We are also especially indebted to the following scientists for their generous donations of material for use in this study: Prof. Hans Tore Rapp and Dr. Jon Anders Kongsrud for material from Loki's Castle hydrothermal vent field, Prof. Monika Bright for material from the Gulf of Mexico, and Dr. Ann Andersen for material from Håkon Mosby Mud Volcano. Thank you to Alex Ball and Tomasz Goral (NHM) for help with imaging, Laura Hepburn for guidance regarding sulphur lump analyses, and to Gabrielle Kennaway and Tony Wighton (NHM) for their help in the preparation of thin sections. Thank you also to Bob Vrijenhoek , Shannon Johnson, and two anonymous reviewers for valuable comments on this work. MG is funded by NERC CASE PhD studentship no. NE/K500847/1. JB is funded by NERC CASE PhD studentship no. NE/L501542/1. The ChEsSo programme was funded by a NERC Consortium Grant (NE/DO1249X/1) which is gratefully acknowledged.

Author details

[1]Life Sciences Department, Natural History Museum, London, UK. [2]School of Earth and Environment, University of Leeds, Leeds, UK. [3]School of Geography, University of Leeds, Leeds, UK. [4]Centre for Geobiology, University of Bergen, Bergen, Norway. [5]Department of Biology, University of Bergen, Bergen, Norway. [6]Ocean and Earth Science, National Oceanography Centre Southampton, University of Southampton, Southampton, UK.

Received: 7 October 2015 Accepted: 6 December 2015
Published online: 14 December 2015

References

1. Brandt A, De Broyer C, De Mesel I, Ellingsen KE, Gooday AJ, Hilbig B, et al. The biodiversity of the deep Southern Ocean benthos. Philos Trans R Soc B. 2007;362:39–66.
2. McClain CR, Schlacher TA. On some hypotheses of diversity of animal life at great depths on the sea floor. Mar Ecol. 2015;36:849–872.
3. Hilário A, Metaxas A, Gaudron SM, Howell KL, Mercier A, Mestre NC, et al. Estimating dispersal distance in the deep sea: challenges and applications to marine reserves. Front Mar Sci. 2015;2:1–14.
4. Goffredi SK, Hurtado LA, Hallam S, Vrijenhoek RC. Evolutionary relationships of deep-sea vent and cold seep clams (Mollusca: Vesicomyidae) of the '*pacifica/lepta*' species complex. Mar Biol. 2003;142:311–20.
5. Raupach MJ, Malyutina M, Brandt A, Wägele JW. Molecular data reveal a highly diverse species flock within the munnopsoid deep-sea isopod *Betamorpha fusiformis* (Barnard, 1920) (Crustacea: Isopoda: Asellota) in the Southern Ocean. Deep Sea Res II. 2007;54:1820–30.
6. Brix S, Riehl T, Leese F. First genetic data for species of the genus *Haploniscus* Richardson, 1908 (Isopoda: Asellota: Haploniscidae) from neighbouring deep-sea basins in the South Atlantic. Zootaxa. 2011;2838:79–84.
7. Zardus JD, Etter RJ, Chase MR, Rex MA, Boyle EE. Bathymetric and geographic population structure in the pan-Atlantic deep-sea bivalve *Deminucula atacellana* (Schenck, 1939). Mol Ecol. 2006;15:639–51.
8. Havermans C, Sonet G, d'Udekem d'Acoz C, Nagy ZT, Martin P, Brix S, et al. Genetic and morphological divergences in the cosmopolitan deep-sea

amphipod *Eurythenes gryllus* reveal a diverse abyss and a bipolar species. PLoS ONE. 2013;8:e74218.
9. Bano N, Ruffin S, Ransom B, Hollibaugh J. Phylogenetic composition of Arctic Ocean Archaeal assemblages and comparison with Antarctic assemblages. Appl Environ Microbiol. 2004;70:781–9.
10. Brinkmeyer R, Knittel K, Jürgens J, Weyland H, Amann R, Helmke E. Diversity and structure of bacterial communities in Arctic versus Antarctic pack ice. Appl Environ Microbiol. 2003;69:6610–9.
11. Pawlowski J, Fahrni J, Lecroq B, Longet D, Cornelius N, Excoffier L, et al. Bipolar gene flow in deep-sea benthic foraminifera. Mol Ecol. 2007;16:4089–96.
12. Herrera S, Shank TM, Sánchez JA. Spatial and temporal patterns of genetic variation in the widespread antitropical deep-sea coral *Paragorgia arborea*. Mol Ecol. 2012;21:6053–67.
13. Vogler AP, Monaghan MT. Recent advances in DNA taxonomy. J Zool Syst Evol Res. 2007;45:1–10.
14. Vrijenhoek RC. Cryptic species, phenotypic plasticity, and complex life histories: Assessing deep-sea faunal diversity with molecular markers. Deep Res II. 2009;56:1713–23.
15. Nygren A. Cryptic polychaete diversity: A review. Zool Scr. 2014;43:172–83.
16. Hilário A, Capa M, Dahlgren TG, Halanych KM, Little CTS, Thornhill DJ, et al. New perspectives on the ecology and evolution of siboglinid tubeworms. PLoS ONE. 2011;6:e16309.
17. Southward E, Schulze A, Gardiner S. Pogonophora (Annelida): form and function. Hydrobiologia. 2005;535:227–51.
18. Dubilier N, Bergin C, Lott C. Symbiotic diversity in marine animals: the art of harnessing chemosynthesis. Nat Rev Microbiol. 2008;6:725–40.
19. Dando PR, Southward AJ, Southward EC, Lamont P, Harvey R. Interactions between sediment chemistry and frenulate pogonophores (Annelida) in the north-east Atlantic. Deep Sea Res I. 2008;55:966–96.
20. Coykendall DK, Johnson SB, Karl SA, Lutz RA, Vrijenhoek RC. Genetic diversity and demographic instability in Riftia pachyptila tubeworms from eastern Pacific hydrothermal vents. BMC Evol Biol. 2011;11:96.
21. Zhang H, Johnson SB, Flores VR, Vrijenhoek RC. Intergradation between discrete lineages of Tevnia jerichonana, a deep-sea hydrothermal vent tubeworm. Deep Sea Res II. 2015;121:53–61.
22. Cowart DA, Huang C, Arnaud-Haond S, Carney SL, Fisher CR, Schaeffer SW. Restriction to large-scale gene flow vs. regional panmixia among cold seep *Escarpia* spp. (Polychaeta, Siboglinidae). Mol Ecol. 2013;22:4147–62.
23. Li Y, Kocot KM, Schander C, Santos SR, Thornhill DJ, Halanych KM. Mitogenomics reveals phylogeny and repeated motifs in control regions of the deep-sea family Siboglinidae (Annelida). Mol Phylogenet Evol. 2015;85:221–9.
24. Webb M. A new bitentaculate pogonophoran from Hardangerfjorden, Norway. Sarsia. 1964;15:49–55.
25. Smirnov RV. Two new species of Pogonophora from the arctic mud volcano off northwestern Norway. Sarsia. 2000;85:141–50.
26. Southward EC. On some Pogonophora from the Carribbean and the Gulf of Mexico. Bull Mar Sci. 1972;22:739–76.
27. Eichinger I, Hourdez S, Bright M. Morphology, microanatomy and sequence data of Sclerolinum contortum (Siboglindae, Annelida) of the Gulf of Mexico. Org Divers Evol. 2013;13:311–29.
28. Southward EC. Pogonophora. In: Weber M, editor. Siboga - Expeditie. Leiden: Brill; 1961. p. 1–22.
29. Ivanov A, Selivanova R. *Sclerolinum javanicum* sp.n., a new pogonophoran living on rotten wood. A contribution to the classification of Pogonophora. Biol Morya. 1992;1–2:27–33.
30. Sahling H, Wallmann K, Dählmann A, Schmaljohann R, Petersen S. The physicochemical habitat of *Sclerolinum* sp. at Hook Ridge hydrothermal vent, Bransfield Strait, Antarctica. Limnol Oceanogr. 2005;50:598–606.
31. Sahling H, Galkin S, Salyuk A, Greinert J, Foerstel H, Piepenburg D, et al. Depth-related structure and ecological significance of cold-seep communities—a case study from the Sea of Okhotsk. Deep Sea Res I. 2003;50:1391–409.
32. Kojima S, Segawa R, Hashimoto J, Ohta S. Molecular phylogeny of vestimentiferans collected around Japan, revealed by the nucleotide sequences of mitochondrial DNA. Mar Biol. 1997;127:507–13.
33. Kojima S, Ohta S, Yamamoto T, Yamaguchi T, Miura T, Fujiwara Y, et al. Hashimoto Molecular taxonomy of vestimentiferans of the western Pacific, and their phylogenetic relationship to species of the eastern Pacific III. Alaysia-like vestimentiferans and relationships among families. Mar Biol. 2003;142:625–35.
34. Aquilina A, Homoky WB, Hawkes JA, Lyons TW, Mills RA. Hydrothermal sediments are a source of water column Fe and Mn in the Bransfield Strait, Antarctica. Geochim Cosmochim Acta. 2014;137:64–80.
35. Vanreusel A, Andersen AC, Boetius A, Connelly D, Cunha MR, Decker C, et al. Biodiversity of cold seep ecosystems along the European margins. Oceanography. 2009;22:118–435.
36. Lazar CS, Dinasquet J, Pignet P, Prieur D, Toffin L. Active archaeal communities at cold seep sediments populated by Siboglinidae tubeworms from the Storegga Slide. Microb Ecol. 2010;60:516–27.
37. Pedersen RB, Rapp HT, Thorseth IH, Lilley MD, Barriga FJAS, Baumberger T, et al. Discovery of a black smoker vent field and vent fauna at the Arctic Mid-Ocean Ridge. Nat Commun. 2010;1:126.
38. Kongsrud JA, Rapp HT. *Nicomache* (*Loxochona*) *lokii* sp. nov. (Annelida: Polychaeta: Maldanidae) from the Loki's Castle vent field: An important structure builder in an Arctic vent system. Polar Biol. 2012;35:161–70.
39. Gaudron SM, Pradillon F, Pailleret M, Duperron S, Le Bris N, Gaill F. Colonization of organic substrates deployed in deep-sea reducing habitats by symbiotic species and associated fauna. Mar Environ Res. 2010;70:1–12.
40. Chown SL, Clarke A, Fraser CI, Cary SC, Moon KL, McGeoch MA. The changing form of Antarctic biodiversity. Nature. 2015;522:431–8.
41. Klinkhammer GP, Chin CS, Keller RA, Dählmann A, Sahling H, Sarthou G, et al. Discovery of new hydrothermal vent sites in Bransfield Strait, Antarctica. Earth Planet Sci Lett. 2001;193:395–407.
42. Domack E, Ishman S, Leventer A, Sylva S, Willmott V, Huber B. A chemotrophic ecosystem found beneath Antarctic Ice Shelf. EOS Trans Am Geophys Union. 2005;86:269–76.
43. Rogers AD, Tyler PA, Connelly DP, Copley JT, James R, Larter RD, et al. The discovery of new deep-sea hydrothermal vent communities in the Southern ocean and implications for biogeography. PLoS Biol. 2012;10:e1001234.
44. Amon DJ, Glover AG, Wiklund H, Marsh L, Linse K, Rogers AD, et al. The discovery of a natural whale fall in the Antarctic deep sea. Deep Sea Res II. 2013;92:87–96.
45. Aquilina A, Connelly DP, Copley JT, Green DRH, Hawkes JA, Hepburn LE, et al. Geochemical and visual indicators of hydrothermal fluid flow through a sediment-hosted volcanic ridge in the central Bransfield basin (Antarctica). PLoS ONE. 2013;8:e54686.
46. German CR, Livermore RA, Baker ET, Bruguier NI, Connelly DP, Cunningham AP, et al. Hydrothermal plumes above the East Scotia Ridge: an isolated high-latitude back-arc spreading centre. Earth Planet Sci Lett. 2000;184:241–50.
47. Winkler G, Newton R, Schlosser P, Crone T. Mantle helium reveals Southern Ocean hydrothermal venting. Geophys Res Lett. 2010;37:L05601.
48. Hahm D, Baker ET, Rhee TS, Won Y-J, Resing JA, Lupton JE, et al. First hydrothermal discoveries on the Australian-Antarctic Ridge: Discharge sites, plume chemistry, and vent organisms. Geochem Geophys Geosyst. 2015;16.
49. Tyler PA. Cruise Report No. 05 RRS James Cook Cruise JC55 13 JAN-22 FEB 2011 Bransfield Strait, the East Scotia Ridge and the Kemp Seamount Calderas Cruise 3 of the NERC Consortium Grant *'Chemosynthetically-Driven Ecosystems in the Southern Ocean'*. 2011. p. 1–85.
50. Webb M. Tube abnormality in *Siboglinum ekmani*, *S. fiordicum* and *Sclerolinum brattstromi* (Pogonophora). Sarsia. 1964;15:69–70.
51. Bell JB, Woulds C, Brown LE, Little CTS, Sweeting CJ, Reid WD , Glover, AG. Macrofaunal ecology of sedimented hydrothermal vents in the Bransfield Strait, Antarctica. Front Mar Sci. 2015 (accepted).
52. Dählmann A, Wallmann K, Sahling H, Sarthou G, Bohrmann G, Petersen S, et al. Hot vents in an ice-cold ocean: Indications for phase separation at the southernmost area of hydrothermal activity, Bransfield Strait, Antarctica. Earth Planet Sci Lett. 2001;193:381–94.
53. Hebert P, Ratnasingham S, DeWaard J. Barcoding animal life: cytochrome c oxidase subunit 1 divergences among closely related species. Proc R Soc B. 2003;270:S96–9.
54. Carr C, Hardy S, Brown T. A tri-oceanic perspective: DNA barcoding reveals geographic structure and cryptic diversity in Canadian polychaetes. PLoS ONE. 2011;6:e22232.
55. Longmore C, Trueman CN, Neat F, Jorde PE, Knutsen H, Stefanni S, et al. Ocean-scale connectivity and life cycle reconstruction in a deep-sea fish. Can J Fish Aquat Sci. 2014;71:1312–23.
56. O'Hara TD, England PR, Gunasekera RM, Naughton KM. Limited phylogeographic structure for five bathyal ophiuroids at continental scales. Deep Sea Res I. 2014;84:18–28.
57. Walz KR, Clague DA, Barry JP, Vrijenhoek RC. First records and range extensions for two *Acesta* clam species (Bivalvia: Limidae) in the Gulf of California, Mexico. Mar Biodivers Rec. 2014;7:e60.

58. Breusing C, Johnson SB, Tunnicliffe V, Vrijenhoek RC. Population structure and connectivity in Indo-Pacific deep-sea mussels of the *Bathymodiolus septemdierum* complex. Conserv Genet. 2015;16:1–16.
59. Audzijonyte A, Vrijenhoek RC. When gaps really are gaps: Statistical phylogeography of hydrothermal vent invertebrates. Evolution. 2010;64:2369–84.
60. Marsh AG, Mullineaux LS, Young CM, Manahan DT. Larval dispersal potential of the tubeworm *Riftia pachyptila* at deep-sea hydrothermal vents. Nature. 2001;411:77–80.
61. Feldman R, Shank T, Black M, Baco A, Smith C, Vrijenhoek R. Vestimentiferan on a whale fall. Biol Bull. 1998;194:116–9.
62. Glover AG, Källström B, Smith CR, Dahlgren TG. World-wide whale worms? A new species of *Osedax* from the shallow north Atlantic. Proc R Soc B. 2005;272:2587–92.
63. Fuerst PA, Maruyama T. Considerations on the conservation of alleles and of genic heterozygosity in small managed populations. Zoo Biol. 1986;5:171–9.
64. Riesgo A, Taboada S, Avila C. Evolutionary patterns in Antarctic marine invertebrates: An update on molecular studies. Mar Genomics. 2015;23:1–13.
65. Allcock AL, Strugnell JM. Southern Ocean diversity: New paradigms from molecular ecology. Trends Ecol Evol. 2012;27:520–8.
66. Webb M. Additional notes on *Sclerolinum brattstromi* (Pogonophora) and the establishment of a new family, Sclerolinidae. Sarsia. 1964;16:47–58.
67. Southward EC. Development of Perviata and Vestimentifera (Pogonophora). In: Reproductive Strategies and Developmental Patterns in Annelids. Netherlands: Springer; 1999. p. 185–202.
68. Danise S, Higgs ND. Bone-eating *Osedax* worms lived on Mesozoic marine reptile deadfalls. Biol Lett. 2015;11:20150072.
69. Halanych K, Lutz R, Vrijenhoek R. Evolutionary origins and age of vestimentiferan tube-worms. Cah Biol. 1998;39:355–8.
70. Chevaldonné P, Jollivet D, Desbruyeres D, Lutz R, Vrijenhoek RC. Sister-species of eastern Pacific hydrothermal vent worms (Ampharetidae, Alvinellidae, Vestimentifera) provide new mitochondrial COI clock calibration. Cah Biol. 2002;43:367–70.
71. Hurtado LA. Evolution and biogeography of hydrothermal vent organisms in the Eastern Pacific Ocean. Ph.D. thesis. Rutgers University, New Brunswick, N.J.; 2002
72. Jablonski D. Extinctions: a paleontological perspective. Science. 1991;253:754–7.
73. Southward EC, Tunnicliffe V, Black M. Revision of the species of *Ridgeia* from northeast Pacific hydrothermal vents, with a redescription of *Ridgeia piscesae* Jones (Pogonophora: Obturata = Vestimentifera). Can J Zool. 1995;73:282–95.
74. Tunnicliffe V, St. Germain C, Hilário A. Phenotypic variation and fitness in a metapopulation of tubeworms (*Ridgeia piscesae* Jones) at hydrothermal vents. PLoS ONE. 2014;9:e110578.
75. Baker HG. The evolution of weeds. Annu Rev Ecol Syst. 1974;5:1–24.
76. Van Dover CLL, German CRR, Speer KGG, Parson LMM, Vrijenhoek RCC. Evolution and biogeography of deep-sea vent and seep invertebrates. Science. 2002;295:1253–7.
77. Vrijenhoek RC. Genetic diversity and connectivity of deep-sea hydrothermal vent metapopulations. Mol Ecol. 2010;19:4391–411.
78. Macdonald I, Loope L, Usher M, Hamann O. Wildlife conservation and the invasion of nature reserves by introduced species: a global perspective. In: Biological invasions: a global perspective. New York: Wiley; 1989. p. 215–55.
79. Gordon DR. Effects of invasive, non-indigenous plant species on ecosystem processes: lessons from Florida. Ecol Appl. 1998;8:975–89.
80. Cole CS, James RH, Connelly DP, Hathorne EC. Rare earth elements as indicators of hydrothermal processes within the East Scotia subduction zone system. Geochim Cosmochim Acta. 2014;140:20–38.
81. Rousset V, Rouse GW, Siddall ME, Tillier A, Pleijel F. The phylogenetic position of Siboglinidae (Annelida) inferred from 18S rRNA, 28S rRNA and morphological data. Cladistics. 2004;20:518–33.
82. Weigert A, Helm C, Meyer M, Nickel B, Arendt D, Hausdorf B, et al. Illuminating the base of the Annelid tree using transcriptomics. Mol Biol Evol. 2014;31:1391–401.
83. Kearse M, Moir R, Wilson A, Stones-Havas S, Cheung M, Sturrock S, et al. Geneious Basic: An integrated and extendable desktop software platform for the organization and analysis of sequence data. Bioinformatics. 2012;28:1647–9.
84. Edgar RC. MUSCLE: multiple sequence alignment with high accuracy and high throughput. Nucleic Acids Res. 2004;32:1792–7.
85. Katoh K, Misawa K, Kuma K, Miyata T. MAFFT: a novel method for rapid multiple sequence alignment based on fast Fourier transform. Nucleic Acids Res. 2002;30:3059–66.
86. Posada D. jModelTest: Phylogenetic Model Averaging. Mol Biol Evol. 2008;25:1253–6.
87. Ronquist F, Huelsenbeck JP. MRBAYES 3: Bayesian phylogenetic inference under mixed models. Bioinformatics. 2003;19:1572–4.
88. Tamura K, Peterson D, Peterson N, Stecher G, Nei M, Kumar S. MEGA5: molecular evolutionary genetics analysis using maximum likelihood, evolutionary distance, and maximum parsimony methods. Mol Biol Evol. 2011;28:2731–9.
89. Clement M, Posada D, Crandall K. Tcs: a computer program to estimate gene genealogies. Mol Ecol. 2000;9:1657–60.
90. Librado P, Rozas J. DnaSP v5: A software for comprehensive analysis of DNA polymorphism data. Bioinformatics. 2009;25:1451–2.
91. Excoffier L, Lischer H. Arlequin suite ver 3.5: a new series of programs to perform population genetics analyses under Linux and Windows. Mol Ecol Resour. 2010;10:564–7.
92. Ryan WBF, Carbotte SM, Coplan JO, O'Hara S, Melkonian A, Arko R, et al. Global multi-resolution topography synthesis. Geochem Geophys Geosyst. 2009;10:Q03014.

Graphic design: Communication Division, UiB / Print: Skipnes Kommunikasjon AS

uib.no

ISBN: 978-82-308-3813-6